United States
Environmental Protection
Agency

Industrial Environmental Research
Laboratory
Research Triangle Park NC 27711

EPA-600/7-80-017d
January 1980

EPA

Advanced Combustion Systems for Stationary Gas Turbine Engines: Volume IV. Combustor Verification Testing (Addendum)

Interagency Energy/Environment R&D Program Report

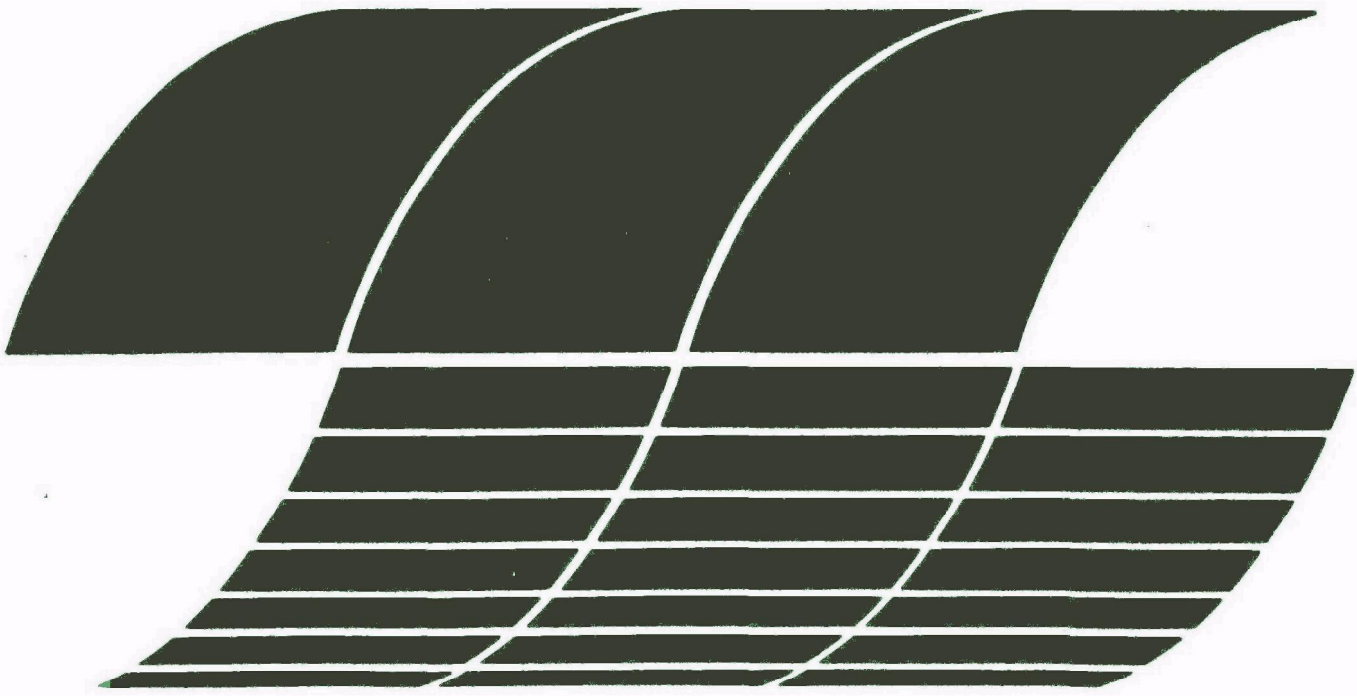

RESEARCH REPORTING SERIES

Research reports of the Office of Research and Development, U.S. Environmental Protection Agency, have been grouped into nine series. These nine broad categories were established to facilitate further development and application of environmental technology. Elimination of traditional grouping was consciously planned to foster technology transfer and a maximum interface in related fields. The nine series are:

1. Environmental Health Effects Research
2. Environmental Protection Technology
3. Ecological Research
4. Environmental Monitoring
5. Socioeconomic Environmental Studies
6. Scientific and Technical Assessment Reports (STAR)
7. Interagency Energy-Environment Research and Development
8. "Special" Reports
9. Miscellaneous Reports

This report has been assigned to the INTERAGENCY ENERGY-ENVIRONMENT RESEARCH AND DEVELOPMENT series. Reports in this series result from the effort funded under the 17-agency Federal Energy/Environment Research and Development Program. These studies relate to EPA's mission to protect the public health and welfare from adverse effects of pollutants associated with energy systems. The goal of the Program is to assure the rapid development of domestic energy supplies in an environmentally-compatible manner by providing the necessary environmental data and control technology. Investigations include analyses of the transport of energy-related pollutants and their health and ecological effects; assessments of, and development of, control technologies for energy systems; and integrated assessments of a wide range of energy-related environmental issues.

EPA REVIEW NOTICE

This report has been reviewed by the participating Federal Agencies, and approved for publication. Approval does not signify that the contents necessarily reflect the views and policies of the Government, nor does mention of trade names or commercial products constitute endorsement or recommendation for use.

This document is available to the public through the National Technical Information Service, Springfield, Virginia 22161.

EPA-600/7-80-017d

January 1980

Advanced Combustion Systems for Stationary Gas Turbine Engines: Volume IV. Combustor Verification Testing (Addendum)

by

R.M. Pierce, C.E. Smith,
and B.S. Hinton

Pratt and Whitney Aircraft Group
United Technologies Corporation
P.O. Box 2691
West Palm Beach, Florida 33402

Contract No. 68-02-2136
Program Element No. INE829

EPA Project Officer: W.S. Lanier

Industrial Environmental Research Laboratory
Office of Environmental Engineering and Technology
Research Triangle Park, NC 27711

Prepared for

U.S. ENVIRONMENTAL PROTECTION AGENCY
Office of Research and Development
Washington, DC 20460

FOREWORD

This report was prepared by the Government Products Division of the Pratt & Whitney Aircraft Group (P&WA) of United Technologies Corporation under EPA Contract No. 68-02-2136, "Advanced Combustion Systems for Stationary Gas Turbine Engines." It is Volume IV of the final report which encompasses work associated with the accomplishment of Phase VI of the subject contract from 1 July 1979 through 12 October 1979. The originator's report number is FR-11405.

Contract 68-02-2136 was sponsored by the Industrial Environmental Research Laboratory of the Environmental Protection Agency (EPA), Research Triangle Park, North Carolina under the technical supervision of Mr. W. S. Lanier.

The authors wish to acknowledge the valuable contributions made to this program by Mr. W. S. Lanier, whose skillful management and insight have been a key factor in the success of the Rich Burn/Quick Quench combustor design concept.

The Pratt & Whitney Aircraft Program Manager is Mr. Robert M. Pierce; the Deputy Program Manager is Mr. Clifford E. Smith. Mr. Stanley A. Mosier is Technology Manager for Fuels and Emissions Programs at the Government Products Division of Pratt & Whitney Aircraft Group. Mr. Bruce S. Hinton has been a principal contributor to the technical effort in Phase VI.

Special recognition is due Mr. E. R. Robertson of the Component Design and Integration Group, who was responsible for all drafting, hardware fabrication, and data processing activities.

TABLE OF CONTENTS

Section		*Page*
1	INTRODUCTION	1
2	PHASE VI — ALTERNATIVE FUELS AND HIGH TEMPERATURE RISE OPERATION	2
	2.1 Phase VI Combustor Designs	2
	2.2 Experimental Rig Hardware and Test Stand Preparation	29
	2.3 Alternative Fuels Testing	31
	2.4 High Temperature Rise Operation	71
3	PROGRAM CONCLUSIONS	84
4	RECOMMENDATIONS	87
	REFERENCES	88
	LIST OF SYMBOLS	89
	APPENDIX A	91
	APPENDIX B	

LIST OF ILLUSTRATIONS

Figure		*Page*
1	Comparison of FRT Combustors Used in Phase IV and Phase VI	3
2	Predicted Variation in Liner Heat Fluxes With Wall Temperature	6
3	Predicted Variation in Liner Heat Fluxes With Wall Temperature	7
4	Baseline Premix Tube	9
5	Inlet Swirler Premixing Tube	9
6	Nonpremixed Arrangement	9
7	Approximate Variation in Specific Gravity With Temperature for Test Fuels	12
8	Approximate Viscosity-Temperature Relationship for Test Fuels	13
9	Surface-Tension-Temperature Relationship for Hydrocarbon Fuels of Varying Specific Gravities	14
10	Predicted Variation in SMD With Fuel Temperature for Shale Residual Oil	16
11	Predicted Variation in SMD With Fuel Temperature for Indonesian/Malaysian Oil	17
12	Full-Scale Combustor Scheme FS-05A (Scheme FS-05B With Premix Tube Variable Damper Removed)	20
13	Nonpremixed Configuration of the FRT/RBQQ Combustor (Scheme FS07A)	21
14	High Temperature Rise Configuration of the FRT/RBQQ Combustor (Scheme FS-08A)	21
15	Burner Scheme Definition (Scheme FS-05B)	22
16	Burner Scheme Definition (Scheme FS-07A)	23
17	Burner Scheme Definition (Scheme FS-08A)	24
18	FRT Combustor (Scheme FS-05A) During Assembly	26
19	FRT Combustor (Scheme FS-05A) Fully Assembled	27
20	Premix Tube With Variable Damper Attached Prior to Final Assembly	28
21	MEL Data System and Emission Equipment	30
22	Schematic Diagram of Smoke Meter	32

LIST OF ILLUSTRATIONS (Continued)

Figure		*Page*
23	Comparison of Variation in NO_x Concentration With Overall Equivalence Ratio for Schemes FS-05A, FS-05B and FS-03A	34
24	Comparison of Variation in CO Concentration With Overall Equivalence Ratio for Schemes FS-05A, FS-05B, and FS-03A	36
25	Comparison of Variation in NO_x Concentration With Overall Euivalence Ratio for Schemes FS-05B, FS-03A, FS-04A, and FS-04B	
26	Comparison of Variation in CO Concentration With Overall Equivalence Ratio for Schemes FS-05B, FS-03A, and FS-04B	39
27	Variation in Emission Concentrations With Overall Equivalence Ratio for Scheme FS-05B Using SRC II Middle Distilate Fuel	41
28	Condition of Premix Tube Swirler and Premixing Passage Following Tests With SRC II Middle Distillate Fuel	42
29	Emission Signature of Scheme FS-05B Firing Shale Residual	43
30	Emission Signature of Scheme FS-05B Firing Indonesian/Malaysian Residual	44
31	Condition of Premix Tube Swirler and Premixing Passage Following Tests With the Residual Fuels	46
32	Emission Signature of Scheme FS-07A Firing No. 2 Fuel	48
33	Effect of Boost Air Pressure Ratio (BAPR) on NO_x and CO Emissions of Scheme FS-07A	49
34	Emission Signature of Scheme FS-07A Firing Indonesian/Malaysian Residual	50
35	Emission Signature of Scheme FS-07A Firing SRC II Middle Distillate	51
36	Condition of Interior Surface of Primary Liner Following Tests Through Scheme FS-07A	53
37	Condition of Nonpremixed Fuel Preparation Following Tests With Residual and SRC II Fuels	54
38	Exit Temperature Profiles (Probe at Mid-Span)	56
39	Exit Temperature Profile (Probe at Mid-Span)	57
40	Exit Temperature Profiles (Probe at Mid-Span)	58
41	Exit Temperature Profiles (Probe at Mid-Span)	59

LIST OF ILLUSTRATIONS (Continued)

Figure		Page
42	Exit Temperature Profiles (Probe at Mid-Span)	60
43	Exit Temprature Profile of Scheme FS-05B Firing Shale Residual (Probe Off Midspan)	61
44	Variation in Temperature Pattern Factor With Overall Equivalence Ratio for Tests Conducted With Schemes FS-05A and FS-05B	62
45	Liner Temperature Rise Factor as a Function of Equivalence Ratio at 50 psia Firing No. 2 Fuel	65
46	Liner Temperature Rise Factor as a Function of Equivalence Ratio at 100 psia	66
47	Effect of Equivalence Ratio and Fuel Type on Secondary Zone Liner Temperature Rise Factor for Scheme FS-05B	67
48	Effect of Equivalence Ratio and Fuel Type on Secondary Zone Liner Temperature Rise Factor for Scheme FS-07A at 100 psia	67
49	Primary Liner Convective Heat Transfer Balance	69
50	Variation in Heat Removed from the Primary Zone Liner by the Convective Cooling Airflow With Equivalence Ratio for Scheme FS-05B Firing Various Test Fuels	70
51	Variation in Heat Removed from the Primary Zone Liner by the Convective Cooling Airflow With Equivalence Ratio for Scheme FS-07A Firing Various Test Fuels	71
52	Emission Signature for Scheme FS-08A Firing No. 2 Fuel	72
53	Emission Signature of Scheme FS-08A Firing No. 2 Fuel at High (Vitiated) Inlet Conditions	74
54	Emissions from Scheme FS-08A Firing No. 2 Fuel at 50 psia and 800°F	76
55	Condition of the Interior Surface of the Primary Liner at the Conclusion of the Test Program (Aft Looking Forward)	77
56	Condition of the Secondary Zone Liner Following Tests of Scheme FS-08A	78
57	Condition of the Nonpremixed Fuel Preparation Device After Operation of Scheme FS-8A on No. 2 Distilate Fuel	79
58	Effects of Equivalence Ratio, Pressure, Temperature and Humidity on Secondary Zone Liner Temperature Rise Factor Firing No. 2 Fuel in Scheme FS-08A	81

LIST OF ILLUSTRATIONS (Continued)

Figure		*Page*
59	Variation in Heat Removed from the Primary Zone Liner by the Convective Cooling Airflow With Equivalence Rati for Scheme FS-08A Firing No. 2 Fuel at Various Rig Inlet Conditions	81
60	Primary Zone Liner Postrun Thermal Paint Analysis	83

LIST OF TABLES

Table		*Page*
I	Characterization of Fuel Preparation Devices Used in SMD Determination	10
II	Comparison of Fuel Properties for Phase VI Test Fuels	11
III	Predicted Values of SMD	15
IV	Summary of Combustor Design Features	25
V	Combustor Operating Conditions in a Typical 25 Megawatt Engine With Free Turbine	33
Appendix A		
I	Combustor Operating Parameter Data	91
II	Emission Concentration Data	93
III	Gas Analysis Parameter Data	95
IV	Combustor Liner Temperature Data	97
V	Performance Parameter Data	101
VI	Combustor Liner Heat Transfer Data	103
VII	Combustor Exit Temperature Data	105

SUMMARY

This report describes an exploratory development program to identify, evaluate, and demonstrate dry techniques for significantly reducing production of NO_x from thermal and fuel-bound sources in burners of stationary gas turbine engines.

In the original program, the Rich Burn/Quick Quench combustor concept, which was identified and evaluated in subscale hardware, was implemented into the design of a full-scale (25 megawatt engine size) gas turbine combustor. Two configurations of the full-scale prototype combustor were designed and constructed. The first provided a primary zone residence time about half as great as that utilized in the bench-scale combustor, but greater than that available in the representative 25 megawatt engine, which had on-board (in-line) burner cans. The second configuration was shorter in length, meeting the basic envelope requirements of the represen-tative engine. Tests of the two configurations were conducted to verify proper implementation of the design concept, and to demonstrate the exhaust emission characteristics attainable in the full-scale design.

Results of this testing showed that the Rich Burn/Quick Quench concept substantially reduced NO_x exhaust emissions for both nitrogenous and non-nitrogenous petroleum distillate fuels. All program exhaust emission goals were met. Having demonstrated effective control of NO_x formed due to fuel-bound nitrogen (which may be present in coal-derived and shale derived feedstocks), it was reasoned that operation of the existing prototype combustor on heavy fuels might also show substantial reductions.

This was the purpose of the additional program effort described herein. A modified version of the longer residence time configuration was successfully tested while burning synthetic liquid and residual fuel oils, demonstrating that the Rich Burn/Quick Quench concept could substantially reduce NO_x formation when these heavy fuels were fired. All exhaust emissions goals of the program were met while burning three test fuels: a middle cut distillate solvent refined coal; a residual shale oil; and an Indonesian/Malaysian residual oil. It was also demonstrated that the exhaust emission goals were met when operating a Rich Burn/Quick Quench combustor at a high turbine inlet temperature (2600°F design point) firing No. 2 fuel oil.

For the sake of convenience, English units of measurements were used in this report. Conversions to SI units may be found in Appendix B on page 101.

SECTION 1

INTRODUCTION

Gas turbine engines currently in use by the electric utilities and by industry account for a relatively small portion of the total quantity of oxides of nitrogen (NO_x) emitted from stationary sources in this country. On a local scale, however, the gas turbine can be a significant contributor to air quality degradation, especially in the vicinity of engine installations where the NO_x background level is already objectionably high. The impact of stationary gas turbines may become even more significant in the future. Along with the present modes of utilization, combined cycle and industrial cogeneration applications are being projected. In these applications the advanced engine technology needed to provide higher cycle efficiencies, and to accommodate the anticipated firing of coal-derived, shale-derived, and petroleum residual fuels, will make it more difficult to meet proposed emission regulations.

Until recently, gas turbine combustors have been designed without regard for exhaust emissions. Initial attempts to control NO_x by modifying existing designs were generally unsuccessful. Although water injection was identified as a potential solution, this approach is expensive and ineffective when nitrogen-laden fuels must be burned. In light of these findings, it was clear that new design concepts specifically addressing exhaust emissions should be considered.

Under EPA Contract 68-02-2136, an exploratory development program was undertaken to identify, evaluate, and demonstrate alternative combustor design concepts for significantly reducing the production of NO_x in stationary gas turbine engines. The investigations were directed toward dry combustion control techniques suitable for use in a 25 megawatt (nominal) engine. Program goals were 50 ppmv NO_x (at 15% O_2) for non-nitrogenous fuels, and 100 ppmv NO_x (at 15% O_2) for fuels containing 0.5% nitrogen by weight. The goal for CO was 100 ppmv (at 15% O_2).

The original program was accomplished in four phases. The first phase consisted of an analytical investigation of combustion concepts considered to have potential for reducing the production of NO_x. In the second phase of work, a number of promising low NO_x production concepts were bench-tested to select the best candidate for implementation into the design of a full-scale, 25-megawatt-size, utility gas turbine engine combustor. In Phase III, a full-scale low NO_x combustor was designed and fabricated. In the fourth phase of work the NO_x reduction capability of the prototype full-scale combustor was demonstrated experimentally at conditions simulating the operating range of a representative 25 megawatt stationary engine.

Phase V of the original program covered the preparation of contract reports. In Phase VI, which is an extension to the original program structure, the Rich Burn/Quick Quench combustor concept was evaluated while burning synthetic and residual fuel oils, and performance under high turbine inlet temperature conditions while burning No. 2 petroleum distillate fuel was documented.

SECTION 2

PHASE VI — ALTERNATIVE FUELS AND HIGH TEMPERATURE RISE OPERATION

In Phase VI, the experimental evaluation of the full-scale Rich Burn/Quick Quench combustor while burning synthetic liquid and residual fuel oils, and while operating in a high temperature rise configuration was accomplished. The three alternative fuels tested were a middle distillate cut solvent refined coal (SRC II), a residual shale oil, and an Indonesian/Malaysian residual oil. This section describes the design modifications to the combustor and fuel preparation devices, the experimental test program, and related results and analysis.

2.1 PHASE VI COMBUSTOR DESIGNS

The purpose of Phase VI testing was to evaluate the Rich Burn/Quick Quench combustor while burning synthetic liquid and residual fuel oils, and to document performance under high turbine inlet temperature conditions. Because two test objectives were being addressed, two combustor airflow distribution schedules (hole-pattern configurations) were required to carry out the evaluation. Also, because of the wide range of properties represented in the three experimental fuels (in comparison to No. 2 distillate), two alternative methods of fuel-air mixture preparation were selected for evaluation in the test program. Drawing upon the experience gained in Phase IV, a revised scheme for the introduction of final dilution airflow was adopted. There were also minor differences in the method of fabrication, consisting primarily of the use of an uncooled cast liner in the aft dilution section of the combustor. A discussion of each of these changes to the configuration of the basic FRT combustor as it had been tested in Phase IV are presented in the following subsections.

2.1.1 Secondary Dilution Airflow and Liner Modifications

The full-scale combustor hardware was restored to the long-length, full-residence time (FRT) configuration tested initially in Phase IV (at the conclusion of testing in Phase IV the hardware had been in the short-length, ECV configuration). Drawing upon the experience gained in Phase IV, an alternative placement of final dilution air holes (axially directed, in the wall of the dump section, rather than radially directed in the wall of the final dilution liner) was also adopted (see Figure 1). This placement, which had been utilized in the ECV combustor in Phase IV, had produced an incremental reduction in thermal NO_x of about 10 ppmv (at 15% O_2). The reduction is illustrated in Figure 106 of Reference 1. In providing for conversion of the hardware to the high temperature rise configuration, the axially directed dilution air holes were covered by a removable metal band. This band also served to cover access ports in the outer shroud leading to the quick quench section. The use of a removable band was a simple modification that allowed a quick and easy change to the high temperature rise configuration without removing the combustor from the test stand.

The aft dilution section, which had been constructed of sheet metal and had employed conventional louver film cooling in scheme FS-03A (the FRT configuration evaluated in Phase IV), was replaced by an uncooled cast liner piece (similar in construction to the primary zone liner) for Phase VI testing. Elimination of the requirement for secondary cooling airflow in this manner made it possible to maintain an identical front-section configuration (down to and including the quick-quench section) in both the baseline and high temperature rise configurations. By maintaining identical front-sections, the same primary zone residence time characteristics could be maintained, allowing a more direct comparison of emission results between the two configurations.

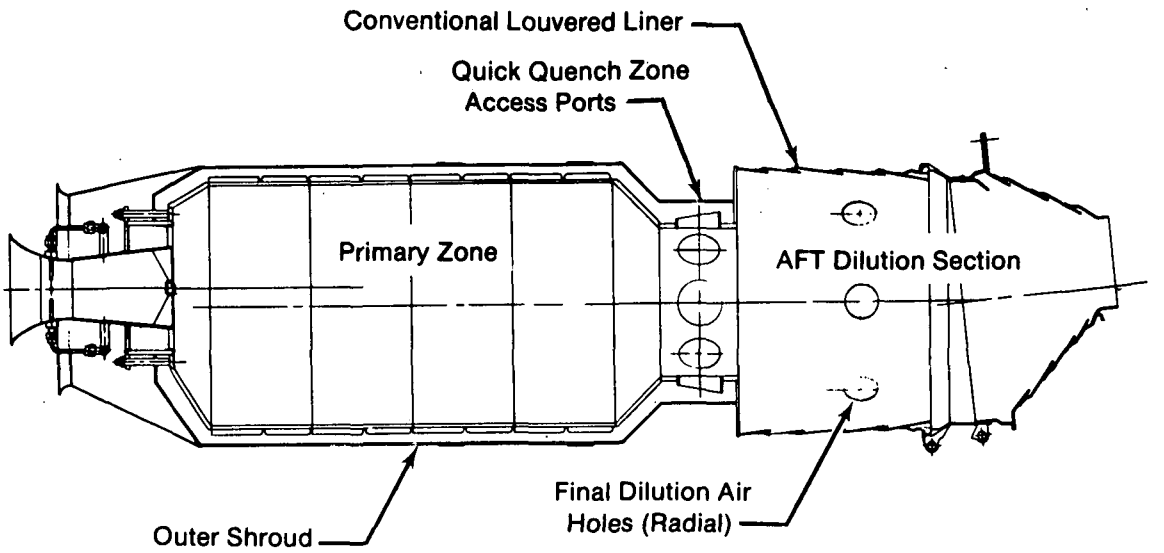

Phase IV Configuration

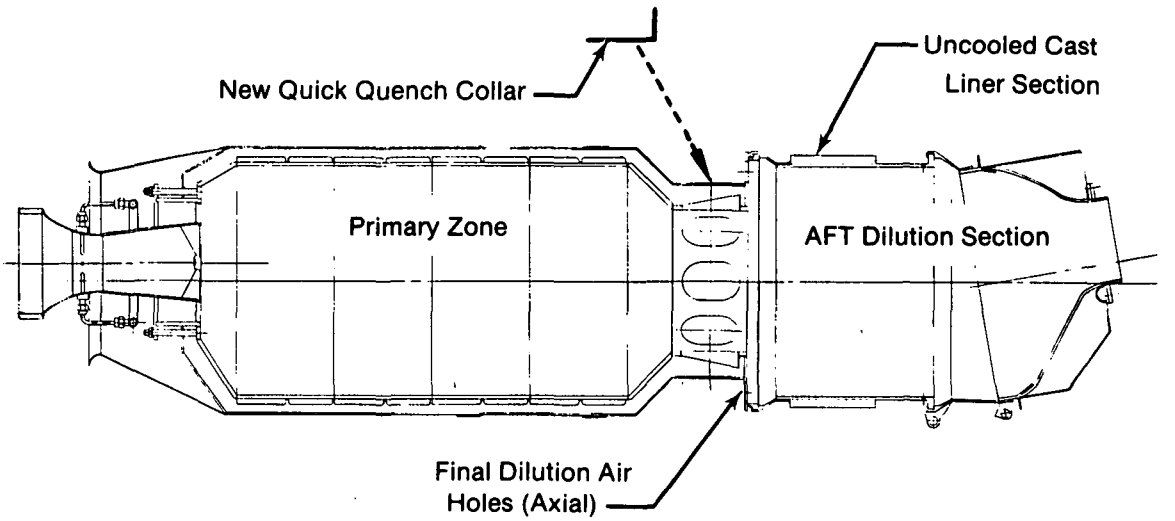

Phase VI Configuration

Figure 1. Comparison of FRT Combustors Used in Phase IV and Phase VI

While the use of an uncooled liner in the aft section of the combustor in Phase VI testing allowed identical operation of the front-section of the combustor, the absence of cooling air caused initial concern regarding the integrity of this aft liner. The axially directed final dilution air jets, which comprise roughly 37% of the total combustor airflow, serve to cool the aft section by forming a thick layer of cool air along the interior surface of the liner. In the high temperature rise configuration (where these dilution holes are blocked), the aft section liner was left uncooled except for radiation to the rig case and slight convection from recirculating airflow. Preliminary calculations were performed to determine whether an uncooled liner could survive during the operation of the high temperature rise configuration of the combustor at the 2600°F exit temperature maximum rig condition.

The analysis of the uncooled aft-section liner was conducted in the manner specified in reference 2, utilizing the following equation, which treats convection and radiation on both the inside and outside surfaces of the liner.

$$C_1 + R_1 = C_2 + R_2 \tag{1}$$

where:

$$C_1 = 0.017 \frac{K}{\mu 0.8} \left(\frac{m_x}{A}\right)_f^{0.8} \left(\frac{1}{d_{n_f}}\right)^{0.2} (T_f - T_w)$$

$$R_1 = \sigma \left(\frac{1 + \alpha_w}{2}\right) \epsilon_f T_f^{1.5} \left(T_f^{2.5} - T_w^{2.5}\right)$$

$$C_2 = 0.020 \frac{ka}{a^{0.8}} \left(\frac{m_x}{A}\right)_a^{0.8} \left(\frac{1}{d_{h_a}}\right)^{0.2} (T_w - T_a)$$

$$R_2 = \sigma \left(\frac{\epsilon_w \epsilon_c}{\epsilon_c + \epsilon_w (1-\epsilon_c) \frac{dw}{dc}}\right) (T_w^4 - T_c^4)$$

and the following terms are defined in consistent units:

σ	=	Stefan-Boltzmann constant
α	=	absorptivity
ϵ	=	emissivity
T	=	temperature
k	=	thermal conductivity
μ	=	dynamic viscosity
m_x	=	mass flowrate
A	=	cross-sectional area
d_h	=	diameter
C	=	convective heat flux
R	=	radiative heat flux

subscripts:

a	=	air
c	=	rig case
f	=	flame
w	=	combustor wall
1	=	designates transfer from flame to liner
2	=	designates transfer from liner to rig case

Solution of equation 1 is effected by evaluating each of the four major net flux terms as a function of the common independent variable, Tw, and by determining the value of Tw for which the equality is valid. The case for operation of the high temperature rise configuration at 2600°F in the test rig is illustrated in Figure 2. It may seem that the greater heat flux from the flame to the combustor liner is by convection, while radiation accounts for nearly all the heat flux from the liner to the rig case. The predicted wall temperature for this case is 1990°F.

In Figure 3, the results of a second heat transfer calculation are shown, in which operation of the combustor in an engine environment was assumed. This case was included so that the predicted effect of increased operating pressure (212 psia vs 100 psia) and a more confined containment vessel surrounding the combustor (a 5-in. gap between the combustor and case was assumed, compared to 10 in. in the plenum-type rig environment) could be assessed. As shown in Figure 3, the radiative and convective heat fluxes to the combustor liner were both increased, while only the convective heat flux increased from the liner to the surrounding engine case. The predicted wall temperature was 2100°F.

A further reduction in the above predicted temperatures was assumed, on the basis of extensive experience with flamespray coating. The application of magnesium zirconate coating to a combustor liner produces a reduction in wall temperature of approximately 100°F under circumstances of predominantly convective heat transfer (a 50°F reduction is ordinarily achieved in the case of radiative heat flux). Because flamespray coating has been applied to the aft section liner, a further reduction in wall temperatures was assumed. The final predicted values are:

Twall = 1890°F (rig operation)
Twall = 2000°F (engine operation).

These values, although relatively high, approach the oxidation temperature (2000°F) of the cast liner material, but are below the range of temperatures (up to 2100°F for brief periods of time) in which other combustors employing the same construction have been operated. Accordingly, it was decided that the uncooled aft section liner should be incorporated into the design of the full-scale combustor for the rig tests to be conducted in Phase VI. It should be noted that no plans now exist for operation of the hardware at 2600°F exit temperature in an engine environment. Before such tests are undertaken, the aft section of the combustor should be redesigned to provide forced convective cooling in the interest of attaining a lower metal temperature.

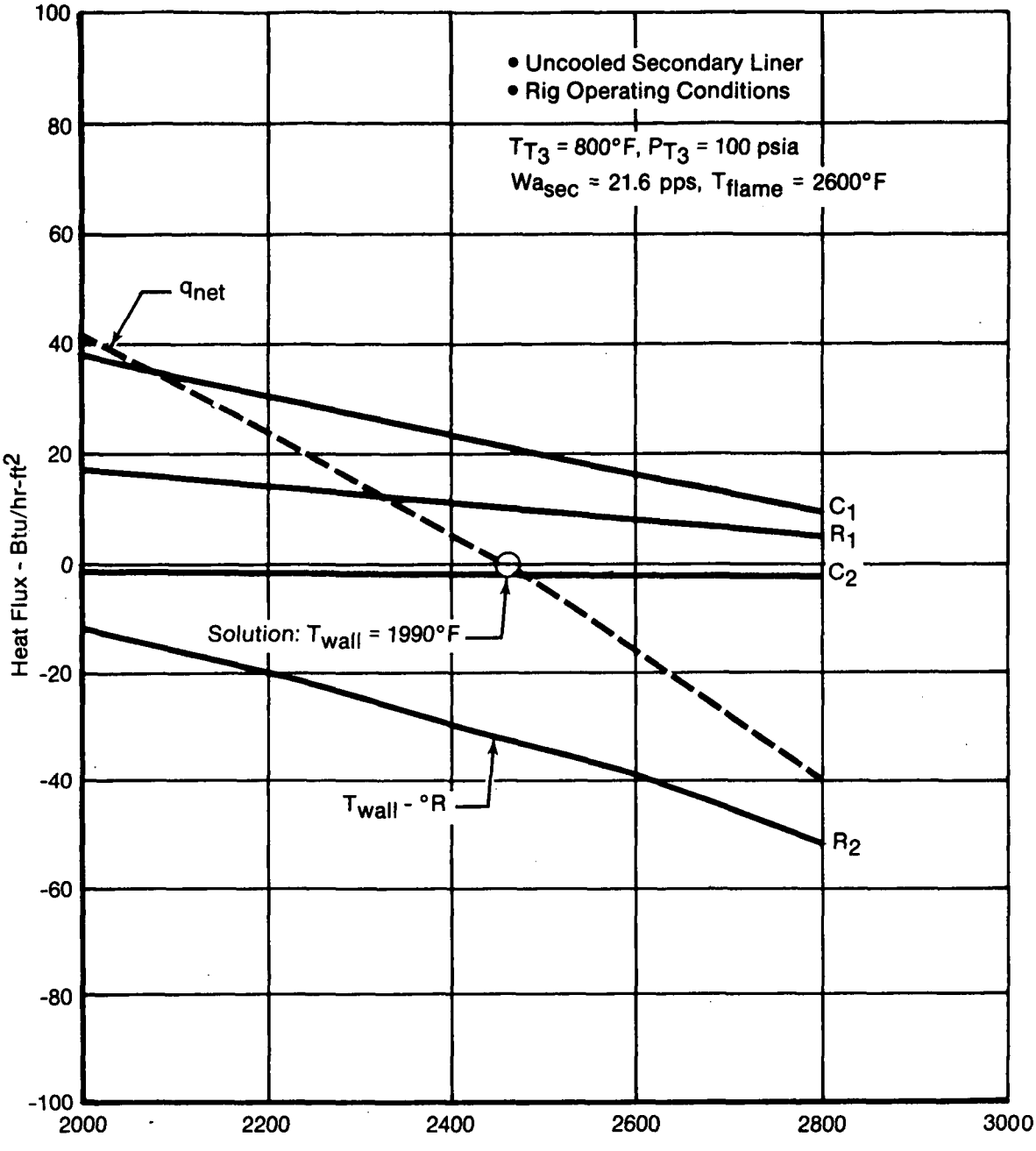

Figure 2. Predicted Variation in Liner Heat Fluxes With Wall Temperature

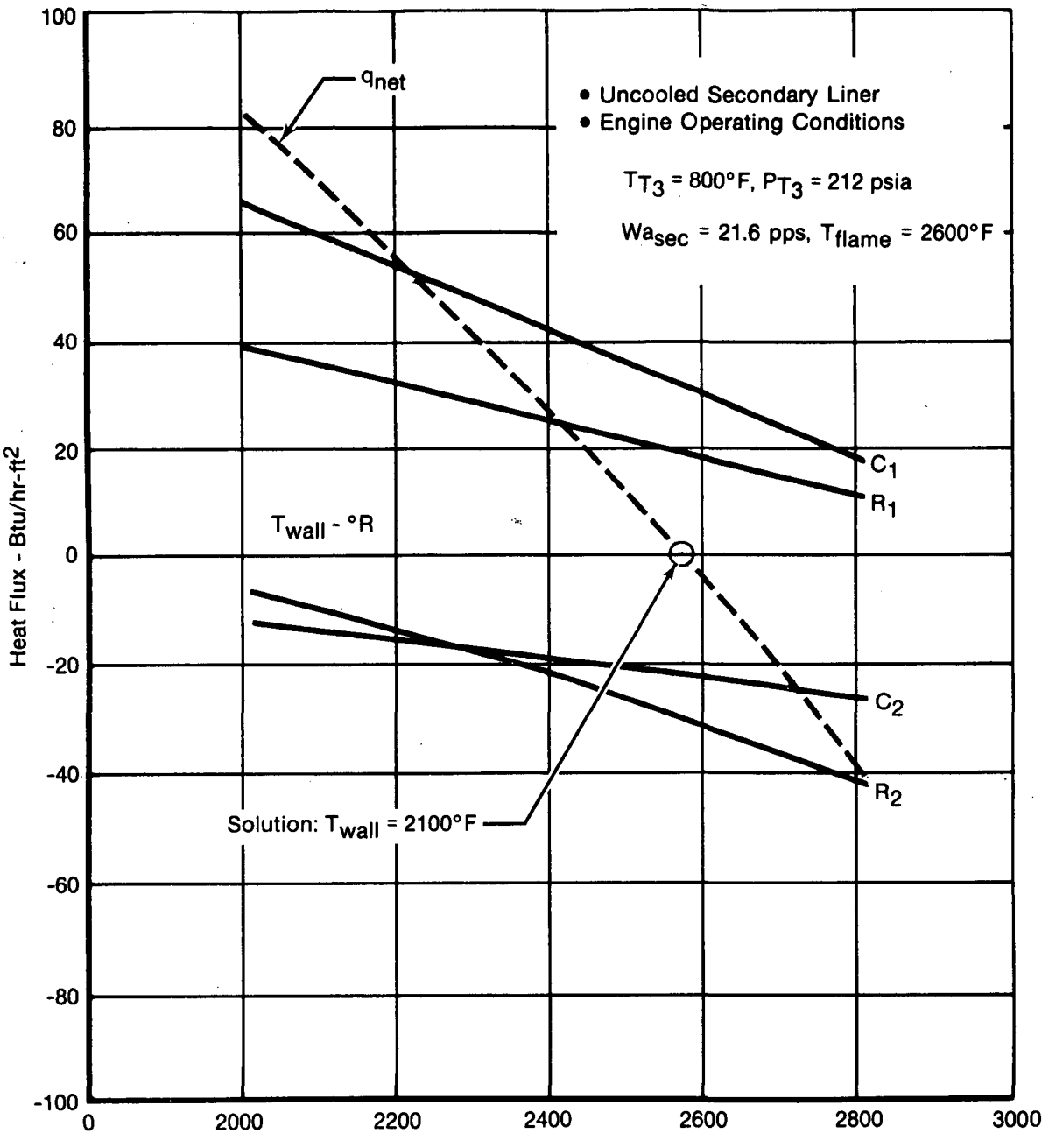

Figure 3. Predicted Variation in Liner Heat Fluxes With Wall Temperature

2.1.2 Fuel Preparation Devices

The fuels that were fired in Phase VI are: a middle distillate cut solvent refined coal (SRC II); a residual shale oil and an Indonesian/Malaysian residual oil. In addition, hardware shakedown tests were conducted initially using No. 2 distillate oil. The wide range of properties represented in the three experimental fuels (in comparison to No. 2 distillate) make it more difficult to achieve a high degree of fuel prevaporization and fuel-air premixing. In particular, variations in viscosity, volatility, and surface tension all affect the atomization and initial burning of fuel. It is possible that the impact of less-than-ideal initial burning conditions on NO_x formation may be eased considerably under the relatively well mixed fuel-rich conditions that prevail in the aft section of the primary zone in the Rich Burn/Quick Quench combustor. In spite of this potential benefit, however, it is desirable to achieve the highest degree of fuel prevaporization and fuel-air premixing possible with available fuel preparation devices. Several classes of fuel injectors, and several fuel-air delivery schemes (including premix tubes, and nonpremixed dome designs) are available and were considered for use in Phase VI testing.

An initial study was conducted to determine the best fuel-preparation device for each experimental fuel. In addition to the premix tube used for distillate fuel in Phase IV, which was eventually used with all three test fuels, consideration was given to air-boost nozzles, to an alternative premix tube having inlet swirl vanes, and to a nonpremixed recessed swirler design. Results of the study are presented in the following paragraphs.

Three specific fuel preparation devices were evaluated: (1) the baseline premix tube with radial "spoke" fuel injectors (Figure 4); (2) the inlet-swirler premix tube in conjunction with an air-boost nozzle (Sonicore Model 281T) shown in Figure 5; and the nonpremixed arrangement shown in Figure 6, consisting of an air-boost nozzle in combination with a recessed swirler.

Predictions of SMD were made using the relationship developed under this program in Phase III and reported in reference 1 for air atomization of liquid fuels.

$$SMD = K(d_f)^{0.375}(\nu_f)^{0.25}\,(\sigma_f)^{0.375}(\rho_f)^{-0.125}(\rho_a)^{-0.5}(V_a)^{-1.0} \qquad (2)$$

where:

ν_f	=	dynamic viscosity of fuel
σ_f	=	surface tension of fuel
ρ_f	=	density of fuel
ρ_a	=	density of air
V_a	=	velocity of air (relative to fuel)
d_f	=	characteristic initial dimension of fuel (diameter, thickness, etc.)
K	=	proportionality constant, dependent on Wa/Wf, the atomizer airflow to fuel flow mass ratio.

Application of equation 2 to predict values of SMD requires that a characteristic initial dimension d_f, and a proportionality constant K be assigned for each fuel injection device, and that the required fuel properties be specified. Data reported in reference 3 indicates that the characteristics of plain-jet air atomizing devices are essentially independent of fuel jet diameter. For large values of the atomizer air-fuel ratio Wa/Wf, reasonable agreement with the experimental data in reference 3 can be obtained by combining the terms K and d_f into a single constant:

$$K\,(d_f)^{0.375} = 0.312\ \text{ft}^{\,0.375}$$

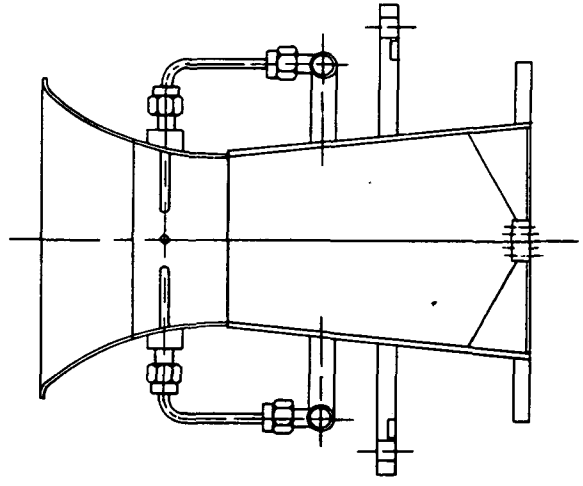

Figure 4. Baseline Premix Tube

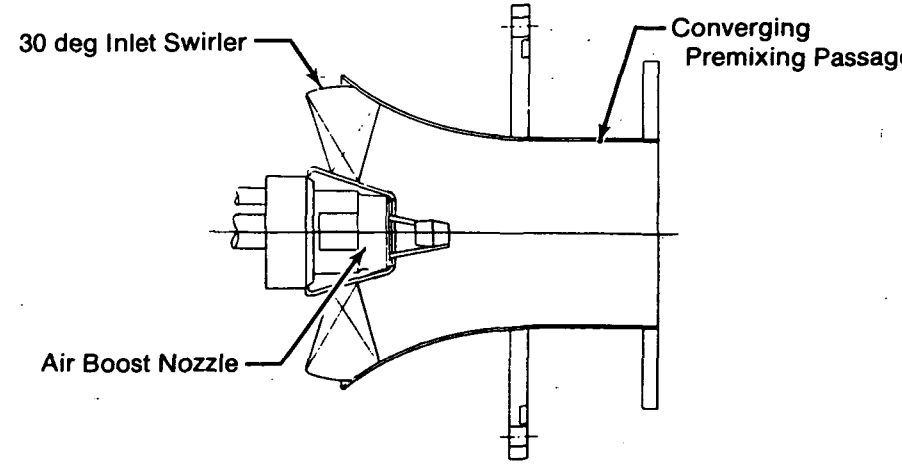

Figure 5. Inlet Swirler Premixing Tube

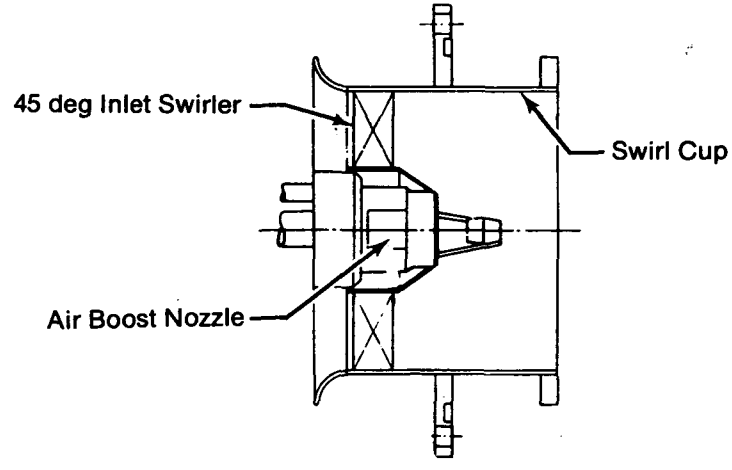

Figure 6. Nonpremixed Arrangement

The component K of this combined-term constant does however vary with atomizer air-fuel ratio in a manner approximated by the following additional term given in reference 3:

$$\left(\frac{1 + \frac{W_A}{W_F}}{\frac{W_A}{W_F}}\right) \quad 1.7$$

In Table I values of the above terms for the three candidate fuel preparation devices (each of which is plain-jet design) are presented. The fuel properties required for use in equation 2 are presented in Table II, along with other important fuel characteristics. Comparisons of the variation in viscosity, specific gravity, and surface tension with fuel temperature for the test fuels are presented in Figures 7, 8, and 9. These curves are based on a limited number of actual data points and were drawn with characteristic slopes for hydrocarbon fuels obtained from reference 4.

TABLE I
CHARACTERIZATION OF FUEL PREPARATION DEVICES USED IN SMD DETERMINATION

Device	$K(d_j)^{0.375}$	Wa/Wf^1	$(K(d_j)^{0.375})$*corrected*
Baseline Premix Tube *(Figure 8)*	0.312 ft.$^{0.375}$	11.3	0.360 ft.$^{0.375}$
Inlet Swirler[2] Premix Tube (Figure 9)	0.312 ft.$^{0.375}$	0.9[3]	1.111 ft.$^{0.375}$
Nonpremixed[2] Arrangement (Figure 10)	0.312 ft.$^{0.375}$	0.9[3]	1.111 ft.$^{0.375}$

NOTES:
[1]Evaluated at maximum fuel setting
[2]These two devices use the same air boost nozzle, Sonicore Model 281 T
[3]Choked nozzle air orifice assumed

TABLE II
COMPARISON OF FUEL PROPERTIES FOR PHASE VI TEST FUELS

	No. 2 (Typical)	*SRC II Middle Distillate*	*Indonesian/ Malaysian Resid*	*Shale Resid*
Specific Gravity	0.84 (60°F)	0.97 (60°F)	0.87 (210°F)	0.82 (210°F)
Viscosity, centistokes	5.0 (60°F)	6.3 (60°F)	11.6 (210°F)	3.3 (210°F)
Surface Tension dynes/cm	25.7 (60°F)	33.3 (60°F)	22.6[2] (210°F)	20.6[2] (210°F)
Heat of Combustion (net) Btu/lbm	18,700	17,235	17,980	18,190
Pour Point °F	<5	<−45	61	90 (remains waxy)
Flash Point °F	>130	>160	210	235
Ultimate Analysis				
Carbon %	87.0	85.77	86.53	86.71
Hydrogen %	12.8	9.20	11.93	12.76
Nitrogen %	<0.02	0.95	0.24	0.46
Sulfur %	0.04-0.48	0.19	0.22	0.03
Ash %	<0.003	0.001	0.036	0.009
Oxygen %	<0.09	3.89	—	0.03
Conradson Carbon, Residue %	<0.30	0.03	3.98	0.19
End Point °F, Atmos. Distillation	640	541	NA	700

NOTES:
[1]Fuel properties are given at stand delivery temperatures to be maintained in test program.
[2]Estimate on basis of fuel specific gravity.

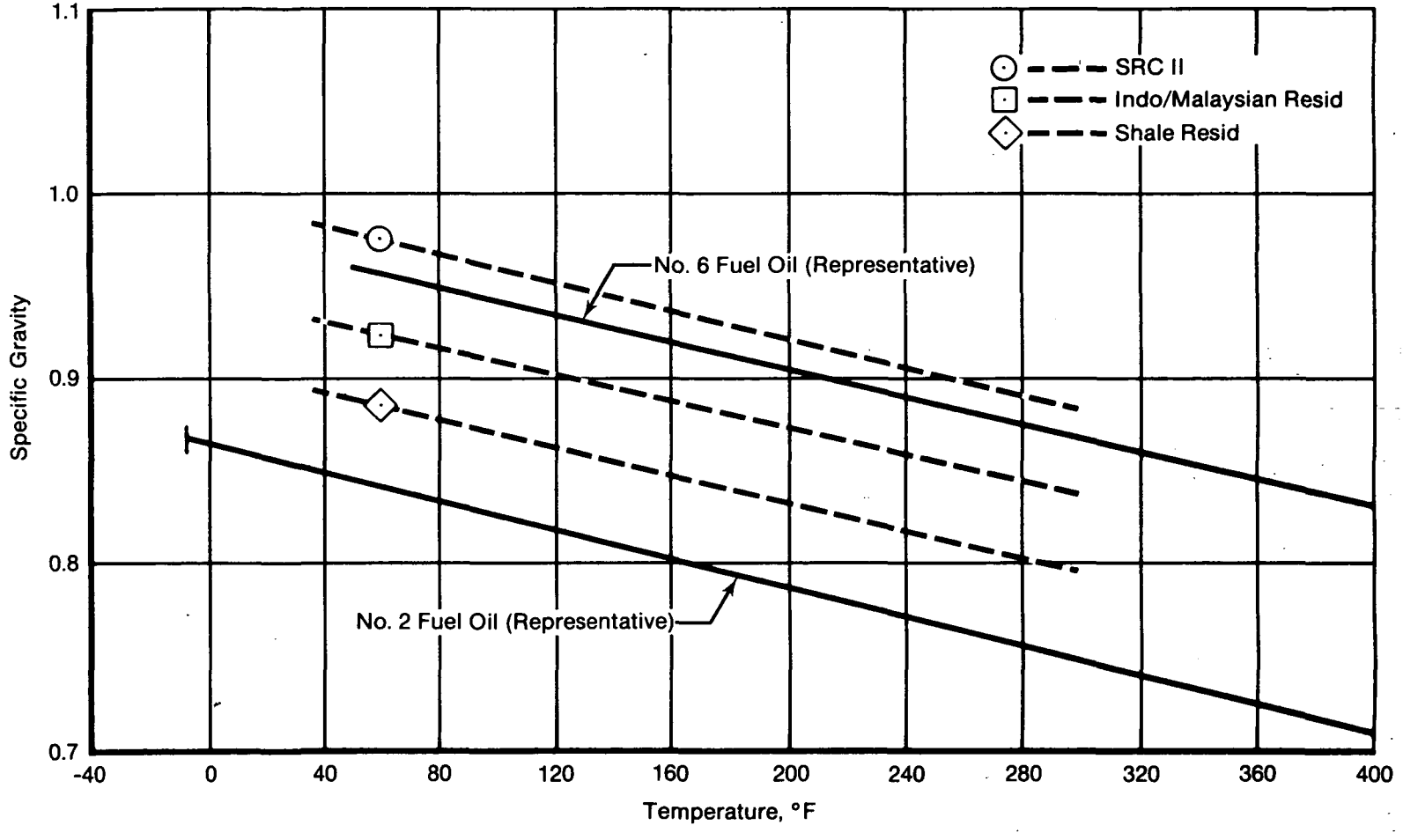

Figure 7. Approximate Variation in Specific Gravity With Temperature for Test Fuels

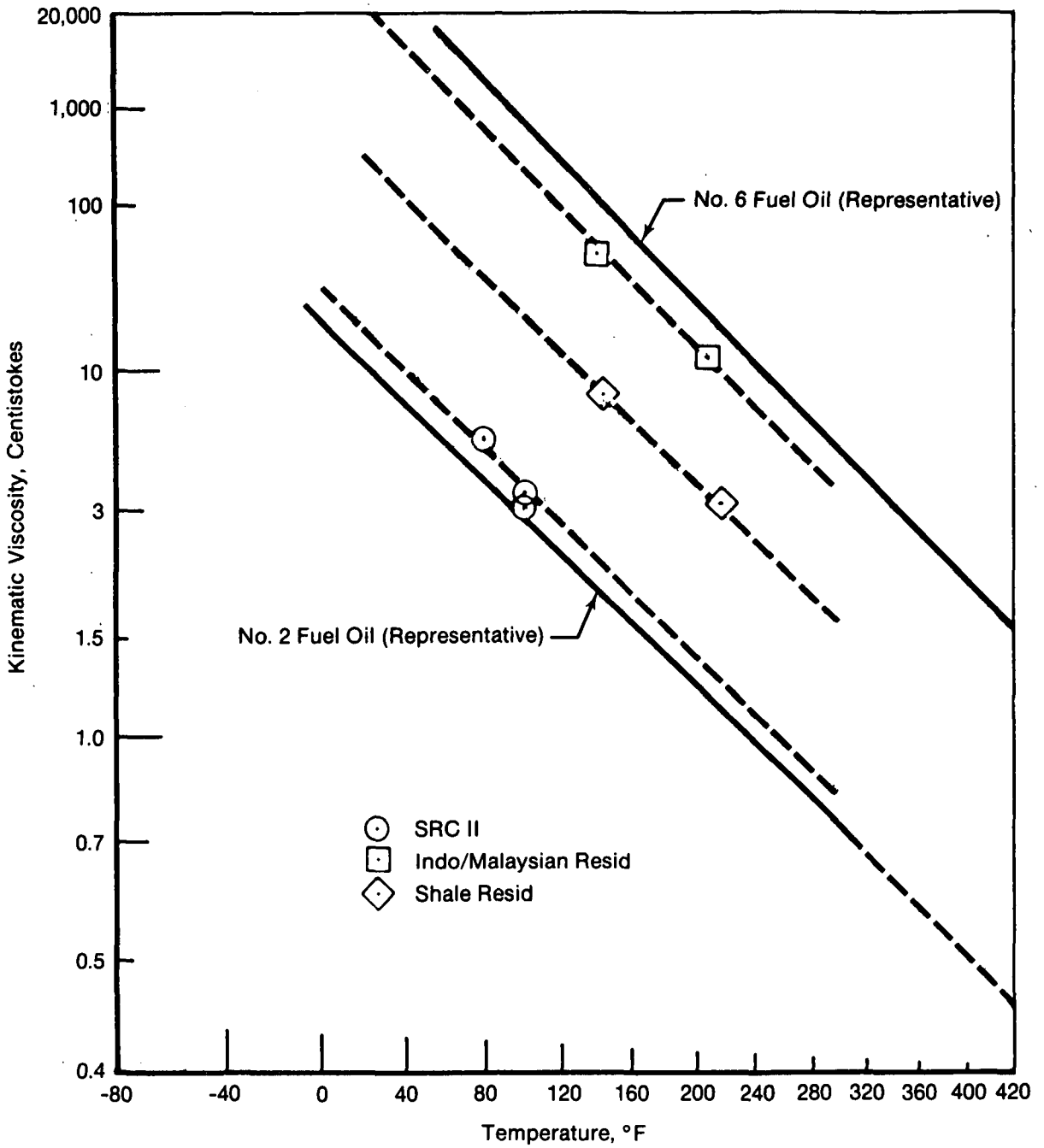

Figure 8. Approximate Viscosity-Temperature Relationship for Test Fuels

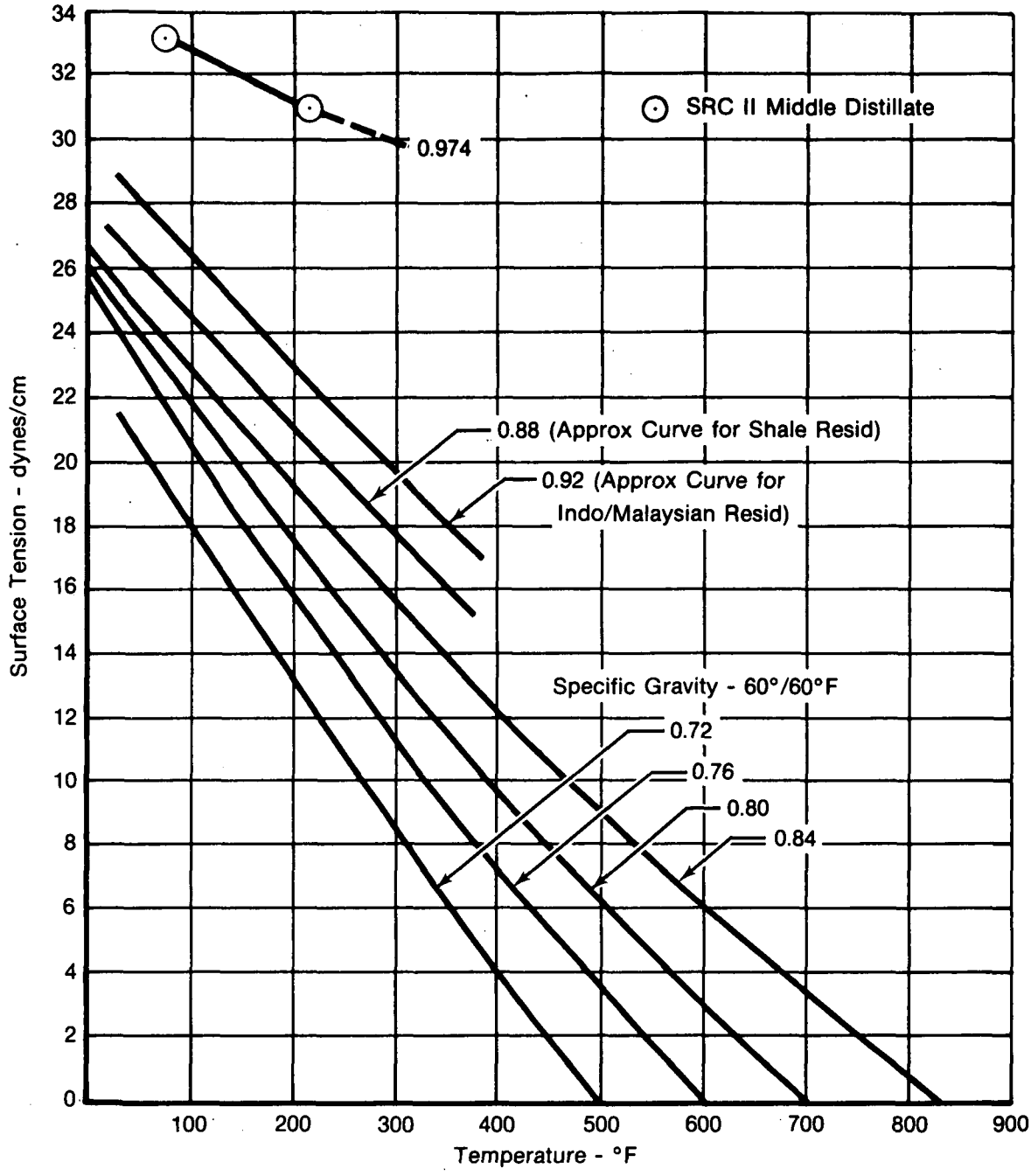

Figure 9. Surface-Tension-Temperature Relationship for Hydrocarbon Fuels of Varying Specific Gravities

Atomization calculations were performed for the baseline premix tube and for the air-boost nozzle (Sonicore Model 281T) used in both the inlet-swirler premix tube and the nonpremixed arrangement, for the four test fuels. The results are presented in Table III. Values of SMD predicted for the baseline premix tube are comparable to those obtained for the air-boost nozzle at maximum rig operating conditions. The predicted variation in SMD with fuel type is also small if it is assumed that the two residual fuels are heated to 210°F. Computations performed for rig idle operating conditions indicate a moderate increase in SMD due to lower air density and, in the case of the baseline premix tube due to reduced air velocity. This effect can be offset in the case of the air-boost nozzle by increasing boost air pressure. A further illustration of the effect of fuel temperature on predicted values of SMD is presented in Figures 10 and 11 for the two residual fuels. The deterioration in SMD at lower fuel temperatures (which is modest) can be offset, if desired, by increasing boost-air pressure in the case of the Sonicore nozzle. The computations indicate that ultrafine atomization (~10 μ) may be possible at 4 to 1 boost air pressure ratio.

TABLE III
PREDICTED VALUES OF SMD

			Rig Conditions			*Primary*	*Boost Air*	
Device	*Fuel*	T_{fuel}	ρ_{T3}	T_{T3}	W_F	*Air Setting*	*Pressure*	*SMD*
Baseline Premix Tube (Figure 8)	No. 2	60°F	94 psia	800°F	1050 pph	Max.	—	26.8
	SRC II	60°F	94 psia	800°F	1050 pph	Max.	—	31.8
	Indo/Malaysian Resid.	150°F	94 psia	800°F	1050 pph	Max.	—	45.4
	Indo/Malaysian Resid.	210°F	94 psia	800°F	1050 pph	Max.	—	31.7
	Shale Resid.	150°F	94 psia	800°F	1050 pph	Max.	—	31.1
	Shale Resid.	210°F	94 psia	800°F	1050 pph	Max.	—	24.6
	No. 2	60°F	40 psia	285°F	258 pph	Idle	—	63.8
	SRC II	60°F	40 psia	285°F	258 pph	Idle	—	75.7
	Indo/Malaysian Resid.	150°F	40 psia	285°F	258 pph	Idle	—	108.4
	Shale Resid.	150°F	40 psia	285°F	258 pph	Idle	—	74.2
Sonicore[1] Model 281T	No. 2	60°F	94 psia	800°F	1050 pph	Max.	200 psia	20.2
	SRC II	60°F	94 psia	800°F	1050 pph	Max.	200 psia	24.0
	Indo/Malaysian Resid.	150°F	94 psia	800°F	1050 pph	Max.	200 psia	34.4
	Shale Resid.	150°F	94 psia	800°F	1050 pph	Max.	200 psia	23.5
	No. 2	60°F	94 psia	800°F	1050 pph	Max.	400 psia	8.4
	SRC II	60°F	94 psia	800°F	1050 pph	Max.	400 psia	10.0
	Indo/Malaysian Resid.	150°F	94 psia	800°F	1050 pph	Max.	400 psia	14.4
	Shale Resid.	150°F	94 psia	800°F	1050 pph	Max.	400 psia	9.9
	No. 2	60°F	40 psia	285°F	258 pph	Idle	80 psia	31.9
	SRC II	60°F	40 psia	285°F	258 pph	Idle	80 psia	38.0
	Indo/Malaysian Resid.	150°F	40 psia	285°F	258 pph	Idle	80 psia	54.4
	Shale Resid.	150°F	40 psia	285°F	258 pph	Idle	80 psia	37.2

[1]Common to Inlet Swirler Premix Tube (Figure 9) and Non-Premix Arrangement (Figure 10).

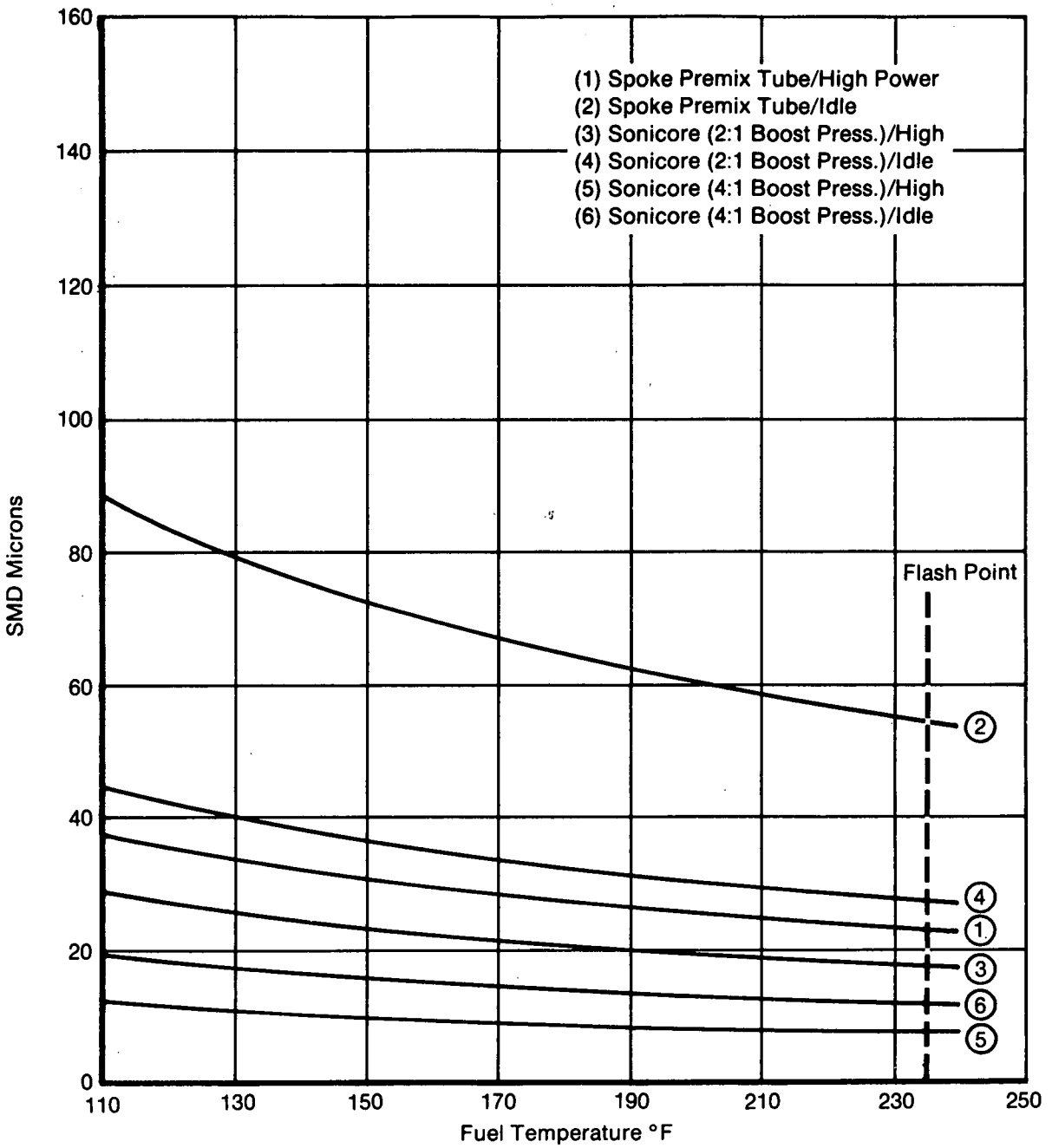

Figure 10. Predicted Variation in SMD With Fuel Temperature for Shale Residual Oil

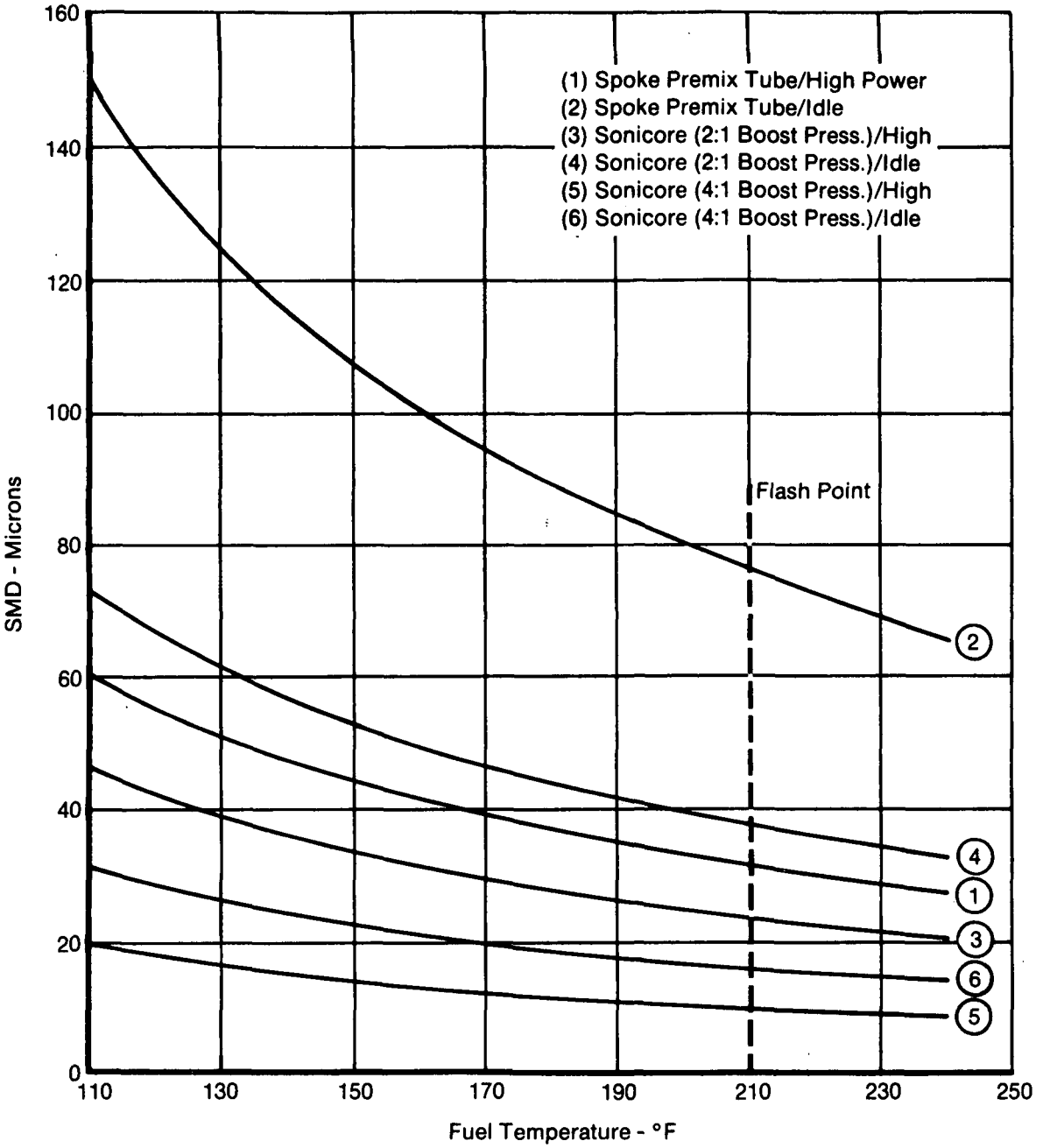

Figure 11. Predicted Variation in SMD With Fuel Temperature for Indonesian/Malaysian Oil

The results described indicate that all four test fuels can be successfully atomized using the baseline premix tube, subject only to the qualification that the two residual fuels be heated to a nominal temperature of 210°F. Atomization produced by the baseline premix tube is almost as good as that achievable using the air-boost nozzle. The air-boost nozzle can provide a means of offsetting the deterioration in SMD encountered at the idle operating point and at reduced fuel temperatures in the case of the residual fuels. The calculations also indicate that ultrafine atomization can be achieved at very high boost air pressure.

Not only the atomization of the fuel, but also the distribution (in an even pattern across the passage into which it is injected) must be provided in an acceptable fuel preparation device. Comparison of the distribution characteristics of the three candidate devices can be made in a qualitative manner by drawing upon prior operating experience. The baseline premix tube can be characterized as having excellent distribution characteristics on the basis of observations made during the Phase IV test program. Atmospheric tests of the nonpremixed, recessed swirler arrangement (Figure 6) conducted in a previous experimental program at P&WA showed a generally good distribution. A uniform, "misty" flame was observed, without streaks. However, a moderate ring of carbon was formed around the inside of the swirl cap, apparently because of the centrifugal effect of swirler airflow on the low-momentum fuel mist produced by the Sonicore nozzle. These results were indicative of moderate wall wetting; however, on balance the distribution was considered good. No tests have been conducted of the inlet swirler premix tube. This device can be expected to be similar to the recessed swirler with regard to wall-wetting tendency, although the longer length of the passage wall may amplify these effects. Aside from the likely wall-wetting tendency, distribution characteristics of this device are unknown.

The tendency to form solid carbon deposits on internal surfaces and exposed parts in the fuel-air passage is accentuated in the case of residual fuels. Even though these fuels may be well atomized and evenly distributed in the primary air flowstream, heavier hydrocarbon compounds are present that do not readily vaporize. These heavier liquids may accumulate on surfaces contacted by the flowstream. In the presence of sufficient heat (due to flame radiation or conduction through the metal surface) pyrolysis can occur before the liquid is vaporized or removed from the surfaces aerodynamically. The tendency to form deposits will be greatest for the two residual fuels. Experience with the baseline premix tube firing a shale DFM was gained during the Phase IV test program. This distillate fuel had been contaminated with heavy earth waxes that were acquired at the refinery when processed fuel was placed in tanks originally used for the crude shale. When this fuel was fired, deposits were formed on the swirler as shown in Figures 87 and 88 in Reference 1. Because the same heavy earth waxes are present in great quantities in the shale resid fuel that was tested in Phase VI, it was expected that heavier deposits might be formed on the baseline premix tube swirler. The same tendency was expected in the case of the Indonesian/Malaysian resid because of the relatively high carbon residue present in this fuel (3.98% Conradson, Table II). Experience gained in a previous experimental program conducted at P&WA to evaluate combustors designed to fire a high-carbon petroleum residual fuel (12% Ramsbottom carbon residue) showed that in general an aerodynamically clean flowpath was required to avoid carbon buildup. In particular, it was concluded that swirlers and other flameholding devices should be removed from the flowpath downstream of the point of fuel injection. These results led to the design of inlet-swirler type configurations such as those shown in Figures 5 and 6.

Two of the three fuel preparation devices just described were used in Phase VI testing; the baseline premix tube, and the nonpremixed, recessed swirler arrangement with the Sonicore air-boost nozzle. Both of these fuel preparation devices produced excellent NO_x emission results and were found to operate in an acceptable manner on all the test fuels. A further description of the emission results, operating characteristics, carbon forming tendencies and conclusions drawn, may be found in Sections 2.3 and 2.4.

2.1.3 Combustor Hardware

The full-scale Rich Burn/Quick Quench combustor was reconstructed to the FRT configuration previously tested in Phase IV. The changes mentioned in the above subsections were incorporated. The initial Phase VI combustor configuration, depicted in Figure 12, is referred to as scheme FS-05A. This configuration employed the baseline premix tube with the variable damper mechanism (described previously in Reference 1) attached for the purpose of staging the quantity of airflow admitted into the primary combustion zone. During the initial checkout tests, the variable damper mechanism became detached from the inlet of the premix tube and it was not reattached. With this occurrence, the airflow distribution was altered slightly and therefore the configuration, absent of the damper, was redefined as scheme FS-05B.

The nonpremixed fuel preparation device (recessed swirler with boost-air nozzle) was also tested in Phase VI. This configuration, shown in Figure 13, is referred to as scheme FS-07A. With the addition of the modified quench zone access port collar, scheme FS-08A, the high temperature rise (2600°F exit temperature design point) configuration was formed. This configuration, which also used the nonpremixed fuel preparation device, can be seen in Figure 14. The modified collar effectively blocked the final dilution air holes which implied that in order to maintain residence times comparable to the other schemes, a reduced airflow was required. A scheme definition sheet for each of the three schemes are presented in Figures 15, 16, and 17. Flow distribution schedules and thermocouple locations are given in these figures.

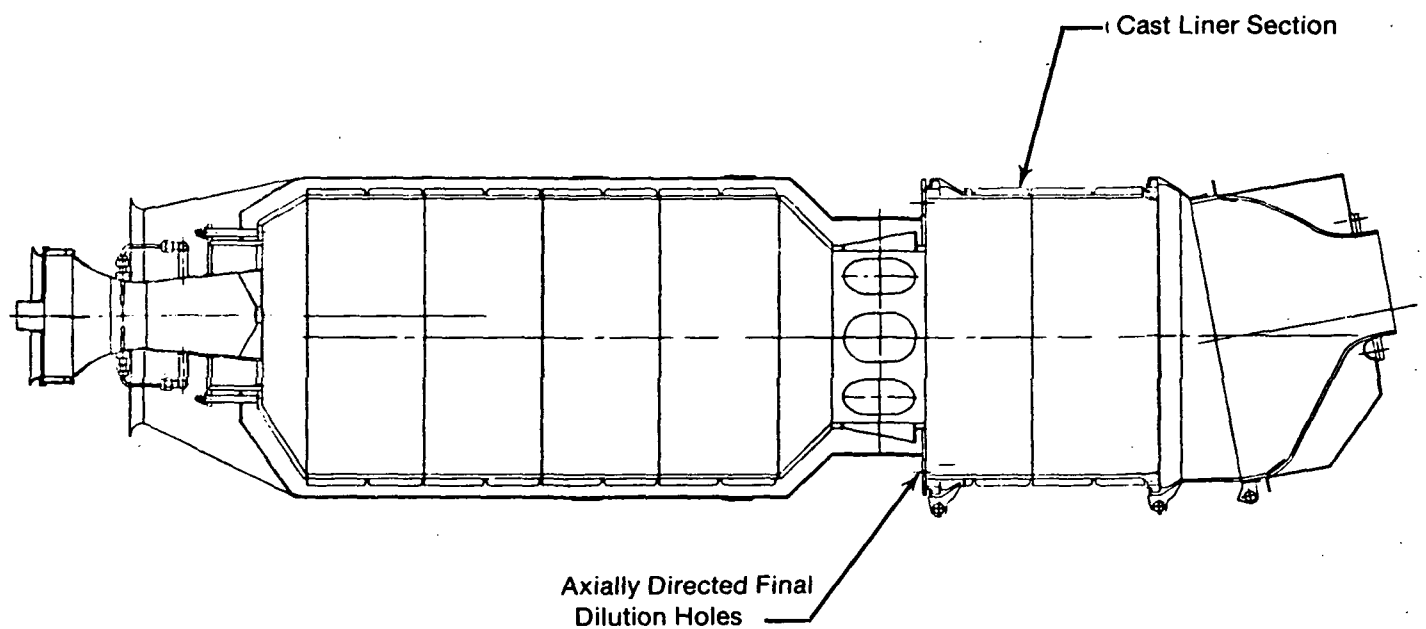

Figure 12. Full-Scale Combustor Scheme FS-05A (Scheme FS-05B With Premix Tube Variable Damper Removed)

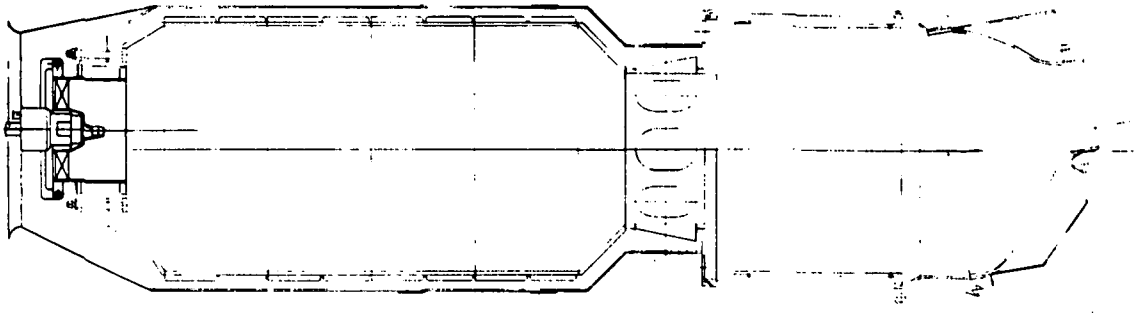

Figure 13. Nonpremixed Configuration of the FRT/RBQQ Combustor (Scheme FS-07A)

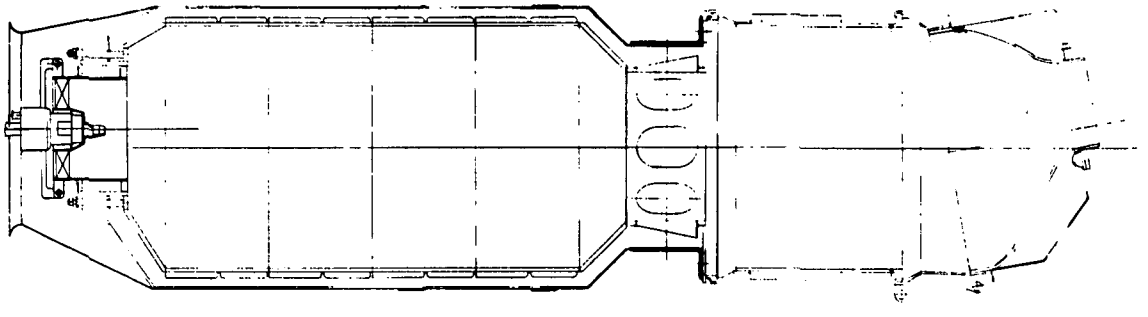

Figure 14. High Temperature Rise Configuration of the FRT/RBQQ Combustor (Scheme FS-08A)

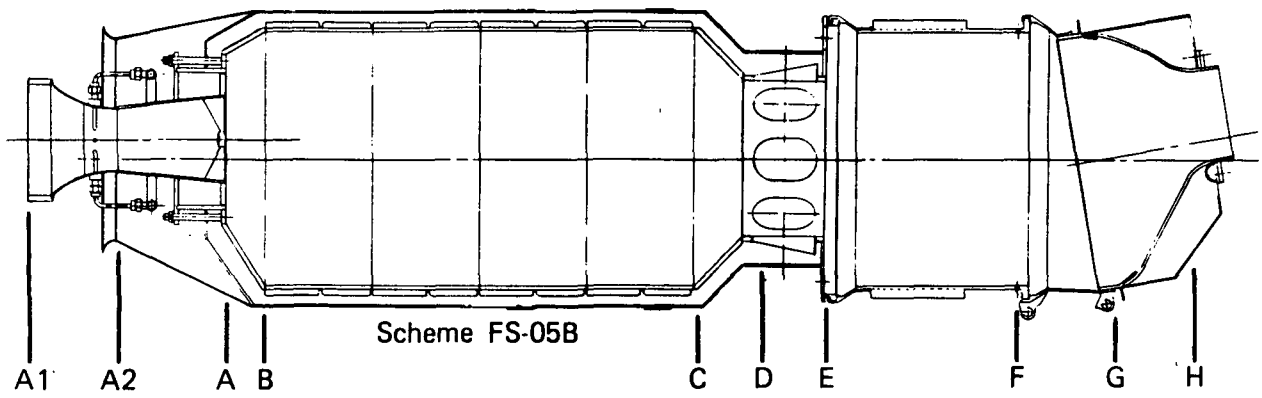

LB	AREF	L/D	VOLREF	ACDSUM
48.01	88.20	4.53	2590.0	27.73

STATION	AX	ACD	WACUM	PHI
A1	13.847	0.0	0.0	0.0
A2	4.335	0.0	0.0	0.0
A	8.038	5.46	19.716	1.307
B	75.391	0.0	19.716	1.307
C	28.280	0.0	19.716	1.307
D	28.280	10.953	59.209	0.435
E	72.346	10.049	95.443	0.270
F	75.391	0.472	97.144	0.265
G	72.348	0.792	100.000	0.258
H	39.337	0.0	100.000	0.258

Headers	Axial Loc.	Rad. Loc.	Circum. Loc
BSTD1	9.0	4.8	0
BSTD2	9.0	4.8	90
BSTD3	9.0	4.8	180
BSTD4	9.0	4.8	252
BST1	14.9	5.0	0
BST2	14.9	5.0	90
BST3	14.9	5.0	180
BST4	14.9	5.0	252
BST5	20.0	5.0	0
BST6	20.0	5.0	90
BST7	20.0	5.0	180
BST8	20.0	5.0	252
BST9	24.5	5.0	0
BST10	24.5	5.0	90
BST11	24.5	5.0	180
BST12	24.5	5.0	252
BST13	36.9	5.0	0
BST14	36.9	5.0	90
BST15	36.9	5.0	180
BST16	36.9	5.0	270
BST17	34.4	5.0	0
BST18	34.4	5.0	90
BST19	34.4	5.0	180
BST20	34.4	5.0	270

Figure 15. Burner Scheme Definition (Scheme FS-05B)

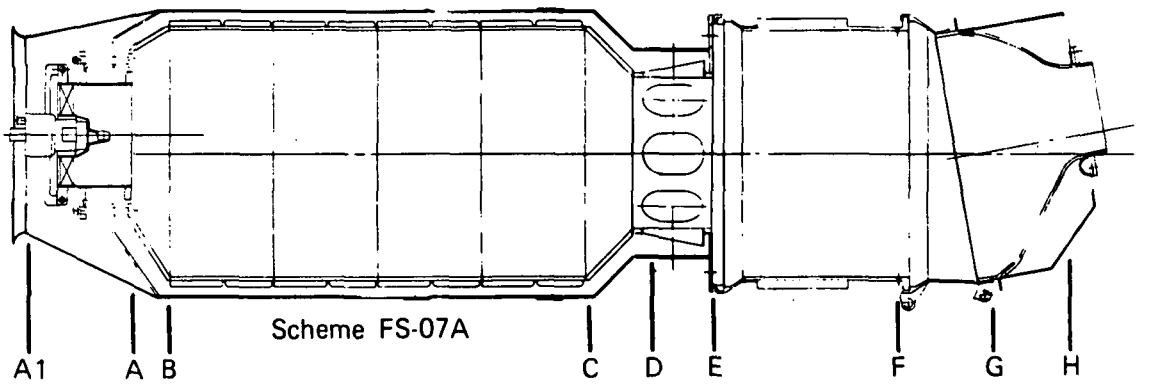

LB	AREF	L/D	VOLREF	ACDSUM
43.19	88.20	4.07	2590.0	27.27

STATION	AX	ACD	WACUM	PHI
A1	9.438	0.0	0.0	0.0
A	12.749	5.005	18.353	1.300
B	75.391	0.0	18.353	1.300
C	28.260	0.0	18.353	1.300
D	28.260	10.953	58.516	0.408
E	72.346	10.049	95.365	0.250
F	75.391	0.472	97.096	0.246
G	72.346	0.792	100.000	0.239
H	39.337	0.0	100.000	0.239

Headers	Axial Loc.	Rad. Loc.	Circum. Loc
BSTD1	9.0	4.8	0
BSTD2	9.0	4.8	90
BSTD3	9.0	4.8	180
BSTD4	9.0	4.8	252
BST1	14.9	5.0	0
BST2	14.9	5.0	90
BST3	14.9	5.0	180
BST4	14.9	5.0	252
BST5	20.0	5.0	0
BST6	20.0	5.0	90
BST7	20.0	5.0	180
BST8	20.0	5.0	252
BST9	24.5	5.0	0
BST10	24.5	5.0	90
BST11	24.5	5.0	180
BST12	24.5	5.0	252
BST13	36.9	5.0	0
BST14	36.9	5.0	90
BST15	36.9	5.0	180
BST16	36.9	5.0	270
BST17	34.4	5.0	0
BST18	34.4	5.0	90
BST19	34.4	5.0	180
BST20	34.4	5.0	270

Figure 16. Burner Scheme Definition (Scheme FS-07A)

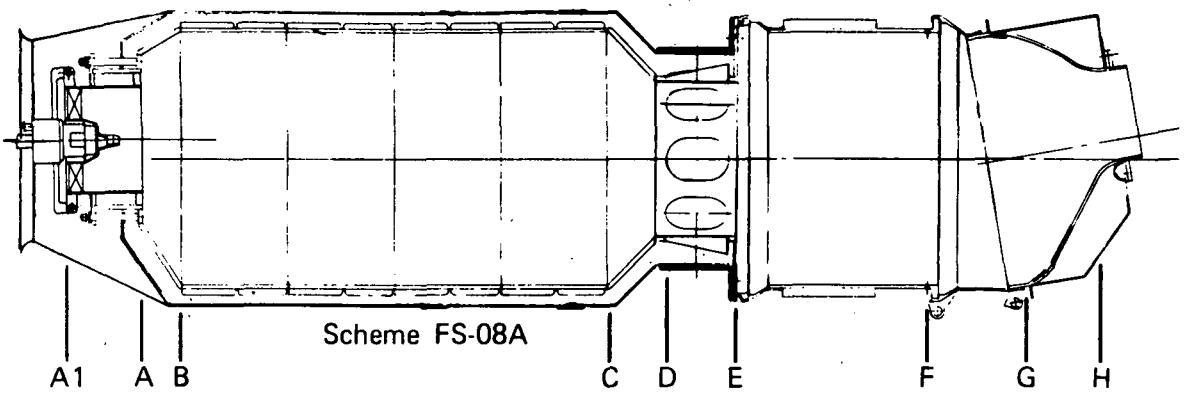

LB	AREF	L/D	VOLREF	ACDSUM
43.19	88.20	4.07	2590.0	17.22

STATION	AX	ACD	WACUM	PHI
A1	9.438	0.0	0.0	0.0
A	12.749	5.005	18.353	1.300
B	75.391	0.0	18.353	1.300
C	28.260	0.0	18.353	1.300
D	28.260	10.953	58.516	0.408
E	72.346	10.049	95.365	0.250
F	75.391	0.472	97.096	0.246
G	72.346	0.792	100.000	0.239
H	39.337	0.0	100.000	0.239

Headers	Axial Loc.	Rad. Loc.	Circum. Loc
BSTD1	9.0	4.8	0
BSTD2	9.0	4.8	90
BSTD3	9.0	4.8	180
BSTD4	9.0	4.8	252
BST1	14.9	5.0	0
BST2	14.9	5.0	90
BST3	14.9	5.0	180
BST4	14.9	5.0	252
BST5	20.0	5.0	0
BST6	20.0	5.0	90
BST7	20.0	5.0	180
BST8	20.0	5.0	252
BST9	24.5	5.0	0
BST10	24.5	5.0	90
BST11	24.5	5.0	180
BST12	24.5	5.0	252
BST13	36.9	5.0	0
BST14	36.9	5.0	90
BST15	36.9	5.0	180
BST16	36.9	5.0	270
BST17	34.4	5.0	0
BST18	34.4	5.0	90
BST19	34.4	5.0	180
BST20	34.4	5.0	270

Figure 17. Burner Scheme Definition (Scheme FS-08A)

The design features of the three FRT combustor schemes tested in Phase VI are summarized in Table IV. A photograph of the Phase VI FRT combustor during construction is shown in Figure 18. The premix tube, primary liner shroud, and aft dilution section were not attached in this figure. The fully assembled configuration with the premix tube is shown in Figure 19. A photograph of the premix tube with variable damper attached is shown in Figure 20.

TABLE IV
SUMMARY OF COMBUSTOR DESIGN FEATURES

	Premixed Configuration (Scheme FS-05A/B)	*Nonpremixed Configuration (Scheme FS-07A)*	*High Temperature Rise Configuration (Scheme FS-08A)*
Type Combustor	Combustor Can, Convective Primary Zone Cooling, Finned Secondary Zone	Combustor Can, Convective Primary Zone Cooling, Finned Secondary Zone	Combustor Can, Convective Primary Zone Cooling, Finned Secondary Zone
Length (Primary)	19.0 in.	19.0 in.	19.0 in.
Length (Dilution)	8.0 in.	8.0 in.	8.0 in.
Length (Overall)	48.0 in. (including transition section to turbine inlet)	43.2 in. (including transition section to turbine inlet)	43.2 in. (including transition section to turbine inlet)
Outer Diameter	11.25 in.	11.25 in.	11.25 in.
Inner Diameter	9.8 in.	9.8 in.	9.8 in.
Combustor Reference Area (Primary)	75.4 in. sq	75.4 in. sq	75.4 in. sq
Type Nozzle (Initial Configuration)	Single-zone low-pressure spraybars (12 with a total of 36 holes at 0.031 dia)	Sonicore Model 281T boost-air nozzle, compressed nitrogen boost supply	Sonicore Model 281T boost-air nozzle, compressed nitrogen boost supply
Swirler (Initial Configuration)	3.20 in. O.D., 0.56 in. I.D., 15 constant solidity vanes with vented, flat centerbody (26 deg swirl angle)	4.03 in. O.D., 1.75 in. I.D., 20 vane recessed swirler (45 deg swirl angle)	4.03 in. O.D., 1.75 in. I.D., 20 vane recessed swirler (45 deg swirl angle)
Combustor Material			
Outer Liner	Type 347 SST	Type 347 SST	Type 347 SST
Inner Liner	Stellite 31 (X40)	Stellite 31 (X40)	Stellite 31 (X40)
Combustor Wall Thickness			
Outer Liner	0.0625 in.	0.0625 in.	0.0625 in.
Inner Liner	0.125 in. on diameter with 0.125 high fins	0.125 in. on diameter with 0.125 high fins	0.125 in. on diameter with 0.125 high fins
Design Point Conditions			
Fuel-Air Ratio	0.0189	0.0189	0.0292
Volumetric Heat Release	2.05×10^6 Btu/(ft^3-hr-Atm)	2.05×10^6 Btu/ft^3-hr-Atm)	2.05×10^6 Btu/ft^3-hr-Atm)
Rate Based on:			
Inlet Pressure	188 psia	188 psia	188 psia
Combustor Airflow	31.5 lb/s	31.5 lb/s	20.4 lb/s
Combustor Reference Velocity (Primary)	29.0 f/s	29.0 f/s	29.0 f/s
Combustor Total Pressure Loss	5.5%	5.5%	5.5%

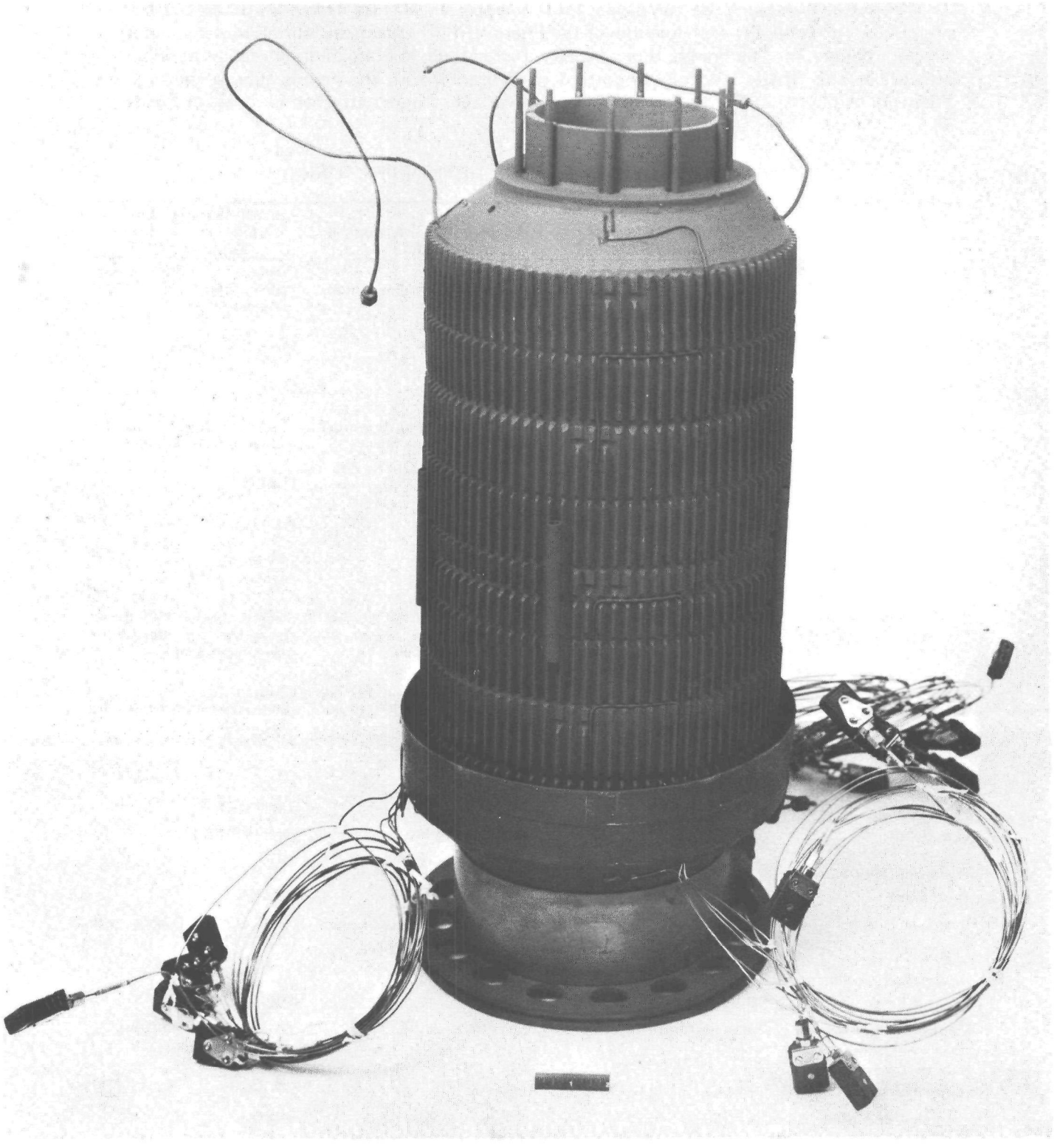

Figure 18. FRT Combustor (Scheme FS-05A) During Assembly

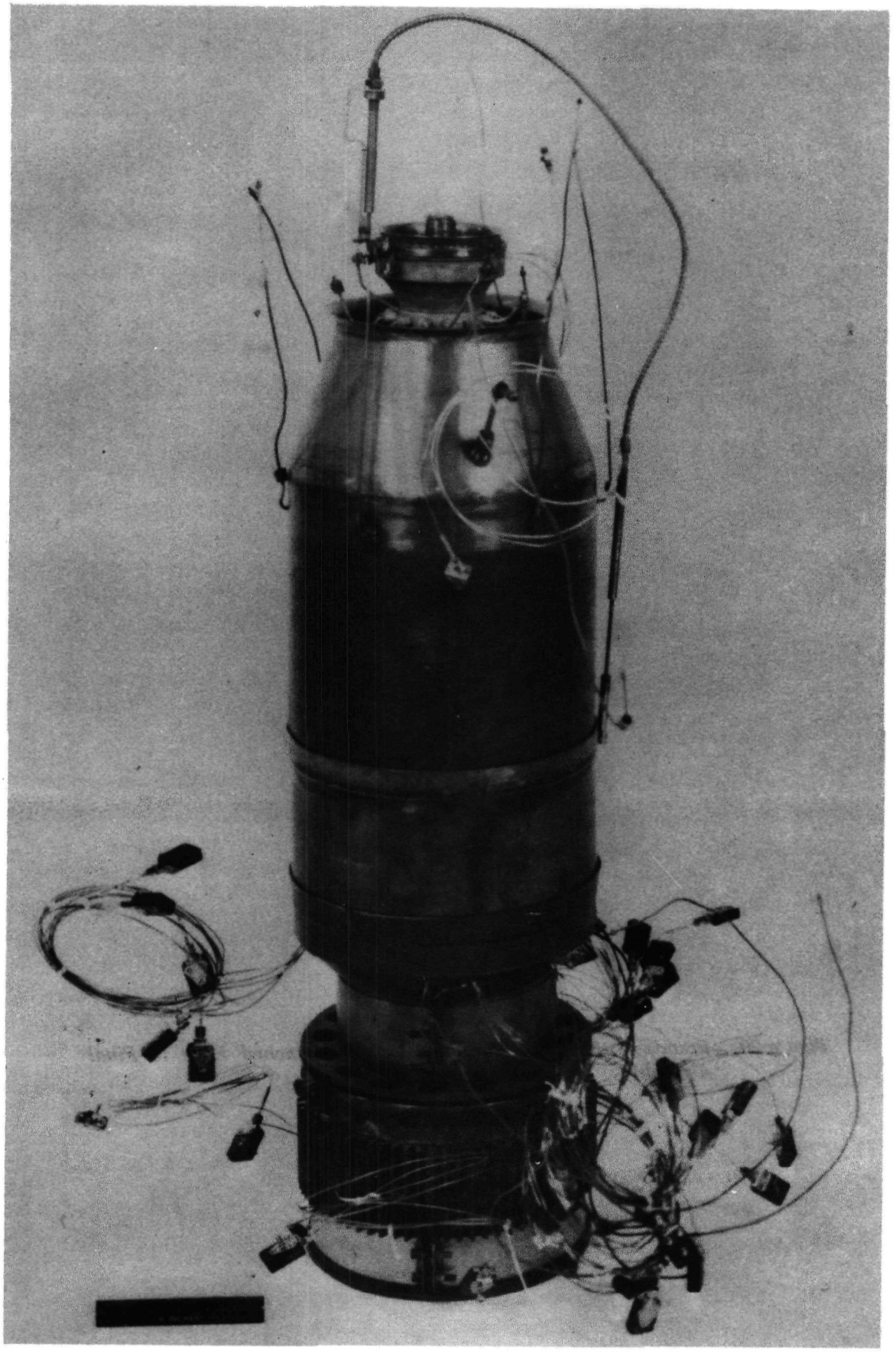

Figure 19. FRT Combustor (Scheme FS-05A) Fully Assembled

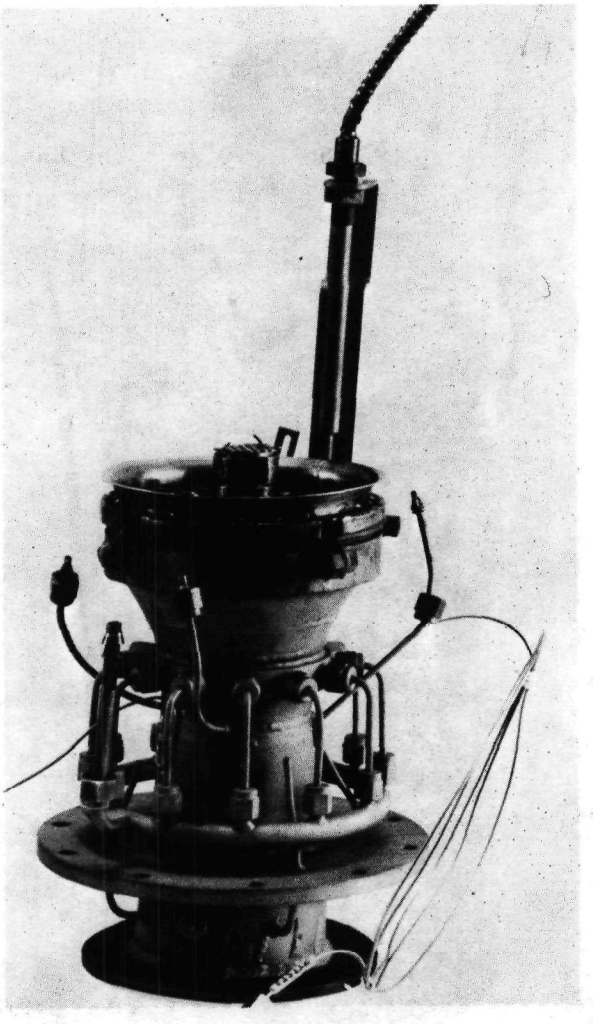

Figure 20. Premix Tube With Variable Damper Attached Prior to Final Assembly

2.2 EXPERIMENTAL RIG HARDWARE AND TEST STAND PREPARATION

The rig hardware and test stand instrumentation used in Phase VI testing were nearly the same as that described for Phase IV testing in Section 2.10.1 (of Reference 1). Additional instrumentation was added to the combustor to allow the measurement of the cooling airflow (quick quench air) temperature rise. The liner was also coated with a temperature sensitive paint to more fully document temperature patterns when examined at the end of the test series.

The P&WA Mobile Emission Laboratory (MEL) was also used in place of the fixed emission equipment used in Phase IV. The Mobile Emissions Laboratory (MEL), shown in Figure 21, is a self-propelled, sound proofed laboratory with an on-board gas analysis and data acquisition/processing system. The gas analysis system consists of individual analyzers for concentration measurements of carbon monoxide (CO), carbon dioxide (CO_2), oxygen (O_2), oxides of nitrogen (NO and NO_x), total unburned hydrocarbons (THC), and sulfur dioxide (SO_2). It also includes a gas chromatograph for measurements of molecular hydrogen (H_2) and nitrogen (N_2). The following analyzers have been incorporated into the gas analysis system:

- Thermo Electron Corp. Model 10A NO/NOX Analyzer, Ranges: 2.5, 10, 25, 100, 250, 1000, 2500, and 10,000 ppm.
- Beckman Model 865 nondispersive Infrared CO Analyzer, Ranges: 100, 500, and 1000 ppm; 1, 5, and 10%.
- Scott Model 250 Paramagnetic O_2 Analyzer, Ranges: 1, 5, 10, and 25%.
- Beckman Model 402 Flame Ionization Total Hydrocarbon Analyzer, Ranges: 1, 5, 10, 50, 100, 500, 1000, and 5000 ppm.
- Thermo Electron Corp. Model 40, Pulsed Fluorescent SO_2 Analyzer, Ranges: 50, 100, 500, 1000, and 5000 ppm.
- Carle Model AGC 311 Gas Chromatograph equipped with both flame ionization and thermal conductivity detectors.

The system is basically a more modern version of that shown schematically in Section 2.10.1 (of Reference 1). It conforms to ARP 1256 and the guidelines specified in the 17 July 1973, Federal Register, "Control of Air Pollution from Aircraft and Aircraft Engines, Emissions Standards and Test Procedures for Aircraft."

A continuous gas sample was abstracted from the burner exhaust and transferred to the MEL system through electrically heated teflon lines. The sample transfer time was less than 2 sec. The sample was cooled in the probe to approximately 300°F, thereby quenching high-temperature oxidation reactions, but maintaining an amount of heat adequate to prevent the loss of unburned hydrocarbons by condensation. The calibration gases that were used were traceable to National Bureau of Standards reference materials. Check calibrations of the testing standards against the primary standards were made periodically to ensure their continued accuracy.

Figure 21. MEL Data System and Emission Equipment

Burner exhaust smoke measurements were obtained through use of a smoke measuring system that conforms to specifications of the Society of Automotive Engineers Aerospace Recommended Practice, ARP-1179. A fixed, single-port smoke sampling probe was located on centerline of the rig exhaust duct near the fixed emission sampling rake. The smoke measuring system is shown in Figure 22. The filter holder, also shown in Figure 22 was constructed with a one-in. dia spot size, a diffusion half-angle of 7.25 deg and a converging half-angle of 27.5 deg. Sample temperature was maintained at 150°F throughout the system. At the required data points, four filter samples were collected at a flowrate of 0.5 ft^3/min from which an average smoke number was determined. A Photovolt Model 670 reflection meter with a type Y search unit conforming to ASA Ph 2.17-1958 "Standard for Diffuser Reflection Density" was used to determine the reflectance of the clean and stained filters. A set of Hunter Laboratory reflectance plaques, traceable to the National Bureau of Standards, were used to calibrate the reflection meter.

The MEL system was also used for data acquisition, recording and reduction of most rig and combustor parameters. Some additional instrumentation was monitored in the control room as were some of the more important parameters on redundant readouts.

2.3 ALTERNATIVE FUELS TESTING

Evaluation of the Rich Burn/Quick Quench combustor operating on synthetic liquid and residual fuels was accomplished using two different fuel preparation devices. Testing was initiated employing the baseline premix tube. The FRT combustor with the premix tube was designated as scheme FS-05A initially. In subsequent testing the premix tube variable damper was removed, and the scheme designation was changed from FS-05A to FS-05B. The non-premixed fuel preparation device was also tested on the FRT combustor. This combustor configuration was designated as scheme FS-07A.

The data obtained for both the premixed configuration and the nonpremixed configuration of the combustor are presented in Tables I through VII of Appendix A. The tables contain the major parameters necessary to specify combustor operating conditions and contain liner temperature and exhaust emission data.

The following subsections describe the emissions and operating characteristics of both the premixed and nonpremixed combustor configurations, as well as exit temperature profiles and the effect that synthetic and residual fuels have on liner temperatures. For comparison purposes, Table V shows the combustor operating conditions of a representative 25 megawatt gas turbine engine. This table contains the inlet pressure and temperature, the operating overall equivalence ratio, and the average combustor exit temperature over the entire range of conditions from cold start to peak load.

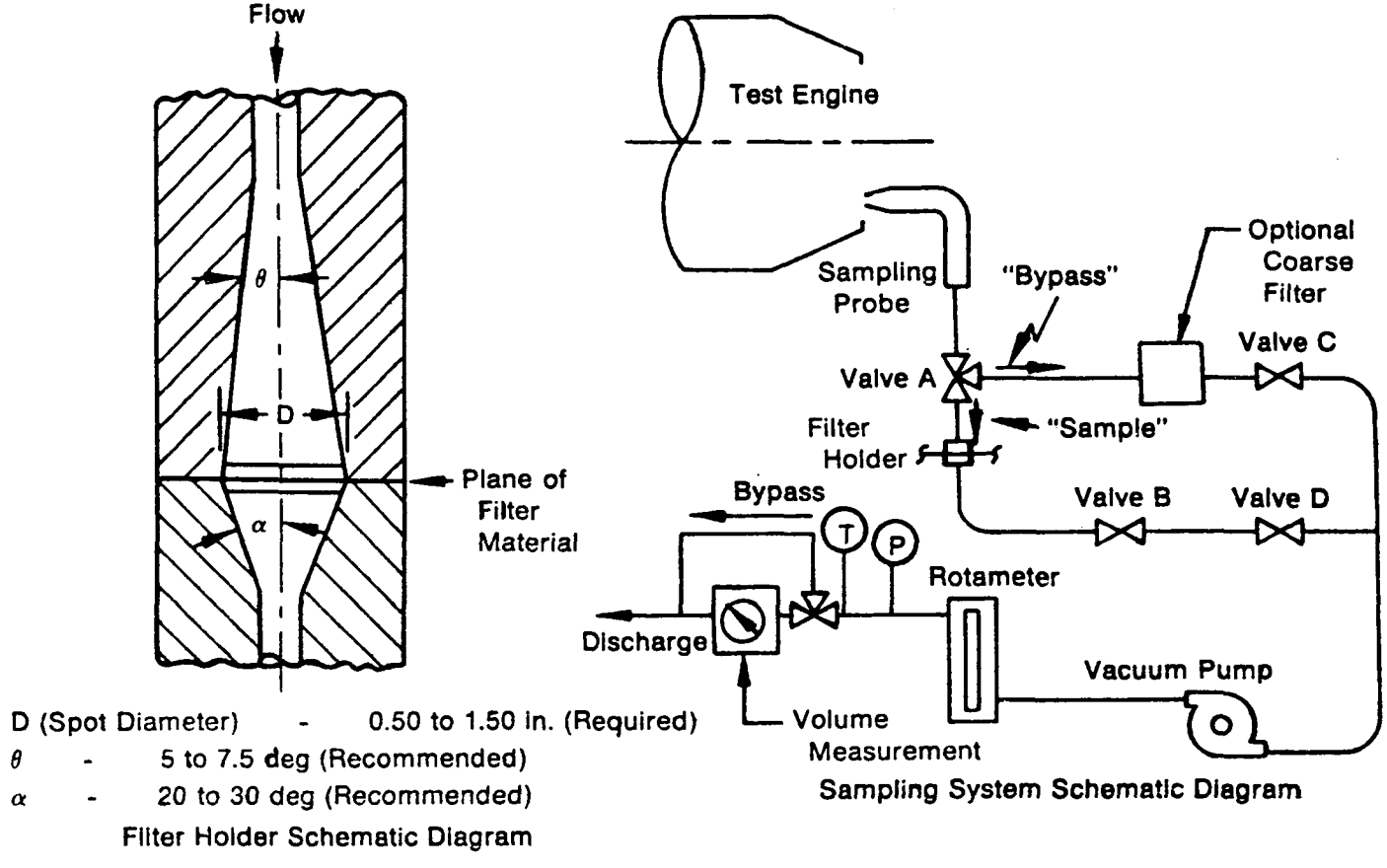

Figure 22. Schematic Diagram of Smoke Meter

TABLE V
COMBUSTOR OPERATING CONDITIONS IN A TYPICAL 25 MEGAWATT ENGINE WITH FREE TURBINE

Operating Point	Inlet Total Pressure (psia)	Inlet Total Temperature (°F)	Exit Equivalence Ratio	Exit Temperature (°F)
Peak Load	208	750	0.31	2100
Baseload (100%)	180	700	0.28	1950
70%	150	600	0.24	1650
50%	120	500	0.20	1450
Sync Idle	50	300	0.13	950
Cold Start	15	70	0.29	1450

2.3.1 Emission and Performance Rig Testing of Scheme FS-05A/B

Operation of the combustor on No. 2 fuel at 50 and 100 psia rig pressure (with nearly constant airflow) was accomplished, and the basic emission signature was obtained (by varying the fuel flowrate) and verified to be consistent with performance measured previously under Phase IV. During the checkout tests, the premix tube variable damper, which had been maintained in the full-open position during all tests up to that point, separated from the premix tube and fell to the bottom of the rig test chamber. There was no damage to any part of the combustor as a result of this occurrence. Examination of the hardware indicated that several welds securing the damper mounting bracket to the premix tube had failed. The variable damper mechanism was removed from the rig and all subsequent tests were conducted without the air staging capability of this mechanism. Tests of the combustor were conducted at 100 psia rig pressure firing SRC II middle distillate fuel. A basic emission signature was generated, and the data indicate that a substantial reduction in the NO_x concentration level was achieved, as described in Subsection 2.3.1.2. Operation of this combustor scheme was also accomplished firing the two residual test fuels, a residual shale oil and an Indonesian/Malaysian residual oil. Both of these test fuels were heated to about 180°F prior to combustion. The No. 2 fuel and SRC II were delivered to the combustor at temperatures just above ambient.

2.3.1.1 Verification of Baseline Exhaust Emission Characteristics

Initial experiments were performed using No. 2 fuel oil to check out the test rig and instrumentation and to verify the baseline performance of the RBQQ combustor. Although the configuration tested, scheme FS-05A, had not been evaluated previously, the arrangement of the hardware was very similar to that of scheme FS-03A, which had been evaluated under Phase IV. As previously described, the principal differences in these two schemes are the alternative placement of final dilution holes in scheme FS-05A (axially directed, in the wall of the dump section, rather than radially directed in the wall of the final dilution liner) and the use of an uncooled secondary liner in scheme FS-05A. As a result of the substitution of alternative final dilution holes, there is a slight shift in the design point airflow distribution in scheme FS-05A, causing a reduction in quick quench airflow from 43.7% of total burner airflow in scheme FS-03A to 40.2% in scheme FS-05A. The same shift in distribution had also been present in scheme FS-04A, tested under Phase IV.

In verifying the baseline performance of the RBQQ combustor, reference was made both to scheme FS-03A, the previously tested full-residence-time (FRT) arrangement of the combustor hardware which had similar primary zone and secondary zone residence times; and to scheme FS-04A, which was shorter in length but had the same design point airflow distribution. Figures depicting these schemes and the emission and performance characteristics are documented in Reference 1.

The initial checkout tests were conducted at 50 psia rig pressure. In Figure 23 a comparison of the NO_x emission characteristics of the combustor to those obtained for the previous FRT configuration (scheme FS-03A) is presented. The curve for schemes FS-05A and FS-05B has the same general shape as the one generated previously for scheme FS-03A. There was a slight decline in the minimum NO_x concentration level achieved (20 ppmv for scheme FS-05B at 15% O_2 compared to 26 ppmv for scheme FS-03A). This result was not unexpected because of the slightly lower inlet air temperature in the case of scheme FS-05B (430°F compared to 450°F for scheme FS-03A), and because of the alternative placement of final dilution holes in scheme FS-05B (axially directed, in the wall of the dump section, rather than radially directed in the wall of the secondary liner — this alternative placement was shown to produce an incremental reduction in thermal NO_x in tests conducted under Phase IV).

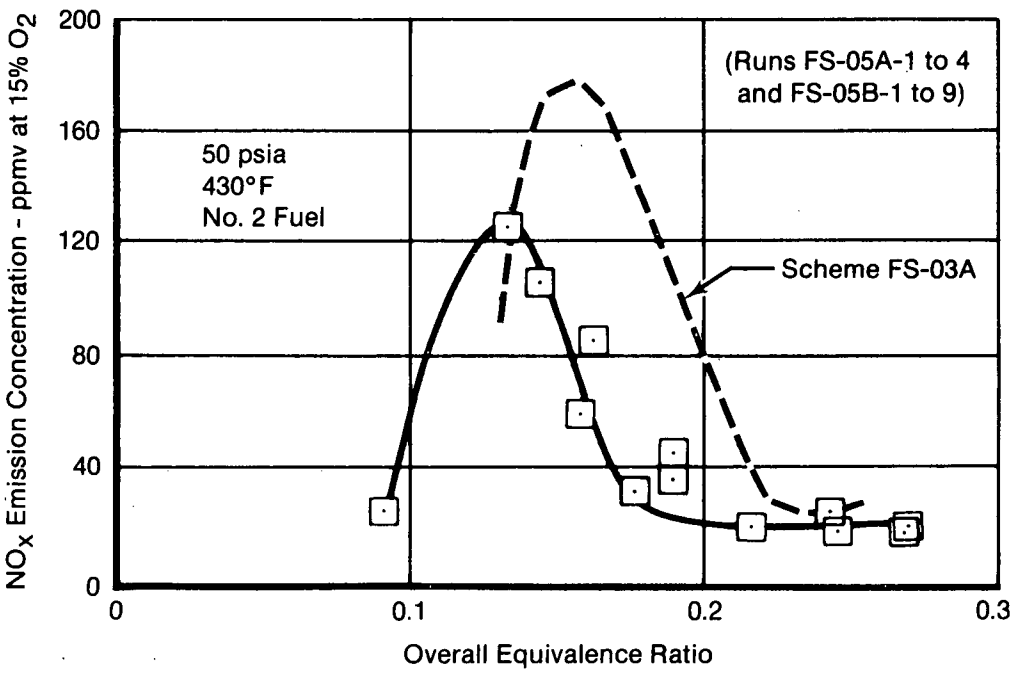

Figure 23. Comparison of Variation in NO_x Concentration With Overall Equivalence Ratio for Schemes FS-05A, FS-05B and FS-03A

In addition, there was a significant shift in the location of the NO_x curve peak in the data for schemes FS-05A and FS-05B (the peak concentration of 123 ppmv for scheme FS-05A, corrected to 15% O_2, occurs at 0.134 overall equivalence ratio, compared to a peak concentration of 178 ppmv for scheme FS-03A, which occurred at 0.160 overall equivalence ratio). This shift was not unexpected because of the altered airflow distribution of scheme FS-05A/5B compared to scheme FS-03A (only 60% of the total airflow is introduced upstream of the secondary-zone dump plane in scheme FS-05B, compared to 65.6% in scheme FS-03A). Although the front sections of both combustor configurations were identical, scheme FS-05B had a greater total open hole area in the secondary zone. As a result, the primary zone equivalence ratio corresponding to a given value of exit-plane equivalence ratio is slightly higher in scheme FS-05B than in scheme FS-03A and the peak NO_x concentration for scheme FS-05A/5B occurs at a lower value of overall equivalence ratio. The lower peak concentration of NO_x measured for scheme FS-05A (123 ppmv compared to 178 ppmv for scheme FS-03A) was an unexpected occurrence. Although no definitive explanation was found, a lower peak concentration of NO_x might be expected to occur due to a slight deterioration in the quality of fuel preparation.

CO data obtained for schemes FS-05A and FS-05B at 50 psia rig pressure are presented in Figure 24. Comparison of the results to those obtained previously for scheme FS-03A indicate that somewhat lower concentrations were measured for scheme FS-05A/5B in the range of overall equivalence ratios to the right of the CO curve peak. In addition, the peak concentration measured was lower for scheme FS-05A/5B. This result is believed to reflect the achievement of more comlete secondary zone oxidation of CO in scheme FS-05A/5B. The improvement may be due to the use of axially-directed final dilution air jets for the first time in this scheme of the FRT configuration of the RBQQ combustor.

Following the initial series of checkout tests at 50 psia rig pressure all subsequent testing of alternative fuels was conducted at 100 psia rig pressure. NO_x emission data obtained firing No. 2 fuel at 100 psia are presented in Figure 25. Included for comparison are the NO_x emission curves obtained in Phase IV for schemes FS-03A, FS-04A, and FS-04B. There is close agreement among the data for these four schemes in terms of the shapes of the curves and the minimum concentration levels achieved. The positions of the curves on the abscissa relative to each other also conform generally to expectations. Thus, the steep portion of the curve for scheme FS-05B coincides closely with the same portion of the curve for scheme FS-04A, which had the same front-end configuration and the same total combustor hole area. At the same time, the curve for scheme FS-05B falls to the left of the curve for scheme FS-03A, which had slightly higher front-end airflow as noted in the previous discussion of the 50 psia data. This curve also lies to the right of the curve for scheme FS-04B which had a slightly lower front-end airflow because of the presence of the premix tube damper.

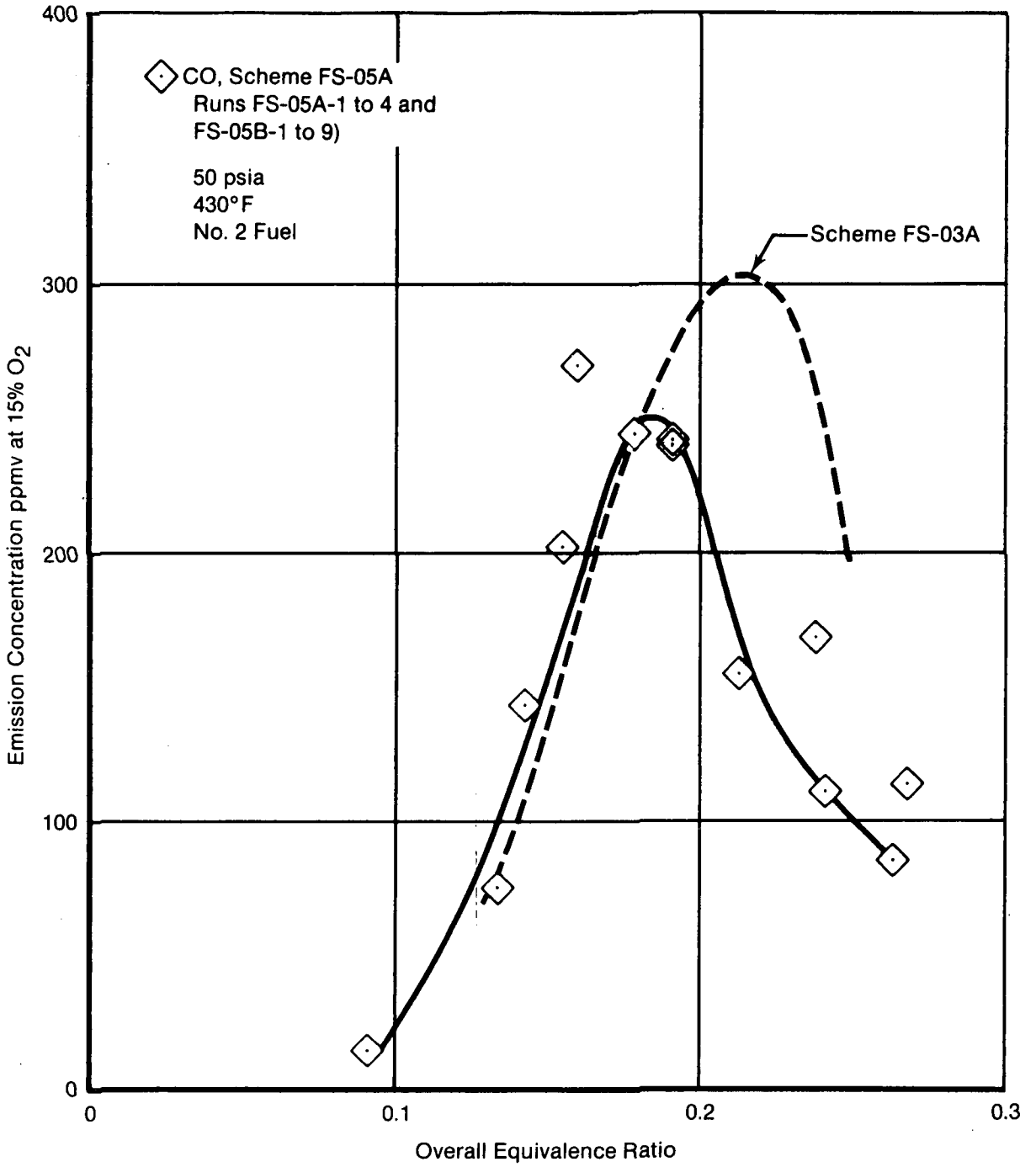

Figure 24. Comparison of Variation in CO Concentration With Overall Equivalence Ratio for Schemes FS-05A, FS-05B, and FS-03A

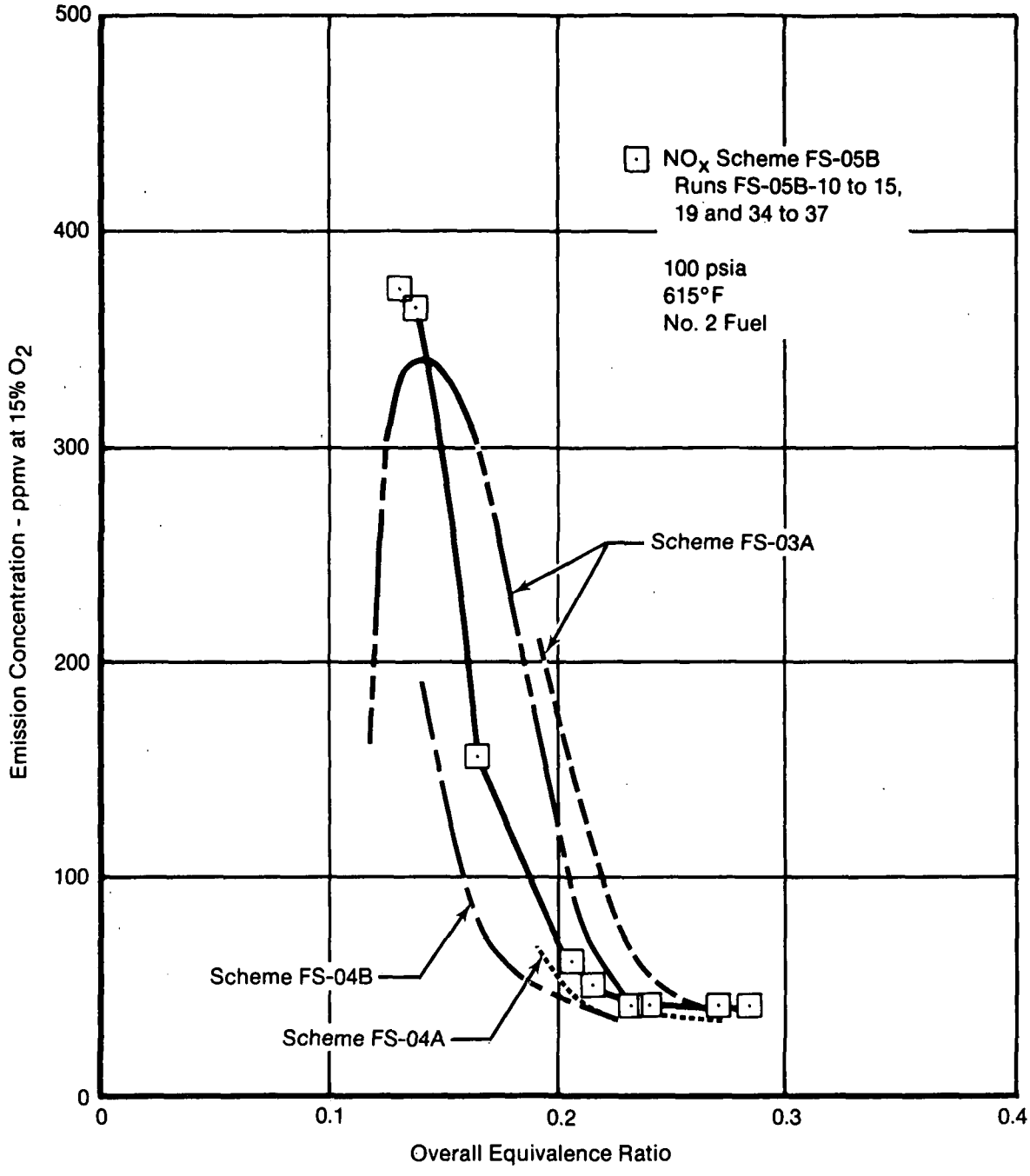

Figure 25. Comparison of Variation in NO_x Concentration With Overall Equivalence Ratio for Schemes FS-05B, FS-03A, FS-04A, and FS-04B

Prior to the resumption of testing of the RBQQ combustor under Phase VI, a projection was made of the minimum NO_x concentration level achievable using the planned configuration (scheme FS-05A) of the burner firing No. 2 fuel. The projection was made with reference to Figure 106, Section 3.2.6, Reference 1, which showed the dependence of minimum attainable NO_x concentration levels on primary zone residence time. Although the referenced curves had been based on only two data points (corresponding to the two values of primary zone residence time represented in the ECV and FRT versions of the RBQQ combustor), it was indicated that the use of axially directed final dilution holes produced an incremental reduction in thermal NO_x of approximately 10 ppmv (corrected to 15% O_2). This observed reduction was combined with the NO_x concentration level achieved in the previously tested FRT combustor which had conventional dilution holes (scheme FS-03A) and a projected minimum NO_x level of 35 ppmv was arrived at for scheme FS-05A. The minimum concentration actually achieved (44 ppmv at 15% O_2) was higher than the projected value. However, the increased level is believed to be attributable to an increase in combustor inlet air temperature from 560°F in the tests of scheme FS-03A to 610°F in the tests of scheme FS-05A/5B. Viewed in this context the results obtained in Phase VI using No. 2 fuel are believed to be consistent with the referenced residence time relationship.

CO emission data obtained firing No. 2 fuel at 100 psia rig pressure are presented in Figure 26. The curve for scheme FS-05B is lower than the curves for schemes FS-03A and FS-04B. This result is believed to reflect the achievement of more complete secondary zone oxidation of CO, and is consistent with the results obtained at 50 psia rig pressure. The following comparisons can be made among data obtained for the three schemes:

1. Two curves of different magnitude were obtained for scheme FS-03A in the Phase IV experimental program. The curve having higher CO concentration values (above 200 ppmv at 15% O_2) was accepted as definitive. The second curve, which had a peak CO concentration only slightly higher than 100 ppmv, was generated during tests in which a metal blockage band on the combustor liner became loosened, causing an alteration in the combustor airflow distribution. Specifically, displacement of the band allowed the direct entry of air from the rig plenum into the quick-quench zone of the combustor. The proper routing of the quick-quench airflow is along a flowpath through the primary liner cooling passage. It is believed that both the quantity and direction of the jets entering the quick-quench section were altered because of the displaced band, and that these alterations caused a net reduction in CO concentration levels. The CO curve for scheme FS-05B is similar to that obtained for scheme FS-03A in the case of the loosened blockage band, indicating that an alteration in the method of introduction of quick-quench airflow and/or final dilution airflow may have been responsible for the general reduction concentration levels.

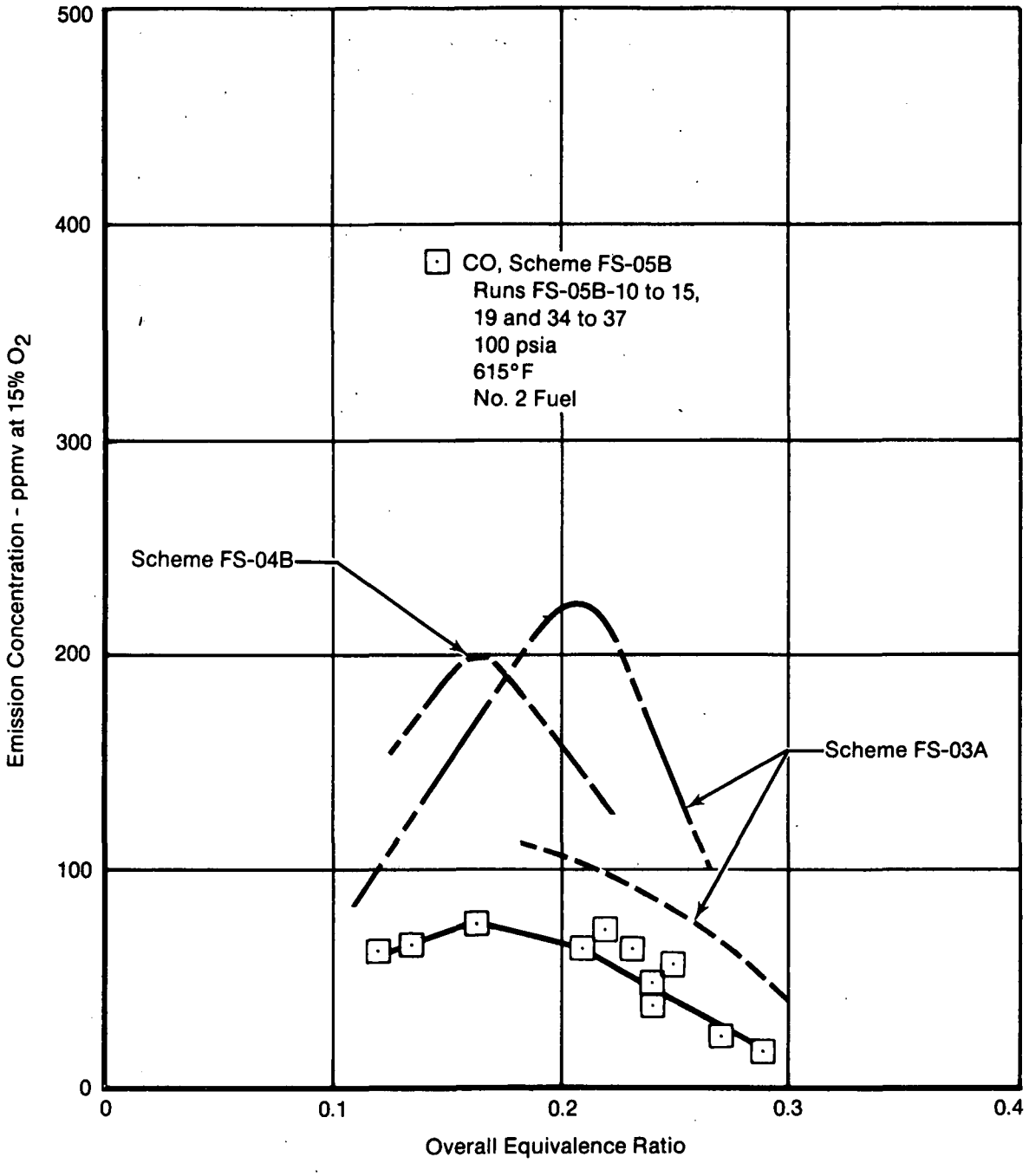

Figure 26. Comparison of Variation in CO Concentration With Overall Equivalence Ratio for Schemes FS-05B, FS-03A, and FS-04B

2. The two major changes incorporated into scheme FS-05B in comparison to schemes FS-03A and FS-04B are the use of axially directed final dilution air jets and the restoration of the secondary zone to full-residence-time length. Because axially directed dilution air jets were also used in scheme FS-04B which produced relatively high CO concentration levels, it has been concluded that the dilution jet feature alone was not responsible for the net reduction in CO measured for scheme FS-05B. Similarly, the extended length full-residence-time secondary zone could not have been solely responsible for the reduction in CO because of its use in scheme FS-03A. It has been tentatively concluded that the reduced CO concentration levels obtained for scheme FS-05B are the result of the combined effect of axial dilution jets and the extended length secondary zone. According to this viewpoint the reduction in CO was similar to that encountered in the same combustor when the quick-quench blockage band became displaced.

Smoke data was recorded at the 100 psia operating conditions for one point. An SAE smoke number (ARP 1179) of 1.8 was obtained for a fuel-lean condition in the primary zone (test No. FS-05B-36).

2.3.1.2 Exhaust Emission and Operating Characteristics With Alternative Fuels

Tests of the FRT combustor (scheme FS-05B) were conducted at 100 psia rig pressure firing an SRC II middle distillate fuel. Exhaust emission data from these tests are presented in Figure 27. As expected, the emission signature of the combustor was generally the same as that documented under Phase IV for other nitrogen bearing fuels (a pyridine-spiked No. 2 fuel and a shale-derived Diesel Fuel Marine). The NO_x curve in Figure 27 has a strong central peak corresponding approximately to the occurrence of stoichiometric operating conditions in the primary zone, and a distinct minimum concentration point or "bucket." The highest NO_x concentration recorded (which may not have represented the peak) was 395 ppmv, corrected to 15% O_2. A minimum NO_x concentration of 93 ppmv (corrected to 15% O_2) was also recorded. Although there is no way to determine the exact rate of conversion of fuel-bound nitrogen to NO_x from these data, it can be noted that complete conversion of the fuel nitrogen present would correspond to an increment in NO_x of 424 ppmv (corrected to 15% O_2). If it is assumed that the thermal NO_x concentration generated while firing SRC II is identical to that obtained while firing No. 2 fuel (43 ppmv, corrected to 15% O_2), then the estimated rate of conversion is 12%.

The CO emission data obtained firing the SRC II middle distillate are also presented in Figure 27. The CO curve is similar to that shown in Figure 26 for No. 2 fuel, except for generally higher concentration levels (116 ppmv corrected to 15% O_2 at the peak of the curve compared to 79 ppmv for No. 2 fuel). Curves for both fuels exhibit peak CO concentrations at approximately the same setting (0.16) of overall equivalence ratio.

Smoke readings were recorded at three test conditions during operation of the combustor on SRC II middle distillate fuel. Values of SAE smoke number obtained were as follows:

Test No.	*SAE Smoke No.* (ARP 1179)*
FS-05B-24	1.6
FS-05B-22	9.9
FS-05B-23	44.9

*An SAE Smoke number in the range of 20 to 25 is generally considered to be the visible threshold.

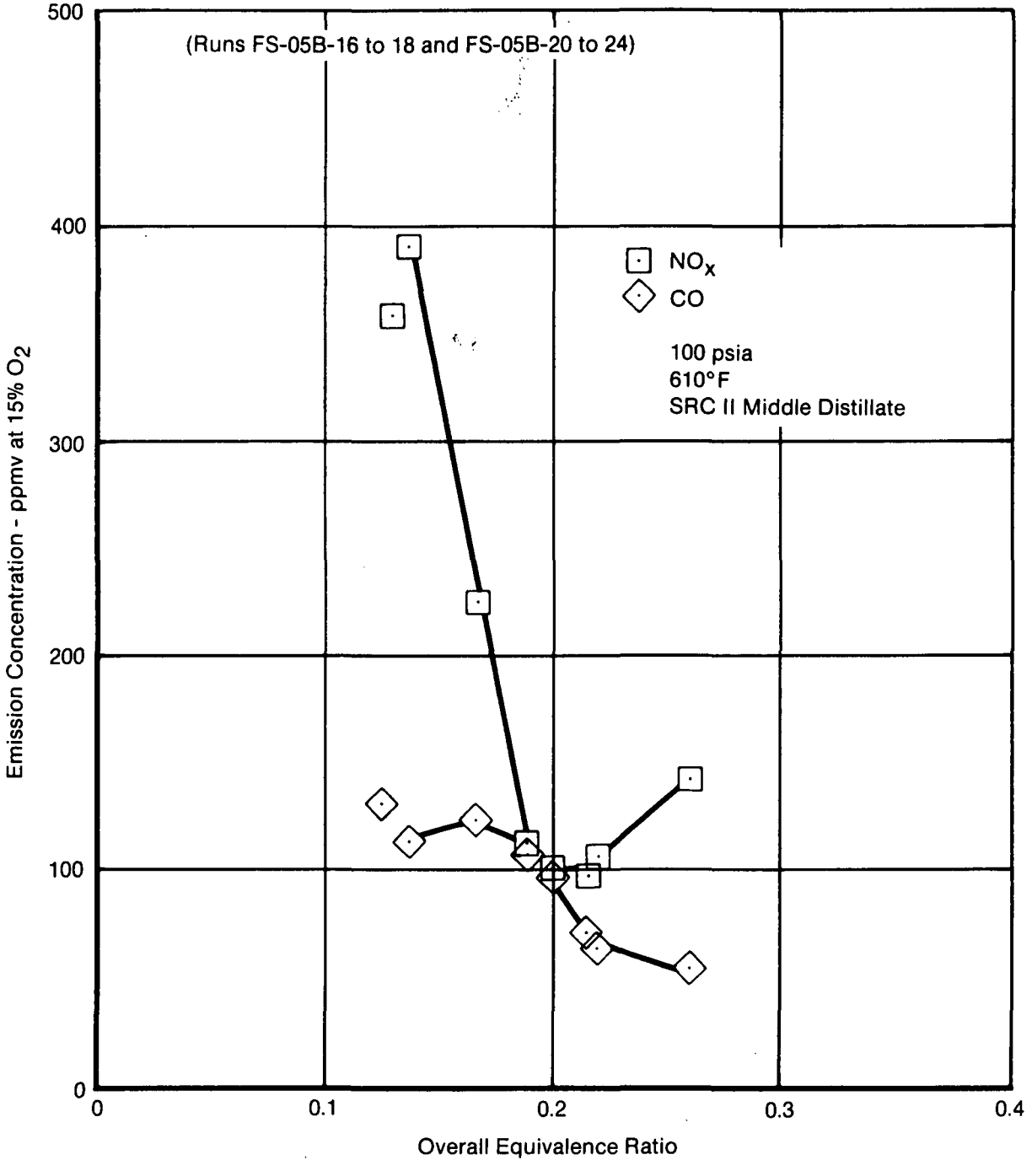

Figure 27. Variation in Emission Concentrations With Overall Equivalence Ratio for Scheme FS-05B Using SRC II Middle Distillate Fuel

The three test conditions represented at these test points correspond to: (1) fuel-lean operation of the primary zone (FS-05B-24); (2) the minimum NO_x level condition (at the bottom of the "bucket" in the NO_x curve, FS-05B-22); and (3) overly fuel-rich operation of the primary zone (FS-05B-23).

No significant change in combustor operating characteristics was noted during the tests of scheme FS-05B conducted with SRC II middle distillate fuel. Inspection of the combustor following the tests revealed that the inside surface of the primary liner was free of carbon deposits. Although there was some deterioration of the flamespray coating within the primary zone, no areas of distress were detected. Examination of the premix tube showed a minor buildup of carbon on the inside surface of the premixing passage and on the premix tube swirl vanes (see Figure 28). The accumulation was slightly greater than that encountered in tests of scheme FS-03A conducted with shale DFM during Phase IV (see Figures 87 and 88 in Subsection 3.2.3.6, Reference 1). The build-up in Figure 28 was present after approximately 1.5 hr of operation at 100 psia rig pressure and subsequent shutdown on SRC II middle distillate fuel.

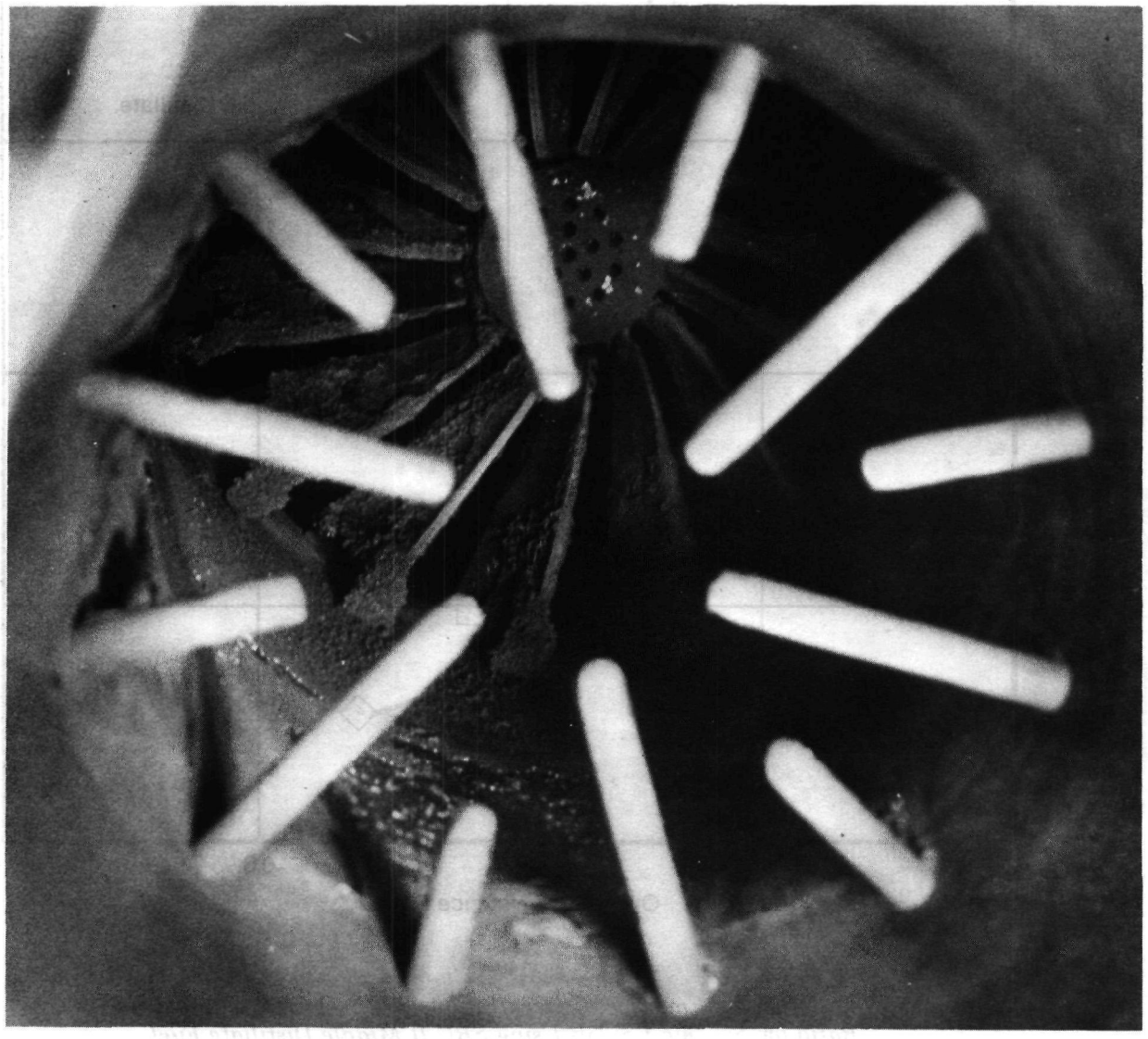

Figure 28. Condition of Premix Tube Swirler and Premixing Passage Following Tests With SRC II Middle Distillate Fuel

Tests of the FRT/RBQQ combustor with premixed fuel preparation device (Scheme FS-05B) were also conducted at 100 psia and 600°F rig inlet conditions firing a shale residual and an Indonesian/Malaysian residual. Exhaust emission data for the shale residual are presented in Figure 29 and for the Indonesian/Malaysian residual in Figure 30. In both cases, the basic emission signatures of the combustor were similar to the SRC II middle distillate fuel and to other nitrogen bearing fuels.

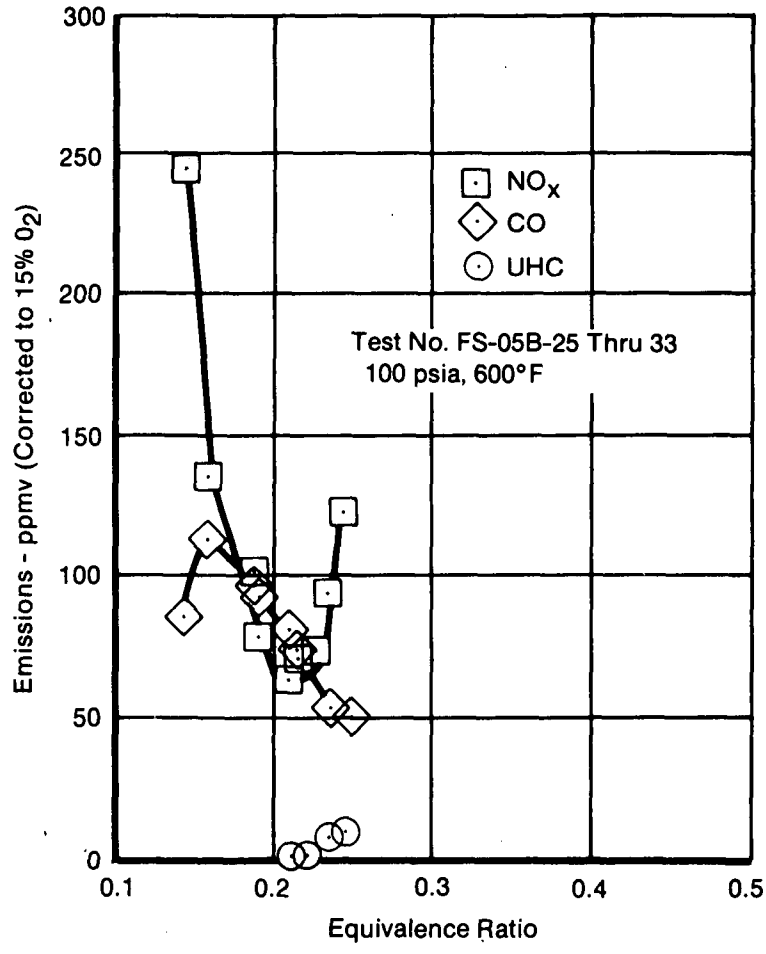

Figure 29. Emission Signature of Scheme FS-05B Firing Shale Residual

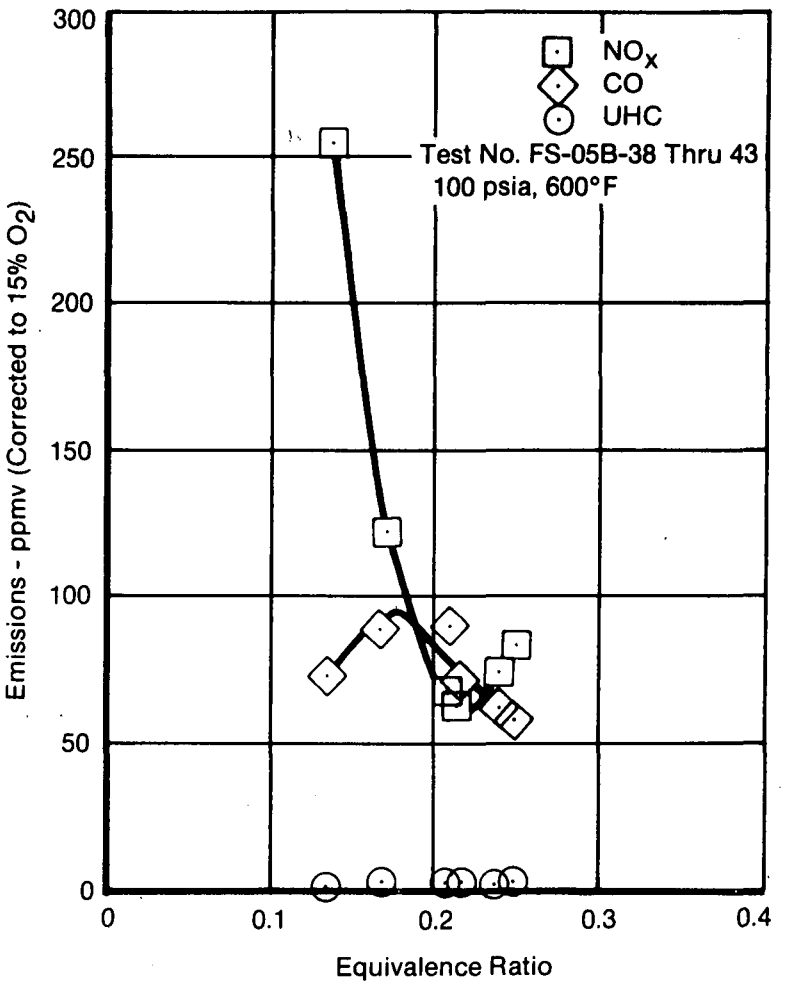

Figure 30. Emission Signature of Scheme FS-05B Firing Indonesian/ Malaysian Residual

The NO_x curve for both fuels again exhibits a strong central peak near the point of stoichiometric combustion in the primary zone and a well defined minimum concentration point or "bucket." The highest NO_x recorded was about 250 ppmv (corrected to 15% O_2) for both the shale and Indo/Malaysian residuals. While these points may not actually be the peak concentration of NO_x, both were taken at nearly the same equivalence ratio as the point of highest recorded NO_x for SRC II. The highest NO_x recorded for these two residual fuels was less than the concentration recorded for SRC II due to the lower nitrogen content in each fuel compared to the SRC II (Shale resid, 0.46% N; Indo/Malaysian resid, 0.24% N; and SRC II 0.95% N). The minimum concentration were 65 ppmv and 67 ppmv (corrected to 15% O_2) for the shale residual and the Indo/Malaysian residual oil, respectively. While both minimum concentrations were lower than that of the SRC II (93 ppmv) as expected due to lower nitrogen contents, both residual oils had nearly equivalent minimum values. This was somewhat unexpected since the Indo/Malaysian fuel has roughly half the fuel-bound nitrogen of the shale residual. However, it has been shown by previous testing in Phase IV that the conversion rate of fuel-bound nitrogen to NO_x tends to decline with increasing nitrogen content (i.e., conversion rate for a shale DFM, 0.24% N, was about 337.; and for pyridine-spiked No. 2 fuel, 0.5% N, was about 21% for the ECV combustor). Calculating the approximate conversion rates for the shale and Indo/Malaysian fuels (making the same assumptions as outlined for the SRC II and noting that complete conversion of fuel nitrogen would correspond to an increment in NO_x of 185 ppmv for the shale resid and 102 ppmv for the Indo/Malaysian resid) yield about

12% for the shale and 24% for the Indo/Malaysian, compared to 12% previously calculated for the SRC II. Also of note, atomization differences between the Indo/Malaysian and the shale residuals could partly account for the NO_x concentration being nearly the same at the minimum point and at the peak for the two residuals, since the Indo/Malaysian fuel is predicted to give larger droplet diameters than the shale residual under the same conditions (Table III). A final possible explanation for the higher than expected NO_x concentration exhibited by the petroleum residual lies in the nitrogen evolution characteristics of the test fuels. Nitrogen is bound mainly in the lighter fractions for the SRC II and the shale residual as evidenced by the fact that nearly all the bound nitrogen evolves by about 600°F. The Indo/Malaysian residual exhibits a different trend in nitrogen evolution: nitrogen still persists at temperatures above 1000°F. This implies that when burning the Indo/Malaysian residual, it is possible that the nitrogen evolution from a fuel droplet persists farther into the flamefront (particularly if vaporization is relatively slow and fuel droplets relatively large), meaning a shorter residence time would be available (due to limited combustion volume) for NO_x reducing reactions to occur. Ultimately, this could potentially lead to higher NO_x emissions.

The CO data obtained firing the shale residual and the Indo/Malaysian residual are also presented in Figures 29 and 30. Both CO curves are similar to that for the SRC II middle distillate fuel except that the peak in the Indo/Malaysian residual curve is somewhat lower than that of the shale and SRC II fuels. This lower peak could be due to a lesser degree of premixing for the Indo/Malaysian residual due to a decrement in atomization just postulated. All three fuels appear to produce a CO concentration level of around 75 ppmv (corrected to 15% O_2) at the equivalence ratio corresponding to the minimum in the NO_x curve.

Smoke data were also obtained while operating the combustor with the shale and Indonesian/Malaysian residuals. Values of SAE smoke number recorded were as follows:

Test No.	*Fuel*	*Equivalence Ratio*	*Primary Zone Condition**	*SAE Smoke No. (APR 1179)*
FS-05B-32	Shale Resid	0.1818	1	14.0
FS-05B-33	Shale Resid	0.2490	2	42.6
FS-05B-42	I/M Resid	0.2370	2	51.2
FS-05B-43	I/M Resid	0.2047	1	46.3

*Primary zone conditions: 1 — equivalence ratio near minimum of NO_x bucket (about 1.3)
2 — equivalence ratio above 1.3 (an overly rich condition)

The smoke number for the Indo/Malaysian residual near the NO_x "bucket" is significantly higher than that recorded for either the shale residual or the SRC II (see table on page 16) which again could be due to atomization differences.

No significant change in the operating characteristics of Scheme FS-05B were noted while firing the shale and Indonesian/Malaysian residual fuels, except for an increase in liner temperature which is described in Subsection 2.3.4. Inspection of the combustor liner following this series of tests revealed no build-up of carbon deposits or regions of distress; however, there was further deterioration of the flamespray coating on the interior surface of the primary liner. The premix tube exhibited light deposits of carbon and a varnish type material (see Figure 31) after operating on the two residuals, but less than the build-up noted after operating on SRC II middle distillate (see Figure 28). The deposits in Figure 31 were present after operating about 4.1 hr on the shale residual and about 1.0 hr on the Indo/Malaysian residual separated by a one hour run with No. 2 fuel all at 100 psia rig pressure.

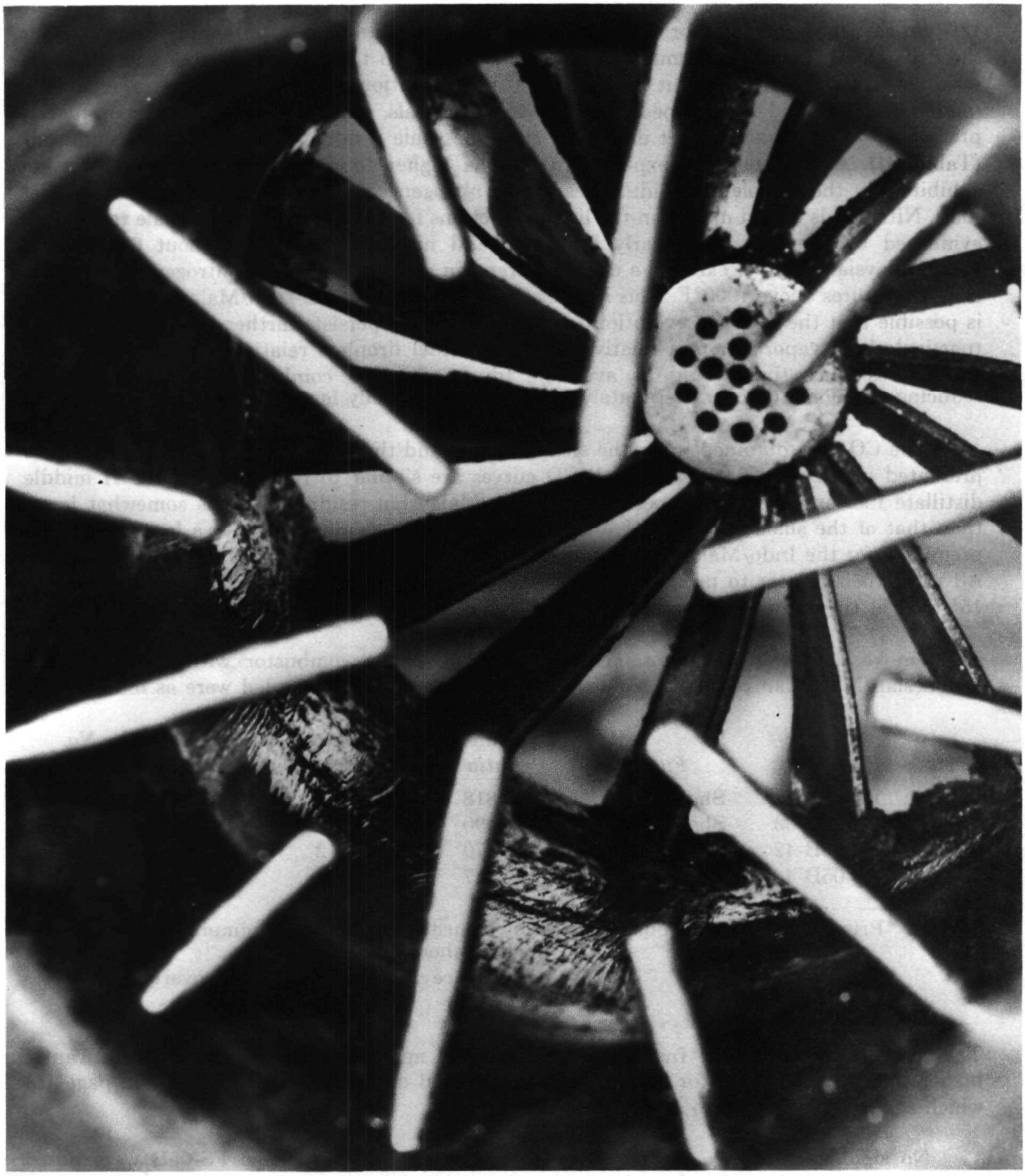

Figure 31. Condition of Premix Tube Swirler and Premixing Passage Following Tests With the Residual Fuels

2.3.2 Emission and Performance Rig Testing of Scheme FS-07A (Nonpremixed Fuel Injection)

It was anticipated (and found to be the case) that operation of the premix tube on the synthetic and residual test fuels could lead to the formation of deposits on the swirl vanes. It was also a concern that by varying the airflow through the premix tube from maximum to minimum (which is necessary for maintaining good emissions from high power to idle conditions for these fuels), velocities within the premixing passage are decreased by a factor of about two. This decrease in velocity would effect not only atomization of the fuel (see Table III) but also the potential for flashback would be increased. In an effort to eliminate the potentially serious swirl vane depositions and to provide a fuel preparation device in which velocity changes would not impact atomization, degree of fuel preparation, or the potential for flashback, a nonpremixed arrangement (shown in Figure 6) was designed. It was reasoned that through the use of a boost air nozzle and from the results of a previous experimental program at P&WA (described in Section 2.1.2), reasonably good fuel preparation could be expected from this device.

A Sonicore model 281T boost-air nozzle fitted in a swirler, which was recessed about three inches from the primary combustion volume, was mounted on the FRT combustor thus comprising scheme FS-07A. In previous atmospheric combustion tests of this fuel preparation device (conducted under a different program), it was observed that a small ring of flame was stabilized within the recirculation zone in the swirl cup. This flame, while tending to increase fuel droplet vaporization and perhaps improve emissions, could tend to produce additional smoke from locally over rich combustion.

No. 2 fuel was first tested in scheme FS-07A. The Indonesian/Malaysian residual and the SRC II were also fired. As with the testing of scheme FS-05B, the No. 2 fuel and the SRC II were not heated, while the temperature of the Indo/Malaysian was elevated to about 180°F by electrical heaters in the supply tank.

2.3.2.1 Emission and Operating Characteristics With No. 2 Fuel

Tests of the RBQQ combustor with a nonpremixed fuel preparation device (Scheme FS-07A, shown in Figure 13) were conducted at 100 psia and 600°F rig inlet conditions firing No. 2 fuel. Exhaust emission data are presented in Figure 32.

In comparing the results of FS-07A (Figure 32) with FS-05B (shown as a dashed line on Figure 32) operating on No. 2 fuel, it can be seen that the minimum NO_x recorded is nearly the same in both cases (about 43 ppmv, corrected to 15% O_2). The flat portion of the curve (which begins at a primary zone equivalence ratio of about 1.3) appears at about the same equivalence ratio which implies that the primary airflow, and likewise residence times are comparable for the two schemes. The peak in the NO_x concentration data is vastly different: about 120 ppmv (corrected to 15% O_2) for the nonpremixed configuration, Scheme FS-07A; and about 372 ppmv (corrected to 15% O_2) using the premix tube, Scheme FS-05B. Since atomization was predicted to be about the same (see Subsection 2.1.2) the difference must be accounted for by the degree of fuel preparation provided by each device. In Figure 33, data are shown in which the supply pressure to the boost air nozzle was varied. It can be seen in this figure that as the boost air pressure and subsequently the boost air pressure ratio (BAPR) is increased, the NO_x concentration declines while the CO increases. This has been shown to be indicative of the degree of fuel preparation. Improved fuel preparation, in this case caused by increased BAPR, results in lower NO_x emissions.

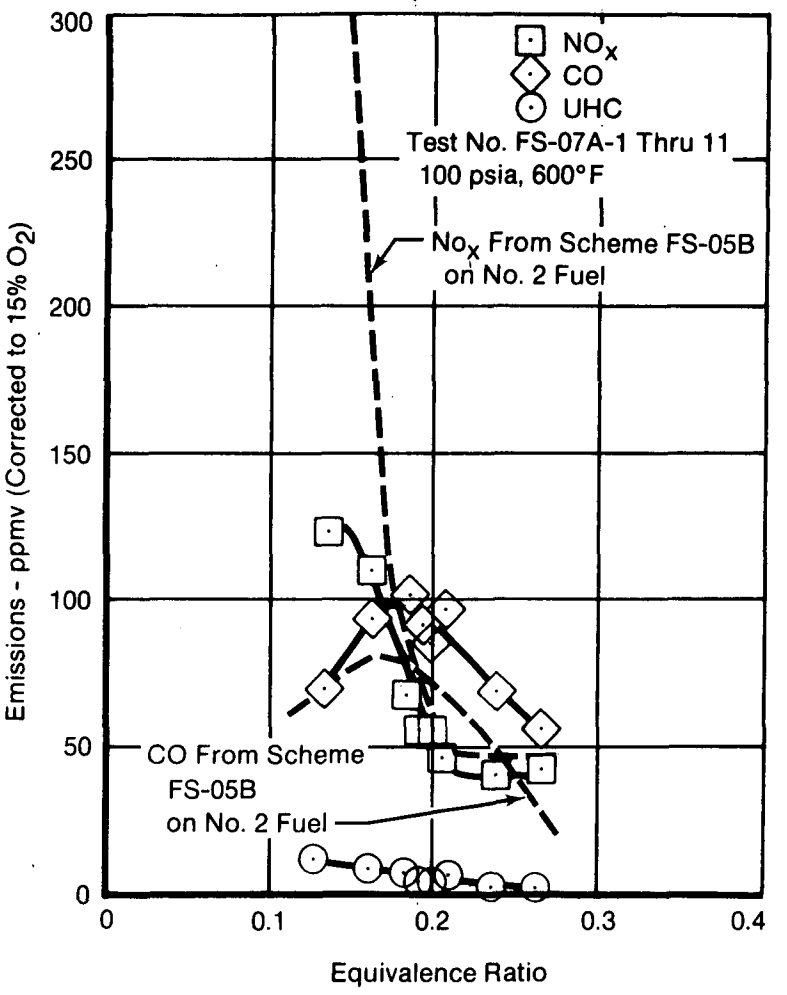

Figure 32. Emission Signature of Scheme FS-07A Firing No. 2 Fuel

CO concentration data for Scheme FS-07A is somewhat higher than for Scheme FS-05B. This result is not fully understood since it was expected that the nonpremixed configuration (FS-07A) would have lower CO than the premixed configuration. Most data points with FS-07A were at an inlet temperature of nearly 620°F while the temperature for FS-05B was about 610°F. This in conjunction with a minor change in airflow distribution (predicted in the scheme definition sheets, Figures 15 and 16) could account for the 20 ppmv difference in CO concentrations.

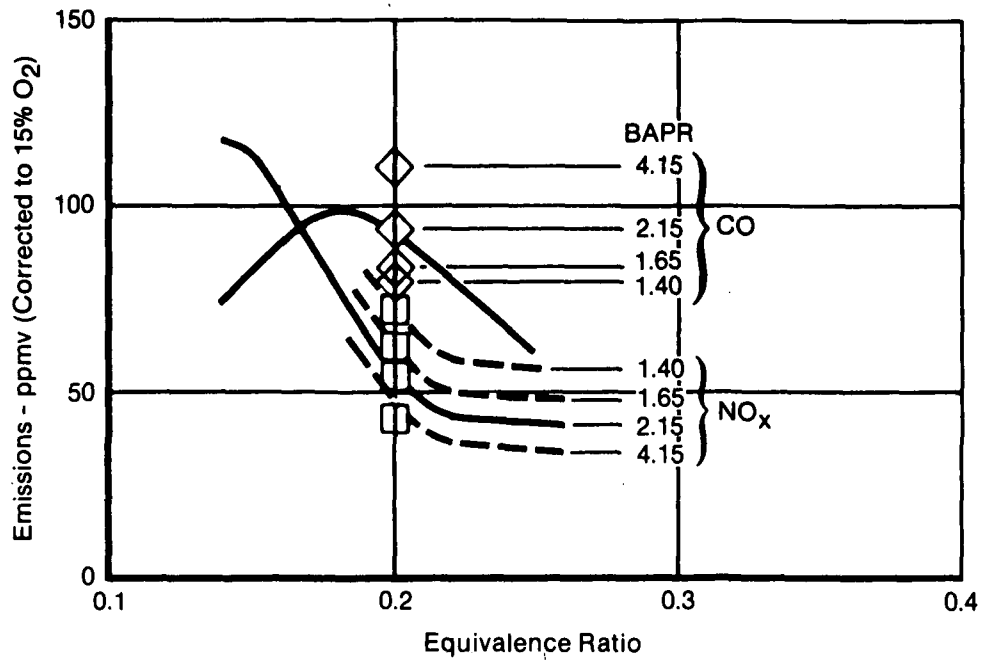

Figure 33. Effect of Boost Air Pressure Ratio (BAPR) on NO_x and CO Emissions of Scheme FS-07A

2.3.2.2 Emission and Operating Characteristics With Alternative Fuels

A limited number of data points were taken with Scheme FS-07A firing the Indonesian/Malaysian residual and SRC II middle distillate fuel to define the bottom of the NO_x "bucket" for each. Test conditions were again 100 psia and 600°F at the rig inlet. The exhaust emission data for the Indo/Malaysian residual and the SRC II are presented in Figures 34 and 35, respectively.

CO data for the two alternative fuels are nearly identical and correspond quite closely to that of No. 2 fuel. Again this data is higher than that obtained for the same fuels when fired in Scheme FS-05B.

The minimum NO_x concentration levels attained with this nonpremixed configuration of the combustor when firing the Indo/Malaysian and SRC II fuels were lower than those attained with the premixed configuration (Scheme FS-05B). Minimum NO_x levels recorded were 56 ppmv for the Indo/Malaysian residual and 80 ppmv for the SRC II middle distillate, compared to 67 ppmv and 93 ppmv obtained with Scheme FS-05B for the same two fuels, respectively (all values corrected to 15% O_2).

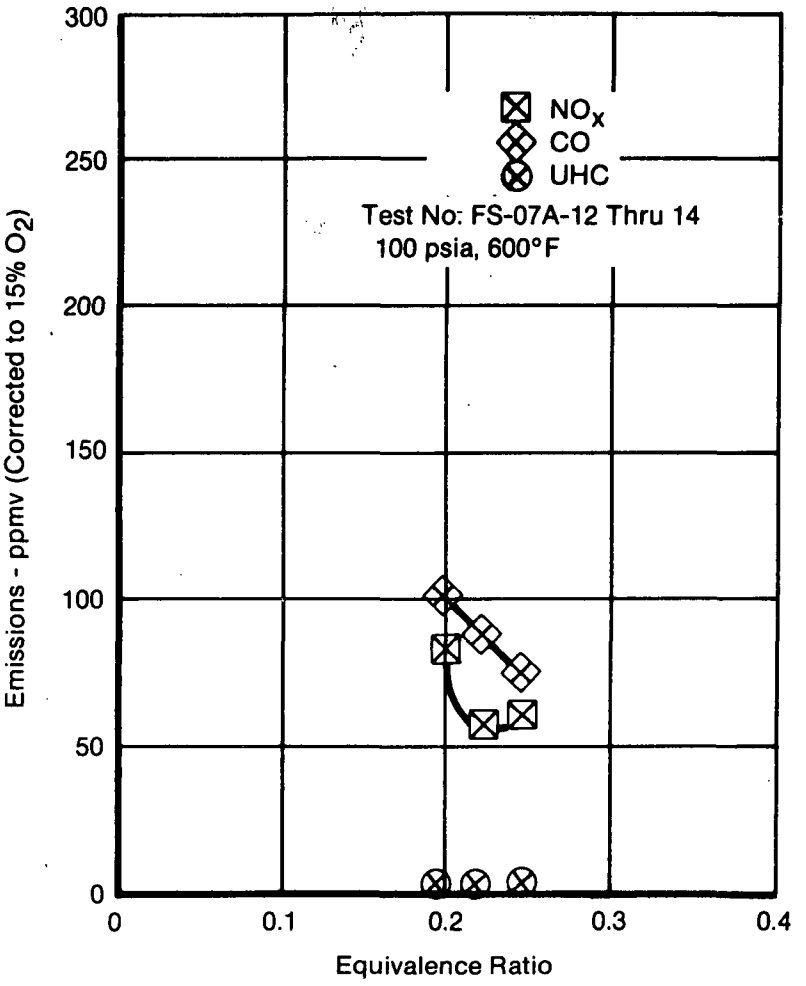

Figure 34. Emission Signature of Scheme FS-07A Firing Indonesian/ Malaysian Residual

By making the same assumptions as previously stated, approximate conversion rates of fuel-bound nitrogen to NO_x were calculated. A summary of the conversion rates follows:

Fuel	*Scheme FS-05B*	*Scheme FS-07A*	*Complete Conversion of Fuel N to NO_x (15% O_2)*
SRC II (0.95% N)	12%	9%	424 ppmv
Shale Resid (0.46% N)	12%	Not Tested	185 ppmv
Indo/Malay. Resid (0.24% N)	24%	15%	102 ppmv

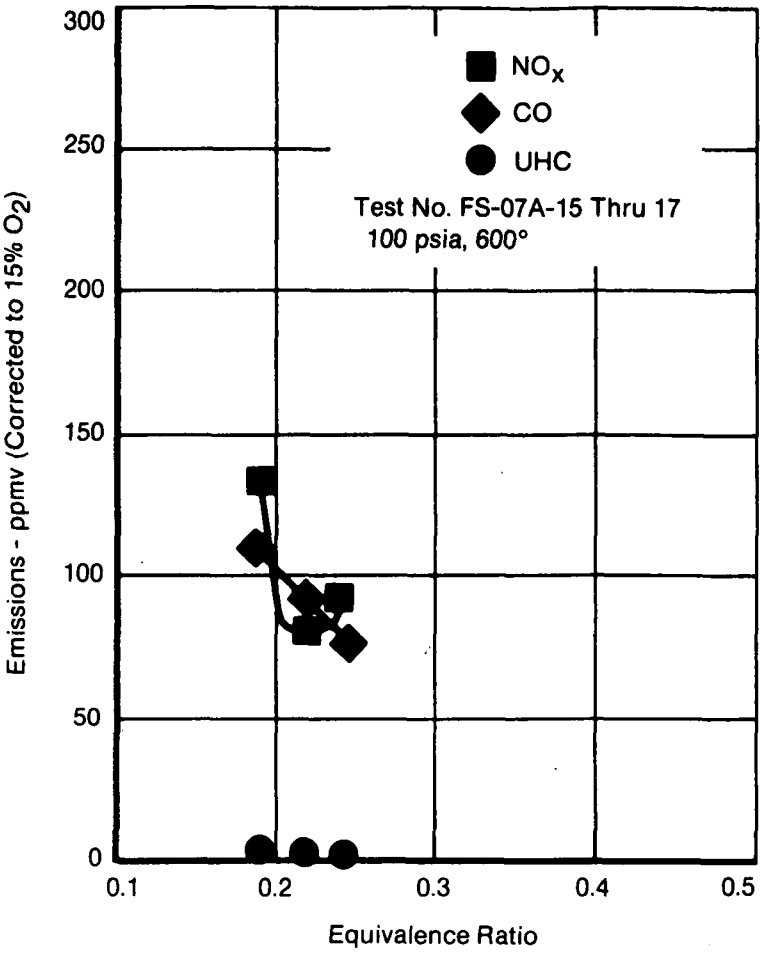

Figure 35. Emission Signature of Scheme FS-07A Firing SRC II Middle Distillate

It was postulated that the reasons for the lower levels of NO_x attained with the nonpremixed configuration of the FRT combustor over those attained with the premixed configuration were:

1. Improved atomization of the heavier fuels by the additional atomizing energy supplied by the boost-air nozzle;

2. Improved atomization would result in more rapid vaporization of the fuel droplets which would evolve the bound nitrogen earlier in the combustion process. This in turn would allow more time for NO_x reducing reactions to occur.

Smoke data were also taken for combustor scheme FS-07A. A summary of the SAE smoke numbers obtained for this version of the FRT combustor as well as for scheme FS-05B for reference is as follows:

Fuel	*Combustor Configuration*	*Test No.*	*Equivalence Ratio*	*Approximate Primary Zone Condition**	*SAE Smoke No. (ARP 1179)*
No. 2 Fuel	Premixed	FS-05B-36	0.1265	3	1.8
	Nonpremixed	FS-07A-1	0.1354	3	0.7
		FS-07A-6	0.2629	2	43.5
		FS-07A-11	0.1988	1	13.9
SRC II Middle Distillate	Premixed	FS-05B-22	0.2134	1	9.9
		FS-05B-23	0.2590	2	44.9
		FS-05B-24	0.1269	3	1.6
	Nonpremixed	FS-07A-16	0.2190	1	31.0
Shale Resid.	Premixed	FS-05B-32	0.1818	1	14.0
		FS-05B-33	0.2490	2	42.6
	Nonpremixed	—	—	—	Not tested
Indo/Malaysian Resid.	Premixed	FS-05B-42	0.2370	2	51.2
		FS-05B-43	0.2047	1	46.3
	Nonpremixed	FS-07A-14	0.1949	1	23.2

* 1 — primary equivalence ratio near the bottom of the NO_x bucket
2 — primary equivalence ratio overly fuel rich
3 — lean primary equivalence ratio

In reviewing the smoke data obtained, there was some indication that more smoke was formed by the nonpremixed configuration compared to the premixed configuration as evidenced by the SRC II data (9.9 for the premixed case versus 31.0 for the nonpremixed). There also appears to be some indication that the premixed configuration formed more smoke when operated on fuels which were insufficiently atomized by the premix tube as seen in the Indo/Malaysian smoke data (23.2 for the nonpremixed configuration versus 46.3 for the premixed configuration). However, the smoke data are inconclusive, except for the expected observation that the smoke formed was generally well below the acceptable level (a smoke number of about 20 is usually considered the visible threshold) until the primary zone equivalence ratio exceeded the design point optimum (about 1.3) by a wide margin, and became overly fuel rich.

The operating characteristics of scheme FS-07A remained nearly the same as scheme FS-05B. A slight change in the flow distribution was noted for this scheme due to minor differences in the flow characteristics of the nonpremixed fuel preparation device compared to the premix tube. Inspection of the combustor primary zone liner again revealed further degeneration of the flamespray coating on the interior surface; however, there were no regions of distress or areas of carbon deposits evident (see Figure 36).

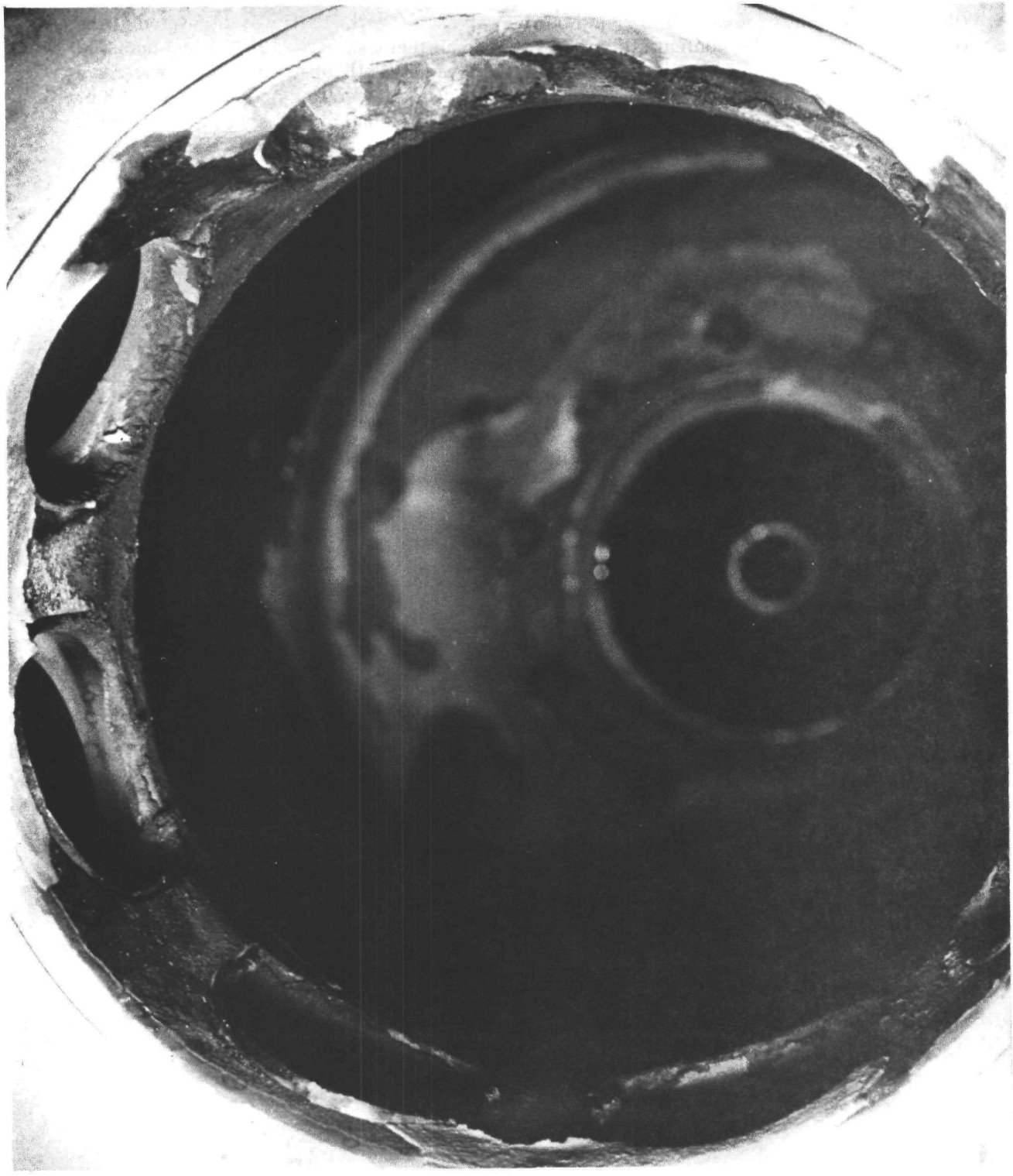

Figure 36. Condition of Interior Surface of Primary Liner Following Tests Through Scheme FS-07A

As seen in Figure 37, the fuel preparation device exhibited minor deposits of carbon on the swirl vanes, on the nozzle shroud, and on the wall of the swirl cup. It was discovered at the conclusion of testing this configuration that a very small fuel leak existed in the fuel manifold which would account for the deposits on the swirl vanes (both upstream and downstream sides). The deposits shown in Figure 37 were present after an operating period of about 1.8 hr on No. 2 distillate, about 0.4 hr on Indonesian/Malaysian residual oil, and about 0.4 hr on SRC II middle distillate fuel at 100 psia with a subsequent shutdown on the SRC II.

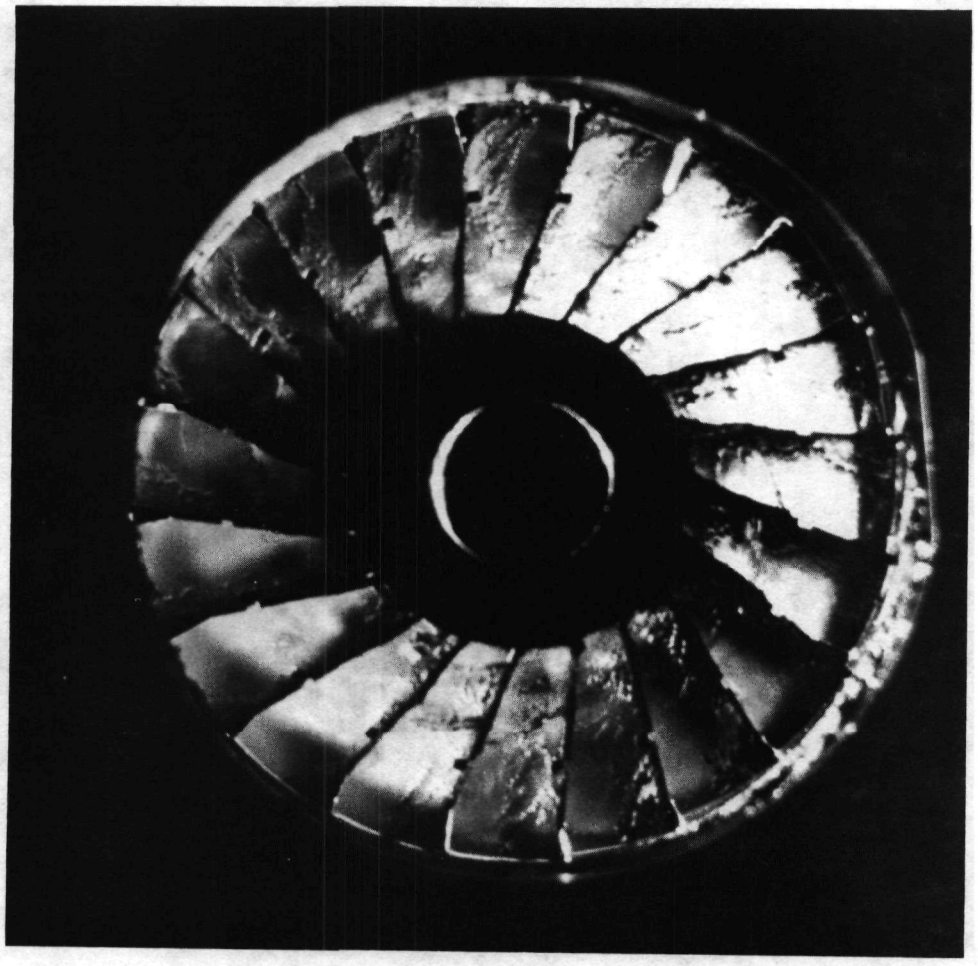

Figure 37. Condition of Nonpremixed Fuel Preparation Following Tests With Residual and SRC II Fuels

2.3.3 Exit Temperature Profiles

Combustor exit gas stream temperatures were measured using the rig traverse probe. Thermocouples are provided at nine locations, equally spaced over the circumference of the annular exit transition piece. In the tests conducted, readings were taken at a fixed radial position near mid-span. The radial traverse capability of the probe was not used in order to maximize the run time available for generating basic emission signatures of the combustor while firing the test fuels.

Exit thermocouple data obtained during operation of the combustor on No. 2 fuel are presented in Table VII of Appendix A, and in Figures 38 through 41. A strong central peak is evident in the circumferential profile of the combustor at all operating conditions, with peak-to-minimum differentials approaching 1600°F at some test points. These results are generally comparable to those obtained in Phase IV testing for scheme FS-03A at 50 psia rig pressure, although the gradients obtained for scheme FS-05B appear slightly more severe in some cases (this difference may result from the use of axially directed final dilution jets in scheme FS-05B, as opposed to conventional radially directed jets in scheme FS-03A).

Exit temperature data obtained during operation of the combustor on SRC II middle distillate fuel are presented in Table VII of Appendix A and Figure 42. The circumferential profiles shown are less well defined than those obtained for No. 2 fuel because of the loss of several thermocouples on the traverse probe. Based on available data however, the measured temperature levels and profile gradients appear to be the same for the two fuels.

With continued testing, there was progressive deterioration of the thermocouples on the exit traverse probe. Readings recorded were often erratic and were considered unreliable. Examination of the hardware indicated that the straps securing the thermocouples to the body of the probe had failed, and that most of the thermocouples were lost due to aerodynamic buffeting.

The thermocouples were refurbished, only to again fail by the same method when testing was resumed. Two test points were obtained with the shale residual fired in scheme FS-05B. These data are shown in Figure 43; however, since the probe was not located at the radial mid-span point, no comparisons could be made.

For the test points where sufficient exit temperature data were available, values of *temperature pattern factor* (peak-to-average temperature differentials normalized to overall temperature rise) were calculated and presented in Table V of Appendix A and Figure 44. The range of values obtained (0.3 to 0.6), while substantially higher than the generally accepted target range of 0.2 to 0.3 is slightly lower than the range of values obtained for scheme FS-03A in Phase IV. As noted in Figure 44, many of the values of TPF reported were computed from partial temperature data because of the progressive loss of thermocouples on the exit traverse probe. It should also be noted that the high values of TPF obtained for schemes FS-05A/5B are consistent with those obtained previously for scheme FS-03A. These high values appear to be the result of ineffective mixing in the aft dilution section of the combustor. Because of high-velocity flow in the center of the passage, it is not unexpected that penetration and mixing in this section may be ineffective. Alternative designs for the aft dilution section, employing perhaps mainstream swirl, or a second quick-quench style mixing section, may ultimately be required if a substantial reduction in pattern factor is sought for industrial gas turbines requiring a retrofittable in-line combustor design.

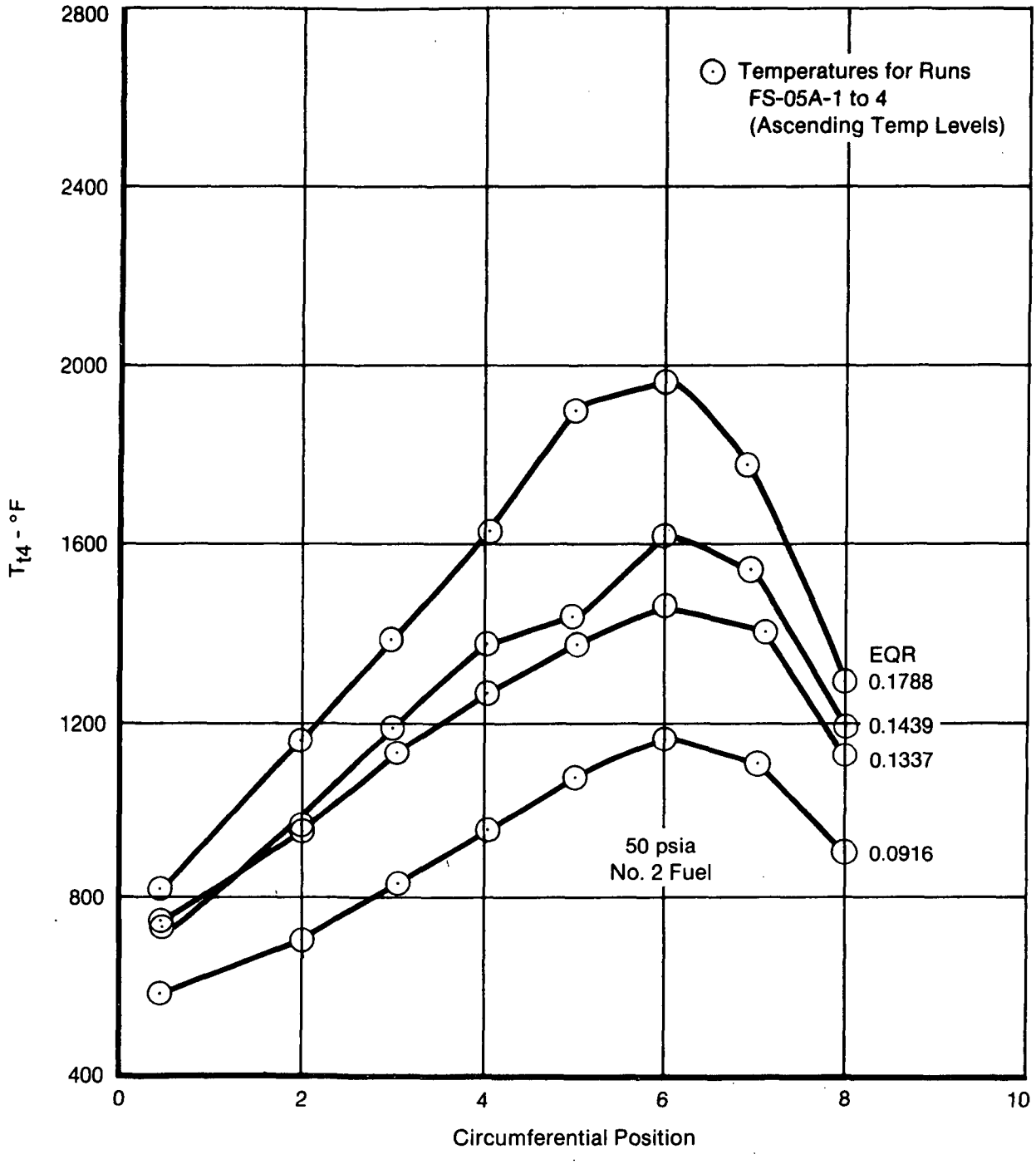

Figure 38. Exit Temperature Profiles (Probe at Mid-Span)

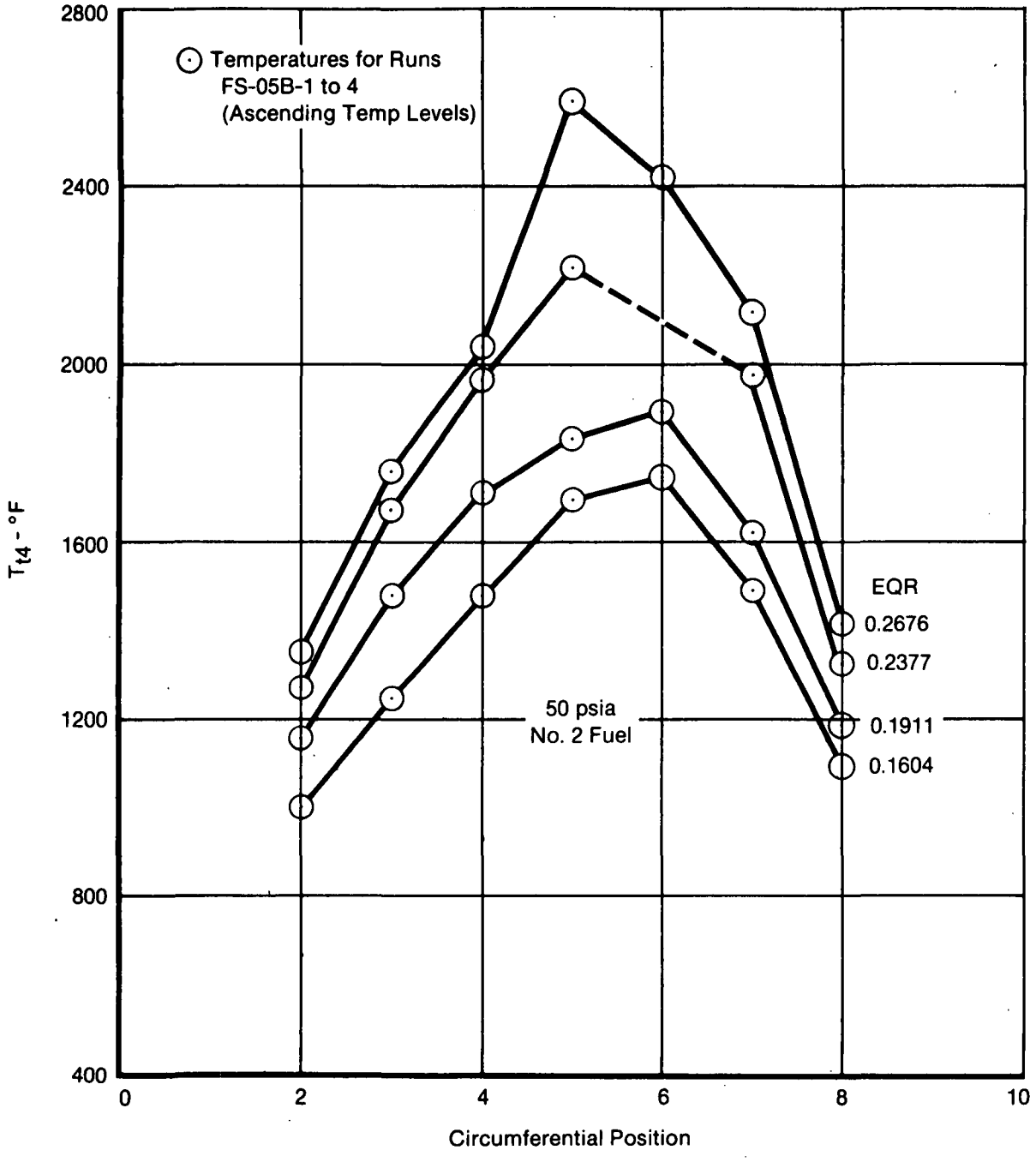

Figure 39. Exit Temperature Profiles (Probe at Mid-Span)

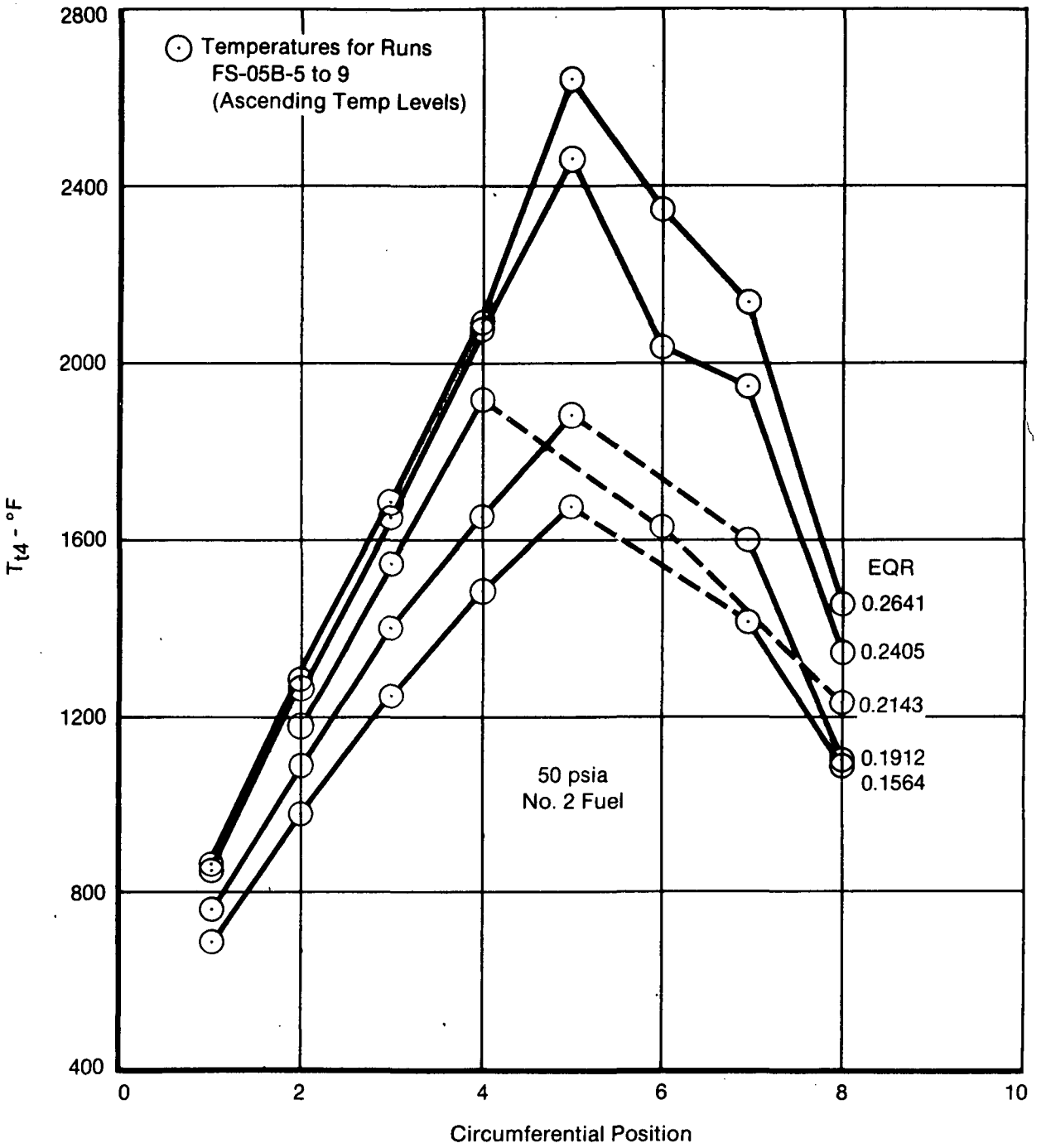

Figure 40. Exit Temperature Profiles (Probe at Mid-Span)

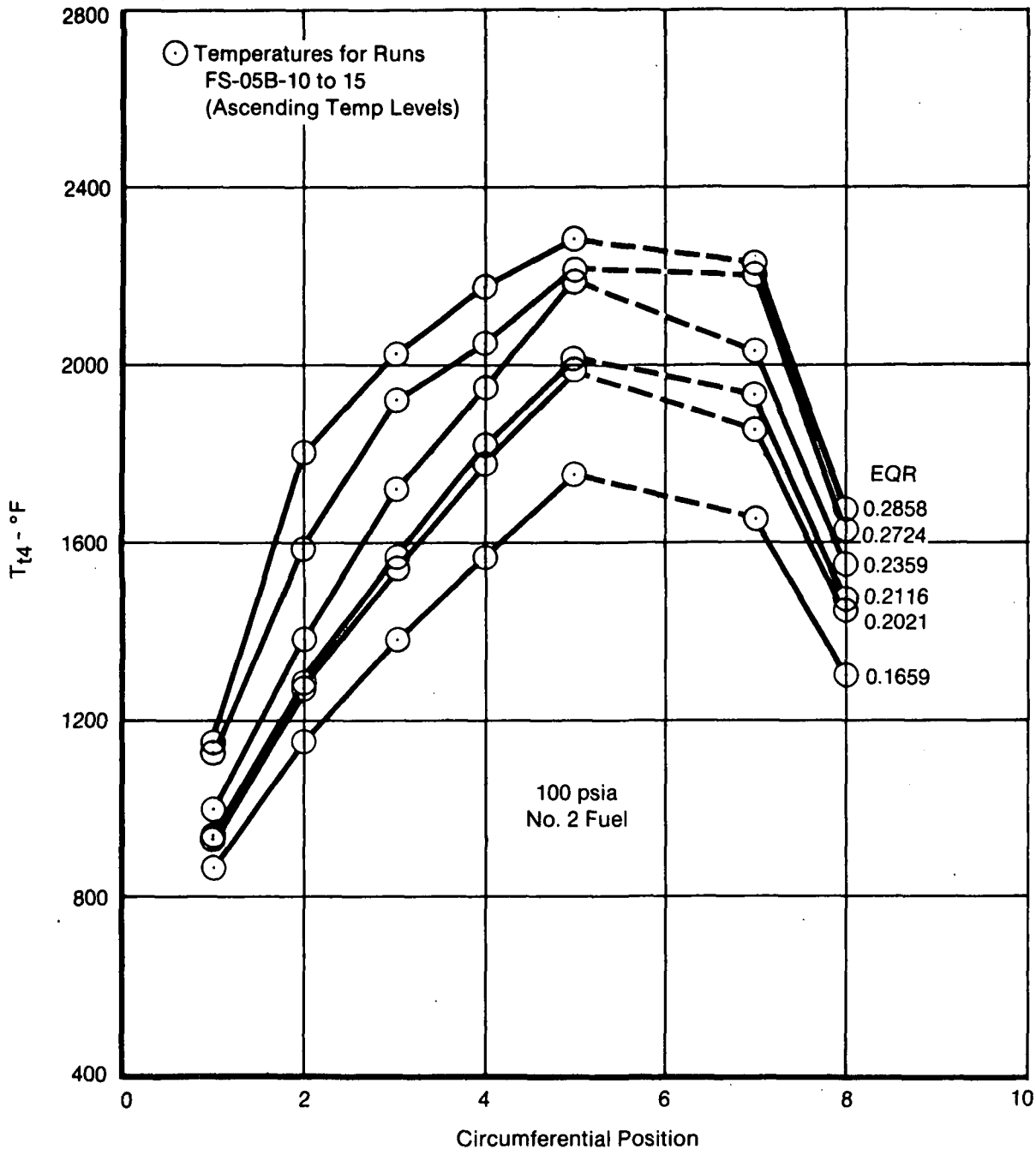

Figure 41. Exit Temperature Profiles (Probe at Mid-Span)

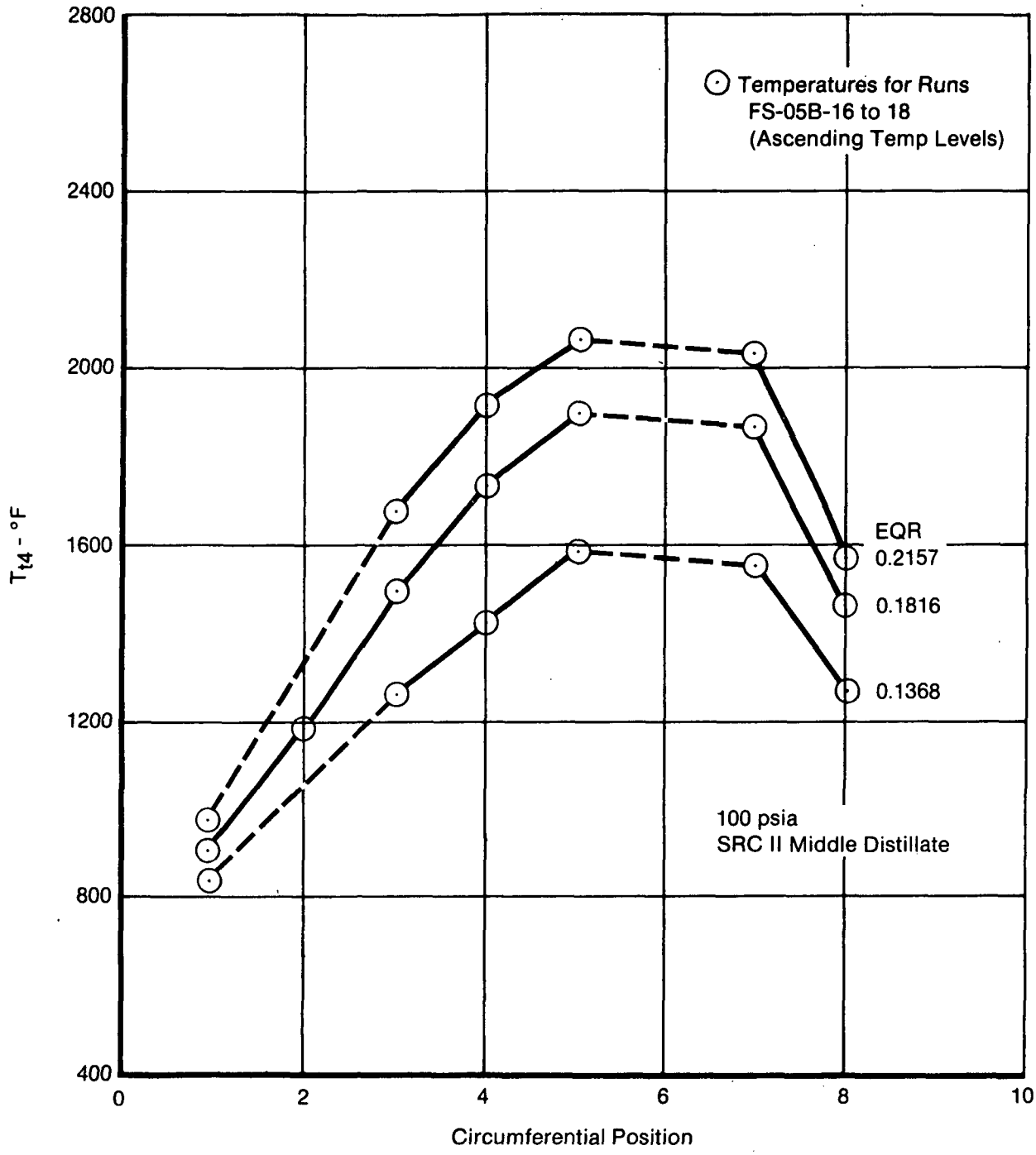

Figure 42. Exit Temperature Profiles (Probe at Mid-Span)

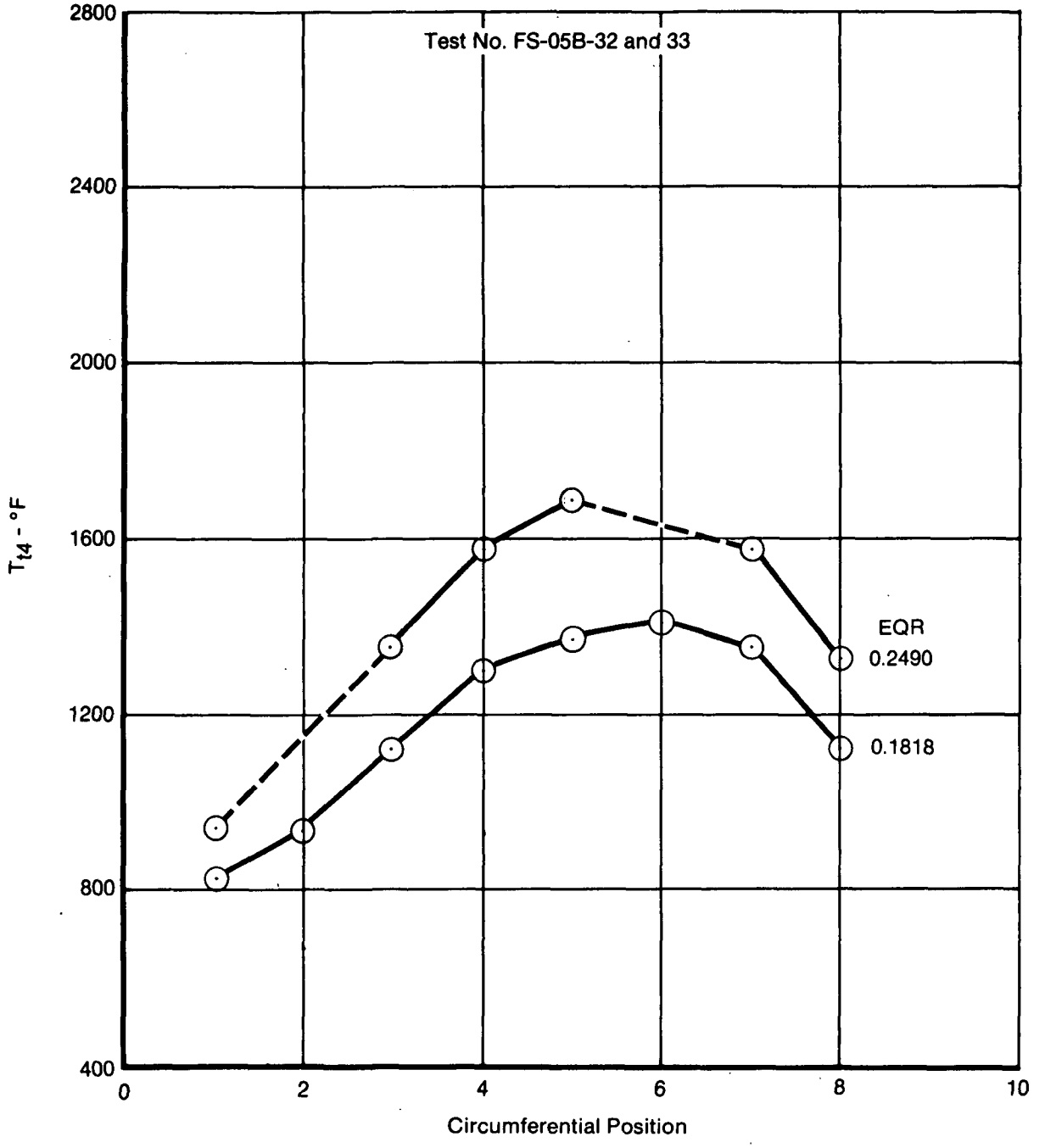

Figure 43. Exit Temperature Profile of Scheme FS-05B Firing Shale Residual (Probe Off Midspan)

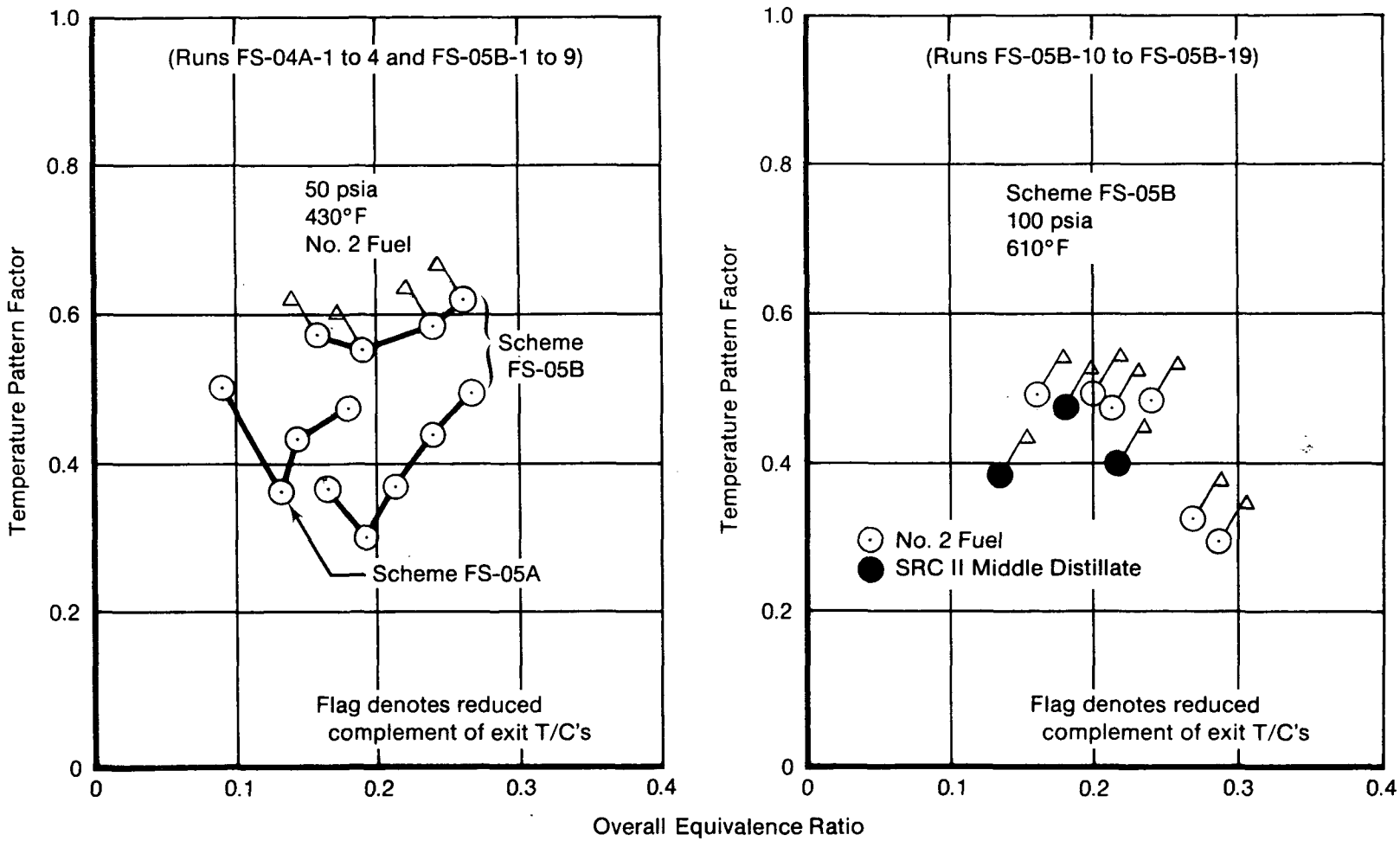

Figure 44. Variation in Temperature Pattern Factor With Overall Equivalence Ratio for Tests Conducted With Schemes FS-05A and FS-05B

2.3.4 Liner Heat Transfer Characteristics

The increased radiation associated with burning synthetic and residual fuels (due to higher carbon content in relation to hydrogen content) can be expected to cause an increase in the heat transmitted to the combustor liner. The carbon content, hydrogen content, and the carbon to hydrogen mass ratio (which is an indication of the molecular make-up of the fuel) of the four test fuels are:

Fuel	*Carbon Content (% wt)*	*Hydrogen Content (% wt)*	*Carbon/ Hydrogen Ratio (by wt)*	*Hydrogen/Carbon Molar Ratio*
No. 2 Fuel	86.763	13.272	6.537	1.823
Shale Resid	86.710	12.760	6.795	1.754
Indo/Malaysian Resid	86.530	11.930	7.253	1.643
SRC II Middle Distillate	85.770	9.200	9.323	1.278

The fuels are listed in order of increasing carbon/hydrogen ratio which is the order of expected increasing combustion radiation if the conditions of combustion are equal. To establish baseline values of the liner heat load, and to determine the variation in heat load with fuel type, extensive instrumentation was added to the combustor to measure the primary zone convective cooling airflow, and to document combustor liner metal temperatures in all sections of the combustor.

Data obtained showing the primary liner convective cooling air temperature rise along with calculated rates of heat removal are presented in Table VI of Appendix A. Also included are normalized liner temperature rise data based on measured combustor liner metal temperatures of the primary and secondary zones. Liner temperature readings are given in Table IV of Appendix A. Combustor liner temperatures were used to compute values of the liner temperature rise factor (LTRF). This parameter provides a basis of comparison for different fuels, or for different methods of fuel preparation in terms of average liner temperature rise (normalized to burner ideal temperature rise). Although values of LTRF can be expected to vary in magnitude with the number and placement of thermocouples, with the movement of the flamefront within the combustor, and perhaps with other factors, it remains a useful indicator of the relative change in liner temperatures when identical tests (same combustor and same operating conditions) are conducted using different fuels or varying degrees of fuel preparation. Liner temperature rise factor is defined by equation 3.

$$LTRF = \frac{(T_{LAVG} - T_{TIN})}{\Delta T_{IDEAL}} \tag{3}$$

where:

T_{LAVG} = average liner temperature from thermocouples — °F
T_{TIN} = combustor inlet temperature — °F
ΔT_{IDEAL} = combustor ideal temperature rise — °F

LTRF was first calculated using the average of all thermocouples affixed to both the primary and secondary liner outer surfaces, for the first several sets of test numbers which had a sufficient number of thermocouples remaining on the primary liner so as not to artificially weight the average temperature toward the secondary liner temperature. When plotted against equivalence ratio (the lower curves in Figures 45 and 46) these data exhibit an apparent peak in LTRF at about 0.15 overall equivalence ratio. Although calculations of LTRF were performed for the purpose of determining the influence of fuel type on liner temperature, no significant differences were noted. At 100 psia rig inlet pressure (Figure 46) there was some apparent scatter in the data for SRC II, however, no clear increase in liner temperature can be claimed when compared to No. 2 fuel data. While half of the SRC II data points lie above the curve, the other half are reasonably close to the line. The highest value of LTRF computed (for SRC II at an overall equivalence ratio of about 0.137) is believed to be in error. This point (which was recorded at a relatively low overall equivalence ratio setting) was taken immediately following a high equivalence ratio point. It apears that insufficient time was allowed for complete liner thermal response and stabilization to occur.

In an attempt to isolate the influence of fuel type on primary liner temperature, LTRF was recalculated using only the primary liner thermocouples for determining the average liner temperature (again for only those test numbers where a sufficient number of thermocouples remained on the primary liner). The results of these calculations appear as the upper curves in Figures 45 and 46. The characteristics exhibited are similar to those obtained for the overall LTRF except that the levels are generally higher. Upon further examination of the data, it appears that the final points taken on SRC II show an increase in LTRF over the trends of the earlier points. This result may indicate a change in the heat transfer characteristics of the combustor liner. It has been postulated that the flamespray coating on the interior liner surface may have deteriorated and caused an increase in the surface emissivity along with a corresponding increase in liner temperature.

While LTRF may be computed based on the reading of only one or two thermocouples, a parameter based on only a few readings would not represent the thermal condition of the entire liner, and would tend to exhibit excessive data scatter. Since nearly all the thermocouples on the primary zone liner were lost only part way through the test program, the LTRF calculated for the primary liner and also for the entire liner were considered unreliable for comparison purposes after Test No. FS-05B-22. For this reason, LTRF based on the average of the secondary zone liner thermocouples (LTRFS) was used in comparing all the data obtained in Phase VI testing.

LTRFS was plotted against equivalence ratio for scheme FS-05B, the premixed configuration of the RBQQ combustor, and is shown for the various test fuels in Figure 47. LTRFS data for scheme FS-07A, the nonpremixed configuration, is presented in Figure 48 with a dashed line representing No. 2 fuel data of scheme FS-05A shown as a reference. It is interesting to note the shape of all the curves in these two figures. LTRF of the secondary liner remains about constant until an equivalence ratio of about 0.2 was reached. At this point LTRFS began to rise quite rapidly followed by a leveling off. This effect can be interpreted as the growth of the flamefront into the secondary, or the point at which the stoichiometry within the secondary zone allows stabilization of flame. When this occurs, radiation from the flame established in the secondary zone begins to have a significant contribution to the heat load on the secondary liner. This is also consistent with the CO emission signature, since CO consumption (decline in the curve) begins at about 0.17 equivalence ratio (EQR) and is well established by 0.2 EQR.

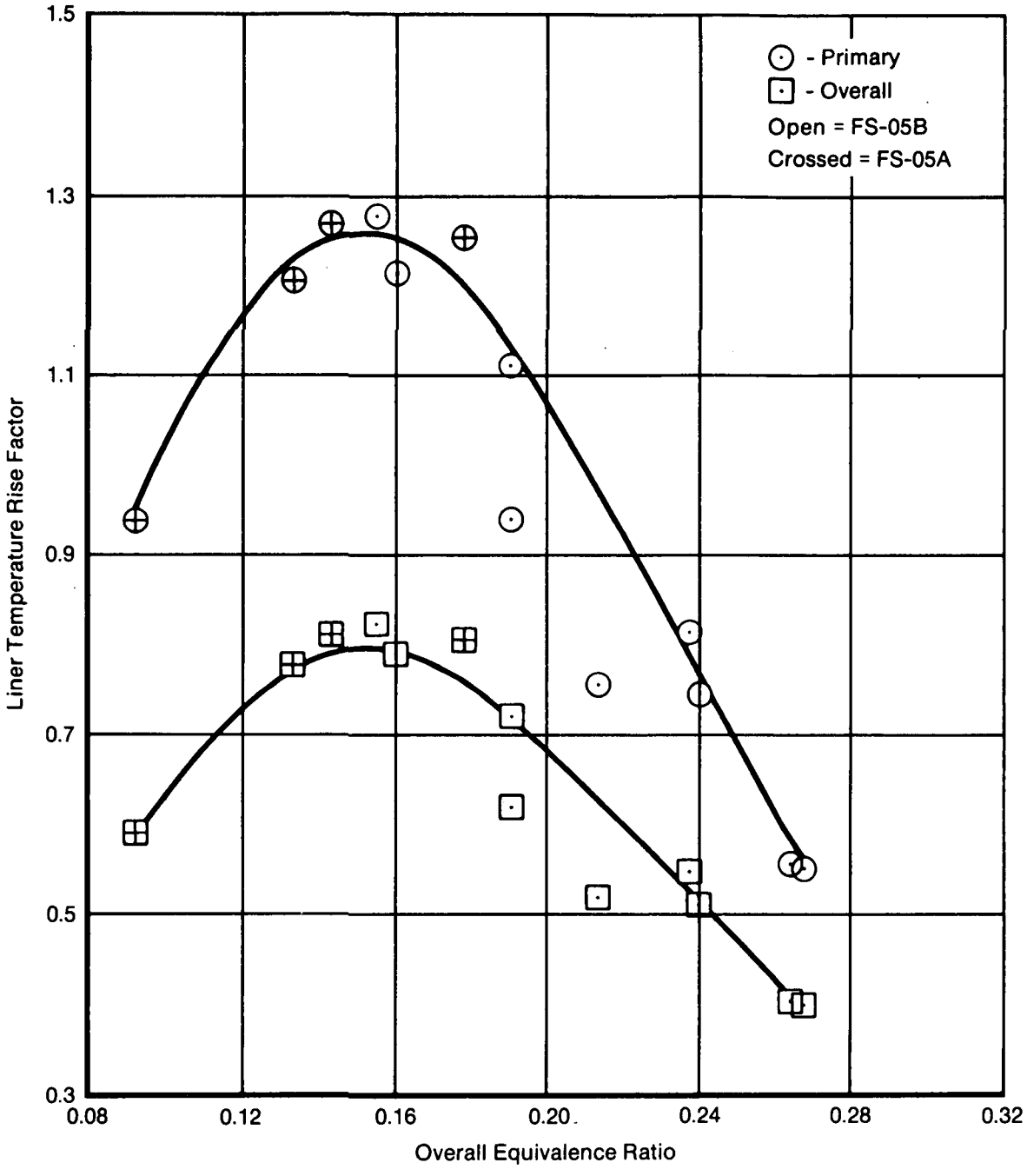

Figure 45. Liner Temperature Rise Factor as a Function of Equivalence Ratio at 50 psia Firing No. 2 Fuel

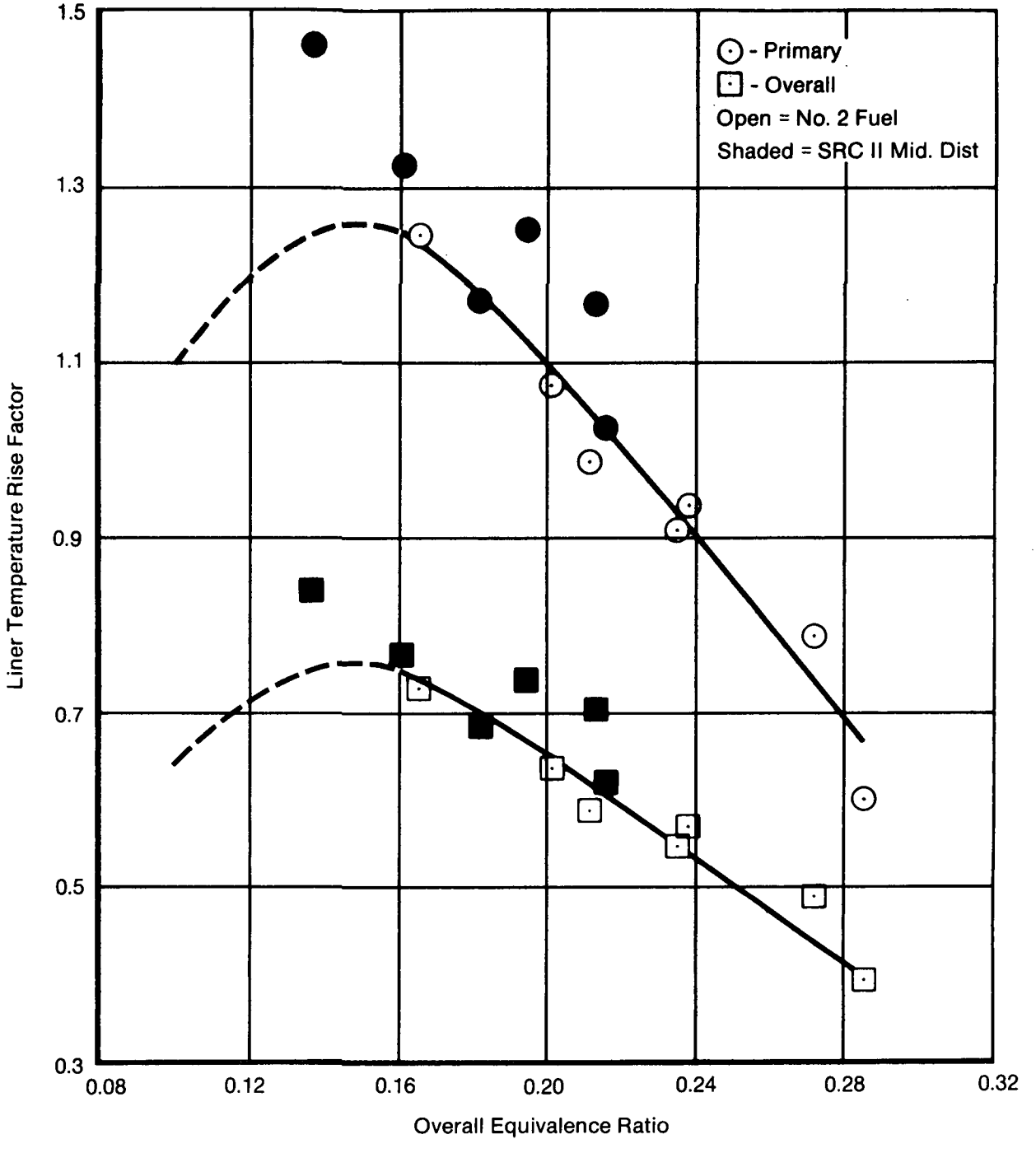

Figure 46. Liner Temperature Rise Factor as a Function of Equivalence Ratio at 100 psia

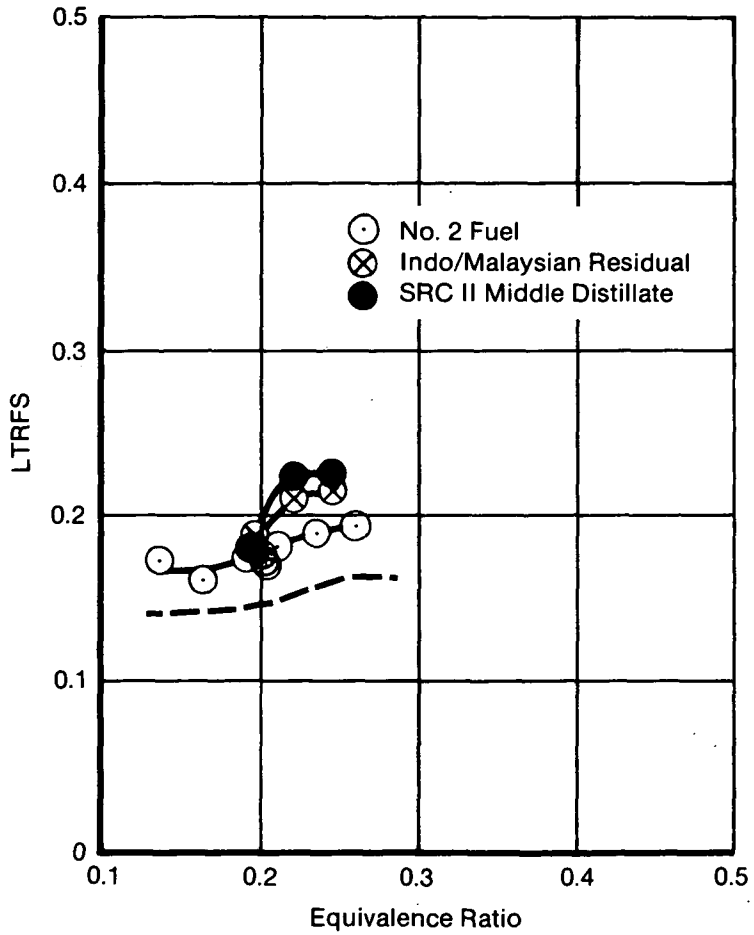

Figure 47. Effect of Equivalence Ratio and Fuel Type on Secondary Zone Liner Temperature Rise Factor for Scheme FS-05B

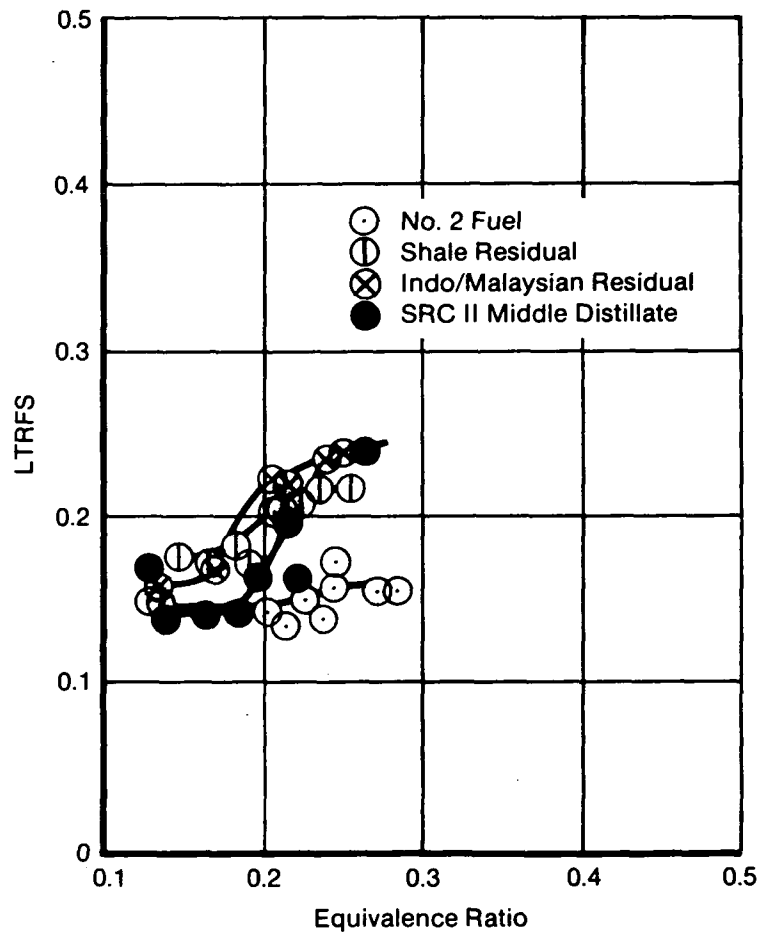

Figure 48. Effect of Equivalence Ratio and Fuel Type on Secondary Zone Liner Temperature Rise Factor for Scheme FS-07A at 100 psia

In examining the data for the nonpremixed combustor (scheme FS-07A), shown in Figure 48, it was evident that the secondary liner experienced a higher temperature rise when the Indo/Malaysian residual or the SRC II was fired than when operating on No. 2 fuel (once flame was established in the secondary zone). There also appears to be consistency between the carbon/hydrogen ratio of the fuel used and the corresponding liner temperature rise. The level of the No. 2 fuel LTRFS for scheme FS-07A is somewhat higher than that generated by scheme FS-05B. The difference is attributed to the degree of fuel preparation. From LTRFS alone it was concluded that the premix tube functioned better than the nonpremixed fuel preparation device on No. 2 fuel.

In examining Figure 47, it can be seen that all the synthetic and residual fuels tested caused an increased LTRFS over that of No. 2 fuel (once flame was established in the secondary zone), although the levels are less distinct than those in Figure 48. This lack of distinction may be attributable to the differences in fuel preparation provided by the premix tube. The degree of fuel preparation of the nonpremixed configuration was more nearly constant for the various fuels (see Table III). Knowledge of this fact implies that the degree of fuel preparation provided by the premix tube may be nearly the same as that provided by the nonpremixed configuration (by looking only at the effect on LTRFS) for SRC II and the Indo/Malaysian residual, since the levels of LTRFS are nearly the same. Another item of interest in Figure 47 is that curves for the two residual fuels exhibit a rapid increase in LTRFS at a lower equivalence ratio. This effect may be due to the higher viscosities of the residual fuels, which cause larger fuel droplets, resulting in an extension of the flamefront into the secondary zone.

For the test numbers where a sufficient number of thermocouples on the primary zone liner were present to allow calculation of an average temperature representative of the actual liner temperature, a convective heat transfer balance for the primary liner was performed using the average primary liner temperatures and the measured quick quench air (primary liner cooling air) temperature rise. The heat removed from the primary liner by convection was calculated using equation 4 and the heat added to the quick quench air was calculated with equation 5.

$$Q_{LIN} = h_c * A * (T_{LIN.PRIMARY} - T_{COOL}) \quad (4)$$

$$Q_{QA} = WA_{SEC} * Cp * (T_{QQ} - T_{IN}) \quad (5)$$

where:

Q_{LIN}	=	heat removed from primary liner — Btu/hr
Q_{QA}	=	heat added to quench air — Btu/hr
$T_{LIN.PRIMARY}$	=	measured average primary liner temperature — °F
T_{QQ}	=	quick quench air temperature — °F
T_{IN}	=	combustor inlet temperature — °F
T_{COOL}	=	average liner cooling gas temperature = $(T_{QQ} + T_{IN})/2$ — °F
C_p	=	specific heat of air at T_{COOL} — Btu/lb — °F
WA_{SEC}	=	measured liner cooling flowrate — lb/hr
A	=	approximate primary liner surface area = 4.694 — ft^2
h_c	=	convective heat transfer coefficient = Btu/hr-ft^2 — °F

From modeling results obtained previously in Phase III, the heat transfer coefficient h_c was estimated to be 225.7 Btu/hr-ft^2-°F for 100 psia operation, and 143.3 Btu/hr-ft^2-°F for 50 psia operation. Ideally, the heat removed from the primary liner should be equal to the heat added to the quench air, neglecting losses and assuming that the heat transfered from the primary liner to the shroud by radiation will be added back to the quench air by convection. Figure 49 shows the data in relation to the ideal heat balance line.

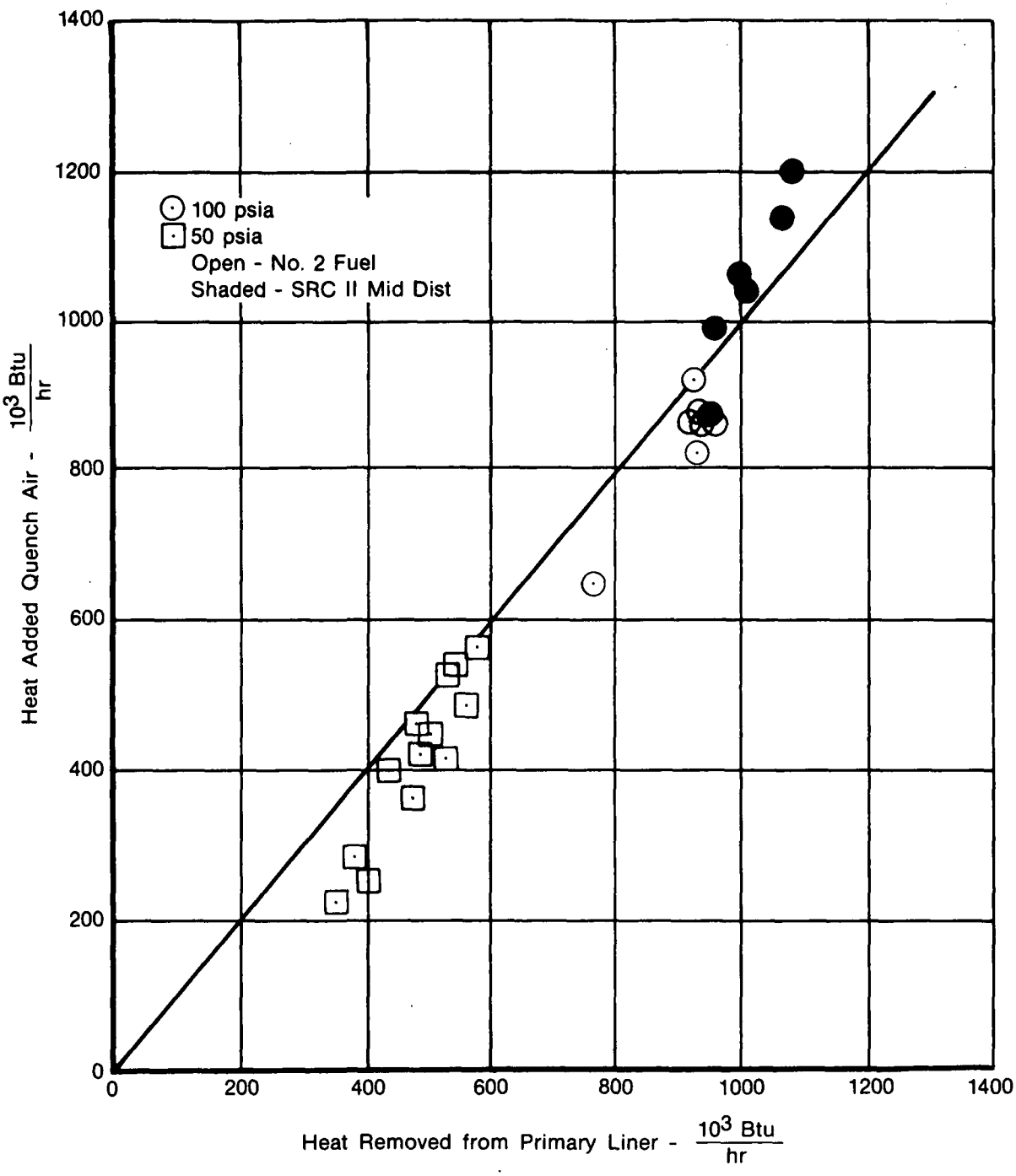

Figure 49. Primary Liner Convective Heat Transfer Balance

The heat removed from the primary zone liner and added to the quick quench air (defined by equation 5) was based on the temperature rise of the quench air. This parameter, called HREMV in Appendix A is plotted against equivalence ratio for schemes FS-05B, and FS-07A and shown in Figures 50 and 51, respectively. In examining these figures, it can be seen that the same trends of the effects of fuel type and degree of preparation on liner temperature (seen here by the resulting heat added to the primary zone convective cooling airflow) are evident as were previously described for the LTRFS curves. This result emphasizes the point that the carbon/hydrogen ratio of the fuel, and the degree of fuel preparation can have an important effect on the temperature of the combustor liner at any given operating condition. It can be noted that the peak and decline in each of the curves shown in Figures 50 and 51 probably coincide with the growth of the flamefront as it begins to extend from the primary into the secondary zone.

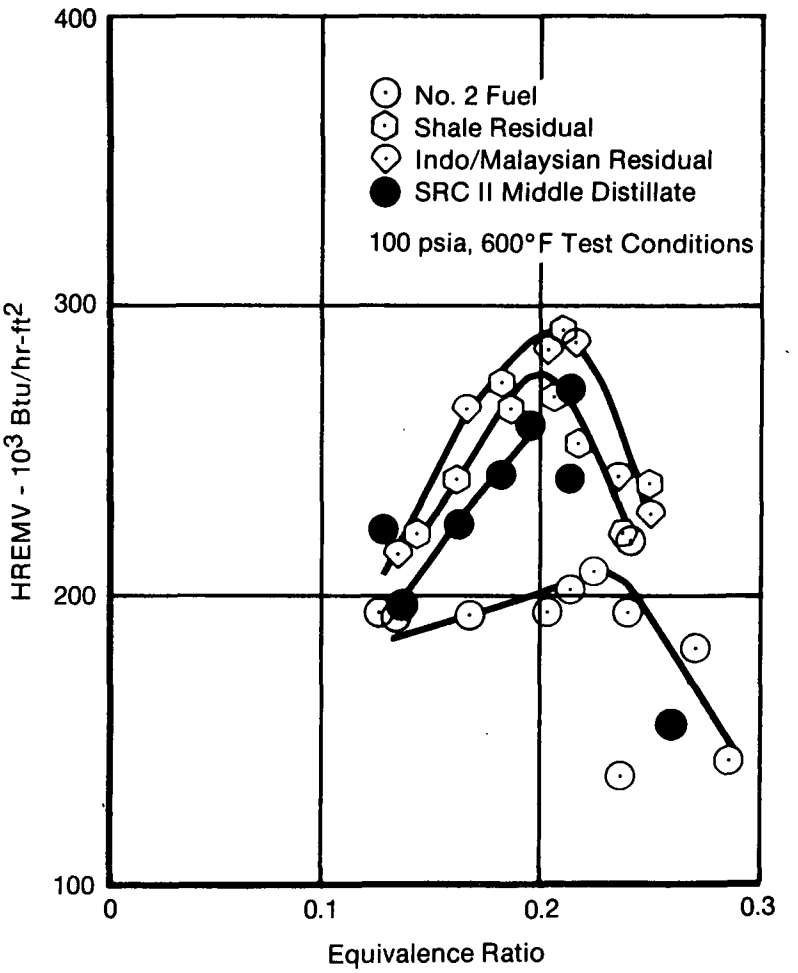

Figure 50. Variation in Heat Removed from the Primary Zone Liner by the Convective Cooling Airflow With Equivalence Ratio for Scheme FS-05B Firing Various Test Fuels

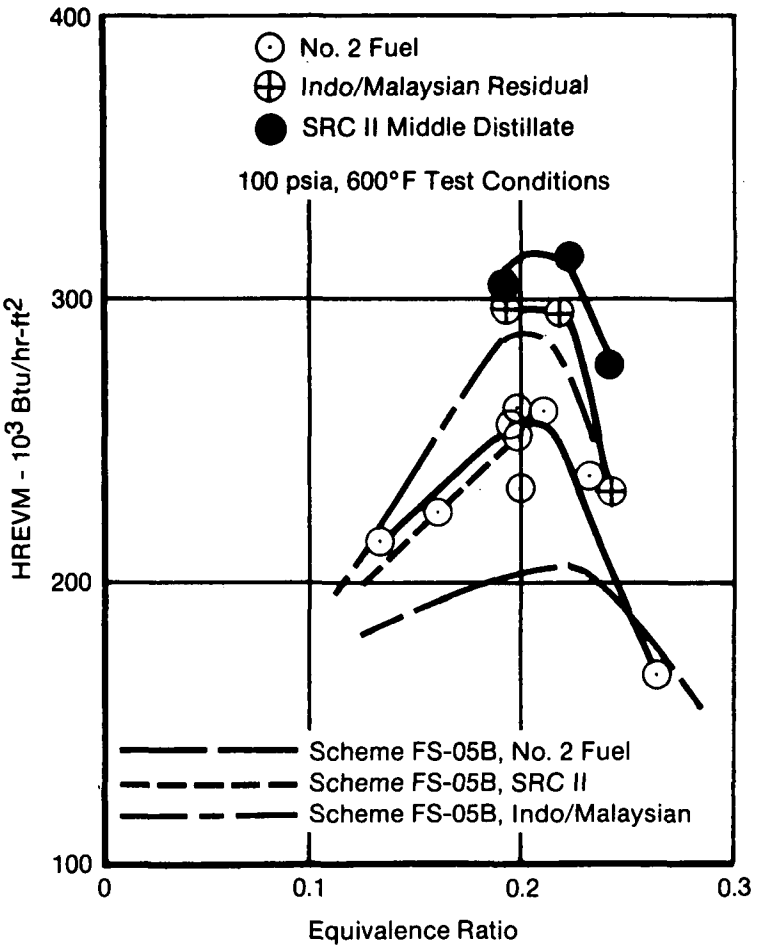

Figure 51. Variation in Heat Removed from the Primary Zone Liner by the Convective Cooling Airflow With Equivalence Ratio for Scheme FS-07A Firing Various Test Fuels

2.4 HIGH TEMPERATURE RISE OPERATION

The FRT combustor was converted to the high temperature rise version, scheme FS-08A, by the addition of the modified quench zone collar which blocked the axial dilution air holes in the secondary zone. This configuration of the combustor was operated at a reduced airflow rate because of the elimination of the final dilution air holes. Primary and quick quench airflow rates were designed to remain the same as the other combustor schemes. The target exit temperature was 2600°F.

Tests of scheme FS-08A were conducted firing No. 2 distillate fuel under various rig inlet conditions. The following subsections describe the emission and performance characteristics of this version of the RBQQ combustor.

2.4.1 Emission and Operating Characteristics of Scheme FS-08A

Tests of the FRT combustor modified to a high temperature rise configuration were conducted firing No. 2 distillate under various rig inlet conditions. At 100 psia and 575°F inlet conditions, a basic emission signature was generated. The exhaust emission data are presented in Figure 52. From this figure, a peak NO_x concentration level of 134 ppmv (corrected to 15% O_2) was recorded at an overall equivalence ratio of 0.2145. This level was comparable to that recorded with scheme FS-07A which used the same nonpremixed fuel preparation device. It can also be observed that a NO_x concentration value of 45 ppmv (corrected to 15% O_2) was attained at the bottom of the "bucket" which was comparable to the NO_x achieved with all other configurations firing No. 2 distillate at the same rig inlet conditions.

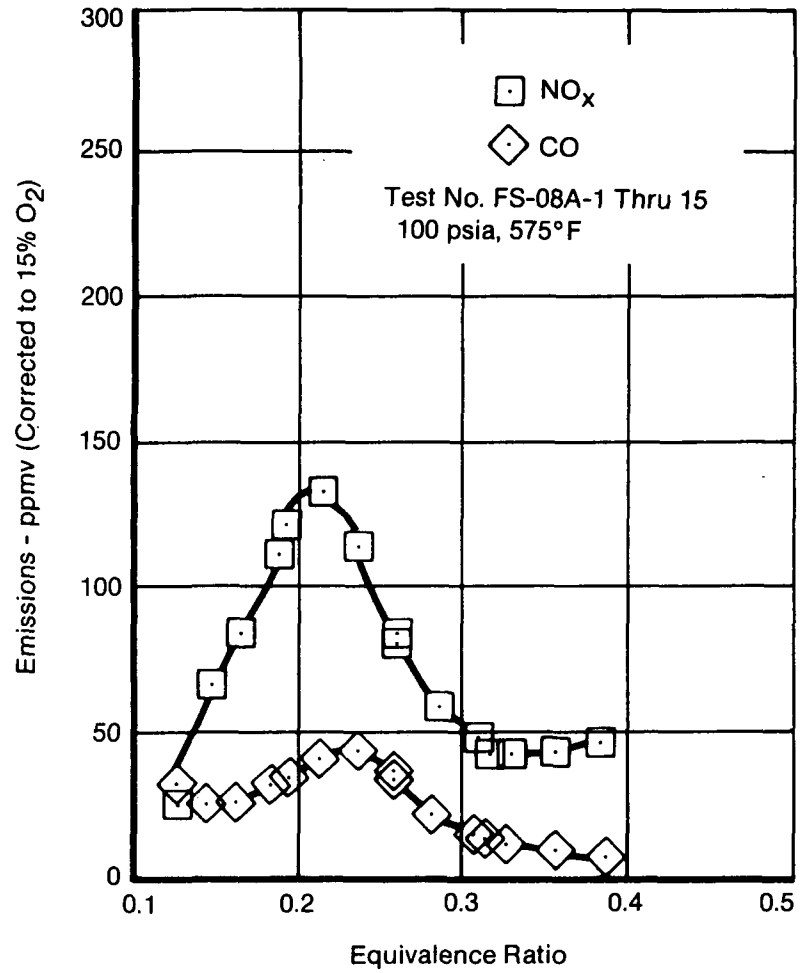

Figure 52. Emission Signature for Scheme FS-08A Firing No. 2 Fuel

It was initially thought that the NO_x level attained by this scheme may be higher without the NO_x reducing effect of the axially directed final dilution air jets, since these air jets were blocked. However, as just mentioned, the NO_x levels observed were nearly the same. It was postulated that while the placement of the final dilution air holes has an effect on the thermal NO_x formation in the secondary zone, the removal of the final dilution airflow entirely could result in the elimination of the NO_x forming potential of diffusion burning between the products from the quench zone and the final dilution jets. Also of note, in examining the flow distribution

data (Table V, Appendix A), it was observed that the combination of the approximate primary zone airflow and the measured cooling passage (quick quench) airflow only comprised about 80% of the total measured airflow. Ideally, the sum of these two airflows should come within about 90% of the total airflow. The emission signature indicated tht the primary zone airflow recorded in the table was a reasonable approximation. This casts some doubt on the measured flow rate through the cooling passage. If this flow rate was actually higher, quenching effectiveness would naturally have been improved resulting in less NO_x formation as the quenching process took place. A final item of note, it can be observed in Table I of Appendix A, that the liner pressure loss (LPL) was about 1% higher for scheme FS-08A than for FS-07A or FS-05B. This would mean that the velocities throughout the combustor would be higher; in particular, the velocities in the quick quench zone would be higher which would tend to increase the quenching effectiveness and reduce the NO_x forming potential in the rich-lean transition.

Concentrations of CO were much lower than other achieved with other configurations. All values recorded were less than 45 ppmv (corrected to 15% O_2). This was to be expected since this configuration of the combustor operates at relatively high equivalence ratios, which means that the temperature in the secondary zone was high enough to efficiently oxidize the CO to CO_2.

The rig inlet air temperature was then raised to 800°F at 100 psia (by the operation of the inlet preheater which vitiates the airflow) in an attempt to operate the combustor near its 2600° exit temperature design point. A brief fuel-air excursion was taken to map the NO_x emissions through the "bucket." The maximum equivalence ratio run was 0.3802 which corresponds to an ideal exit temperature of about 2313°F. While this temperature is somewhat below the intended design point, operation at the minimum NO_x condition had been achieved and several data points in the vicinity of the "bucket" had been documented.

A determination of preheater emission characteristics was subsequently made. At 50 psia and the same rig inlet temperature, a NO_x concentration of 16.4 ppmv (uncorrected) was measured. This value was corrected to the 100 psia operating conditions by the following relationship:

$$NO_{x100} = NO_{x50} * \left[\frac{FA_{100}}{FA_{50}}\right] * e^{19\Delta H} * \left[\frac{P_{100}}{P_{50}}\right]^{1/2} * e^{0.00313(T_{100} - T_{50})}$$

where:

NO_{x100} = NO_x corrected to the 100 psia conditions

NO_{x50} = NO_x at the 50 psia conditions = 16.4 ppmv

FA_{100} = Preheater fuel-air ratio at 100 psia conditions = 0.0035

FA_{50} = Preheater fuel-air ratio at 50 psia conditions = 0.0065

ΔH = Change in specific humidity between 100 and 50 psia conditions = 0

P_{100} = Preheater inlet pressure at 100 psia = 100 psia

P_{50} = Preheater inlet pressure at 50 psia = 49.6 psia

T_{100} = Preheater inlet temperature at 100 psia conditions = 565°F

T_{50} = Preheater inlet temperature at 50 psia conditions = 365°F

This relationship has been shown to be accurate for correcting NO_x over relatively small changes in operating conditions under lean diffusion burning with minor differences in fuel droplet size. Droplet size of the preheater fuel was expected to be nearly the same at the 100 psia conditions as at the 50 psia conditions because the preheater fuel flow and pressure drop were about the same under both conditions. While the temperature and pressure differences are significant, the correction to NO_x is believed to be appropriate in light of the extremely fuel lean operating conditions of the preheater. By applying the relationship, a value of preheater NO_x of 22.4 ppmv was computed, and this estimated value was used in the correction of the 100 psia data.

The emission data for the 100 psia and 800°F (vitiated) rig inlet conditions are shown in Figure 53. A minimum NO_x concentration of 38 ppmv[1] (corrected to 15% O_2) was recorded. The slight reduction in NO_x (38 ppmv versus 45 ppmv) with increased inlet temperature was unexpected. Normally an increase in NO_x is observed as inlet temperature rises.

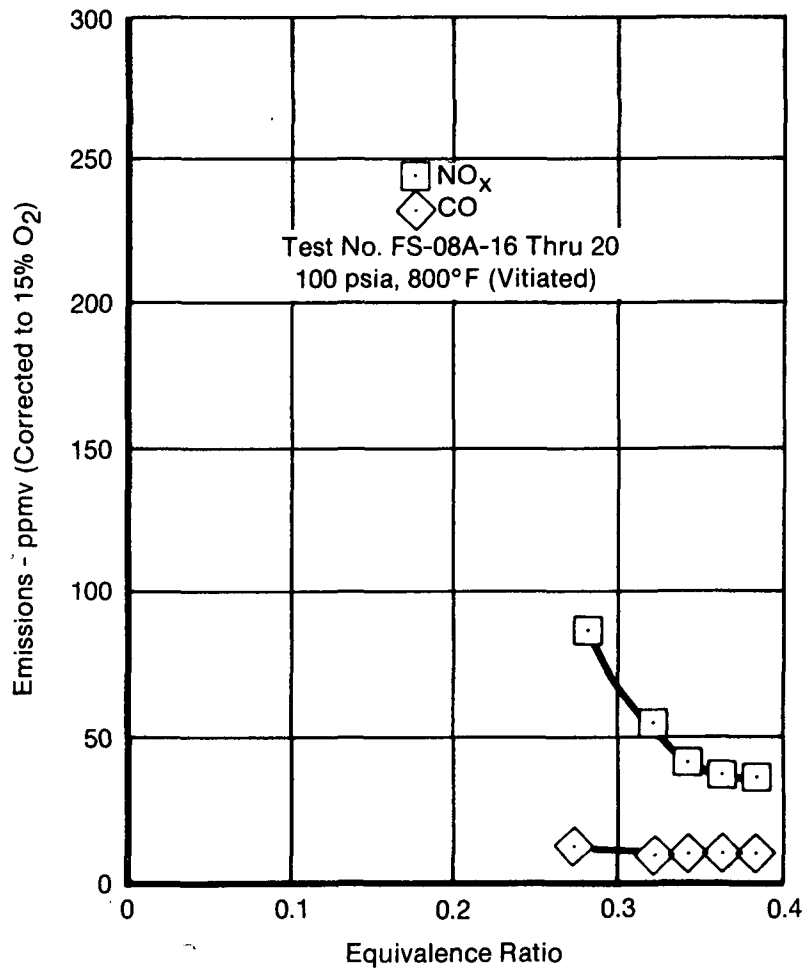

Figure 53. Emission Signature of Scheme FS-08A Firing No. 2 Fuel at High (Vitiated) Inlet Conditions

[1] For vitiated rig conditions, NO_x produced by the preheater was first subtracted from the total measured NO_x and then the 15% O_2 correction was applied through the use of the combustor equivalence ratio.

Several factors are thought to have contributed to the observed reduction of NO_x with the increased inlet temperature.

1. Higher inlet humidity from combustion in the preheater could reduce NO_x by influencing temperature rise. This effect is explained further later in this section.

2. It was postulated that with the absence of secondary dilution airflow in this configuration, the thermal NO_x formed by the diffusion interaction of quench zone discharge products and final dilution air may have been eliminated. This would result in a reduction in NO_x production sensitivity to inlet temperature by reducing the number of regions where thermal NO_x could be formed.

3. It was also postulated that increased turbulence in the primary zone and a more effective quenching process may have been a factor. This configuration was inadvertently operated at a higher pressure loss (8 to 9%) than desired (5 to 6%) because of the loss of a readout in the control room.

All CO concentration data measured at the 100 psia and 800°F rig inlet conditions of the order of 10 ppmv[2] (corrected to 15% O_2) and lower. This result was expected because oxidation reaction rates are increased by the presence of 800°F inlet temperature and high operating equivalence ratios in the secondary zone.

The rig inlet pressure was subsequently decreased to 50 psia while maintaining the inlet temperature at 800°F by the preheater. Three data points were taken to define the NO_x "bucket." The emission data are presented in Figure 54. A minimum NO_x concentration of 31 ppmv (corrected to 15% O_2) was achieved. In Phase II bench scale testing NO_x production for rich burning had been shown to be independent of pressure. However, since the nonpremixed fuel preparation device allows some burning to take place in the recirculation zone of the swirl cup before being discharged into the primary zone, it is expected that some of the NO_x generated by the diffusion burning process taking place in this region will be affected by pressure (generally accepted to be proportional to the square root of the ratio of pressures). In examining the data in Table I of Appendix A, it is observed that the boost air pressure ratio (BAPR) was somewhat higher for the 50 psia points than for the 100 psia points (2.4 versus 2.1, for the same inlet pressures, respectively). This means that the nozzle boost nitrogen flow rate would comprise a higher percentage of the primary airflow at 50 psia than at 100 psia. This slight additional percentage of nitrogen would serve to dilute the species within the primary combustion volume and would affect kinetic reaction rates and, possibly, the production of NO_x. It is perhaps the combination of these factors (and possibly others) that explain the observed reduction in NO_x at the lower inlet pressure.

CO concentrations measured were very low, reaching a minimum of about 7 ppmv (corrected to 15% O_2). Again, high inlet temperature and high secondary equivalence ratios account for the low CO concentration levels.

[2] This data includes the CO produced by the preheater which is also oxidized in the RBQQ combustor.

Inlet humidity was artifically elevated by injecting water through a bank of atomizing nozzles just downstream of the preheater for the last two data points of this test series. The rig inlet pressure and temperature were maintained at 50 psia and 800°F, respectively. The emission data are presented in Figure 54 which also shows the data from the previous 50 psia, 800°F conditions. Note that the specific humidity was increased from about 2.4% (including vitiation) to about 4.5% by the water injection. It can be seen that the increased humidity had no effect on the CO emissions, while NO_x was reduced about 4 ppmv (corrected to 15% O_2). The effect is believed to reflect the increased heat capacity of the air (due to the addition of water) which lowers combustion temperatures, particularly in the second zone where thermal NO_x formation may occur.

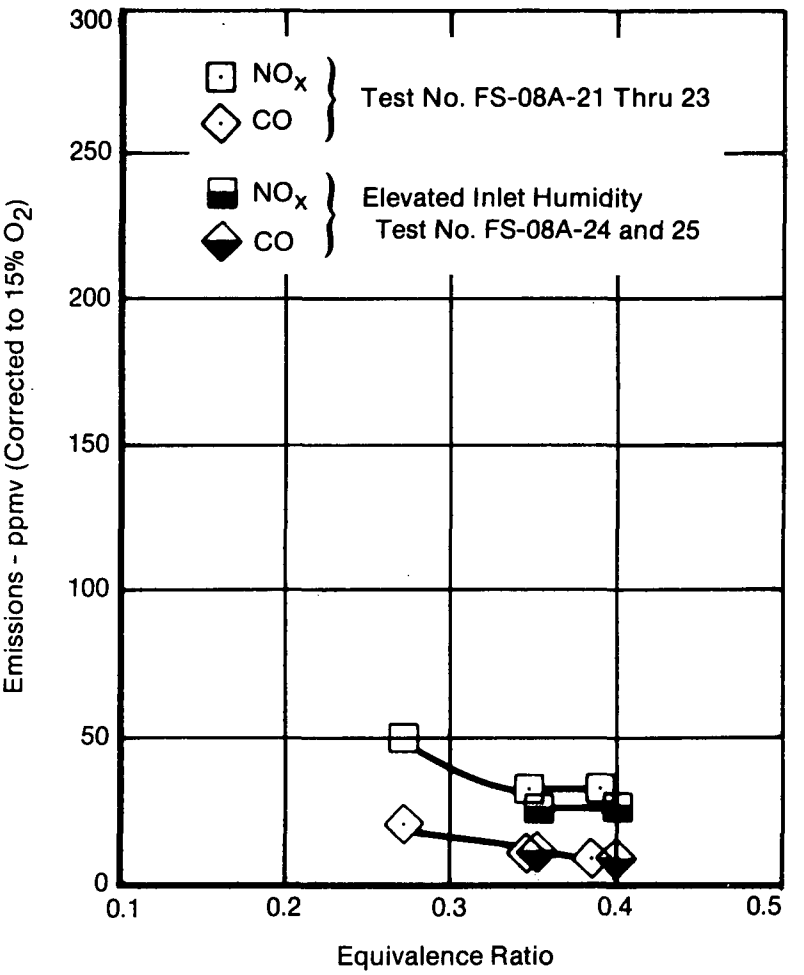

Figure 54. Emissions from Scheme FS-08A Firing No. 2 Fuel at 50 psia and 800°F

Inspection of the combustor following the test series showed no indication of distress on either the primary or secondary liner. Further deterioration of the flamespray coating was noted (see Figure 55) on the interior surface of the primary zone liner. The flamespray coating on the interior surface of the secondary zone liner also experienced very minor deterioration in a few localized areas (see Figure 56).

The fuel preparation device, shown in Figure 57, was found to be free of deposits except for minor carbon deposits on the downstream side of the fuel nozzle and its shroud. This configuration was operated for a total of 4.8 hours at the 50 psia and 100 psia conditions already described.

Figure 55. Condition of the Interior Surface of the Primary Liner at the Conclusion of the Test Program (Aft Looking Forward)

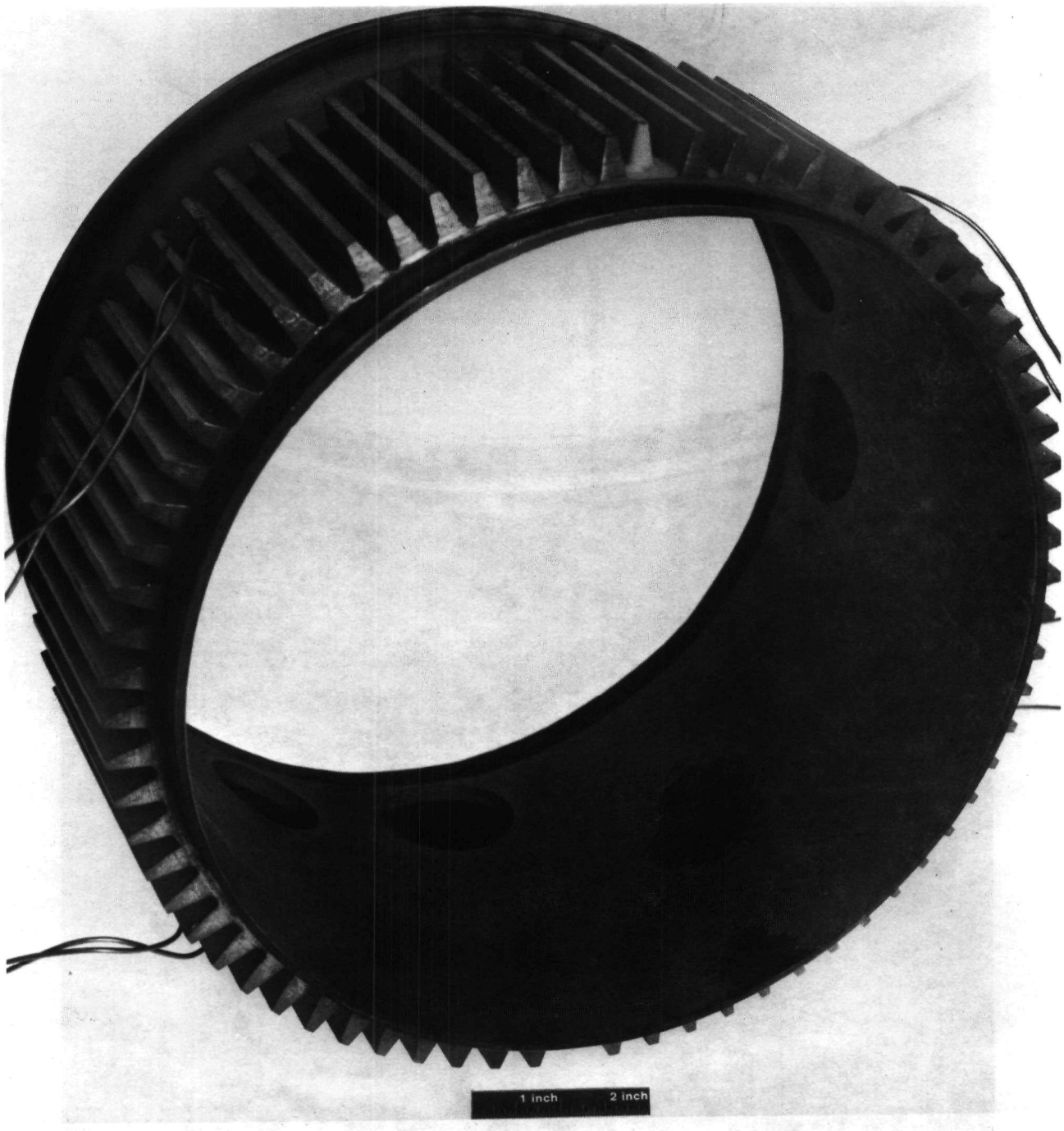

Figure 56. Condition of the Secondary Zone Liner Following Tests of Scheme FS-08A

Figure 57. Condition of the Nonpremixed Fuel Preparation Device After Operation of Scheme FS-8A on No. 2 Distillate Fuel

2.4.2 Exit Temperature Profiles

Insufficient exit temperature data were recorded to compute pattern factor data for the high temperature rise configuration of combustor. The thermocouples damaged on the exit traverse probe in previous testing were not replaced in time for the test series.

It was expected that the exit temperature pattern of the high temperature rise configuration would have been greatly improved over that of schemes FS-05A/B and FS-07A, because of the absence of the final dilution air which was ineffectively mixed at the combustor exit of the other configurations. Because the quick quench zone is considered an effective mixer, the temperature pattern in the gas stream discharged from the quench zone is thought to be nearly uniform. However, the high velocity jet exiting the quench zone most likely would not spread entirely to produce a uniform velocity gradient by the combustor exit plane. This would mean that even though the temperature of the quench zone jet was nearly uniform, there could exist a large enthalpy gradient across the combustor exit plane due to nonuniform mass flow. It should be emphasized that because of the high-velocity flow in the center of passage, alternative designs for the secondary zone need to be considered, perhaps employing mainstream swirl or a rectangular or semi-annular quench zone and secondary liner extending to the turbine inlet, if improved turbine inlet profiles are sought.

2.4.3 Liner Heat Transfer Characteristics

The liner temperature rise factor for the secondary zone liner, LTRFS, was computed for the data of scheme FS-08A. In Figure 58 the LTRFS data are plotted against corresponding equivalence ratios. As expected with the high temperature rise configuration (which has no dilution flow injected along the walls of the secondary liner), the level of LTRFS was much higher than with schemes FS-05A/B and FS-07A. The general result, however, was much the same in that the LTRFS plot exhibits the same general trends as that of the other two schemes. The 800°F inlet temperature resulted in a lowering of LTRFS compared to the 575°F inlet temperature, probably due to the increased heat capacity of the air caused by the higher humidity from vitiation. The data obtained at 50 psia rig inlet pressure are generally at a lower level of LTRFS as expected; however, there was increased scatter and the effect of water injection (which was expected to lower LTRFS) was not well defined.

The heat removed from the primary zone liner and added to the quick quench air (HREMV) was plotted against overall equivalence ratio for scheme FS-08A, and these data are presented in Figure 59. The same comments just mentioned for LTRFS apply here, noting that increased HREMV can be due to either higher liner temperatures or increased heat capacity of the air (due to increased humidity from vitiation of the airflow or water injection).

With reference to Subsection 2.1.1, the secondary zone liner temperature was predicted to reach 1890°F during 100 psia rig operation. In reviewing the liner temperature data in Table IV of Appendix A, the maximum temperatures recorded were about 1450°F. It can be noted that the predicted wall temperature was determined assuming fully developed turbulent flow along the interior surface of the aft liner. This assumption was probably not realistic because of the gas stream leaves the quick quench zone as a high velocity jet, which would not reattach itself to the liner wall for quite some distance downstream. It can also be noted that the model assumed a 2600°F exit temperature while the combustor was run to only about 2300°F due to rig limitations.

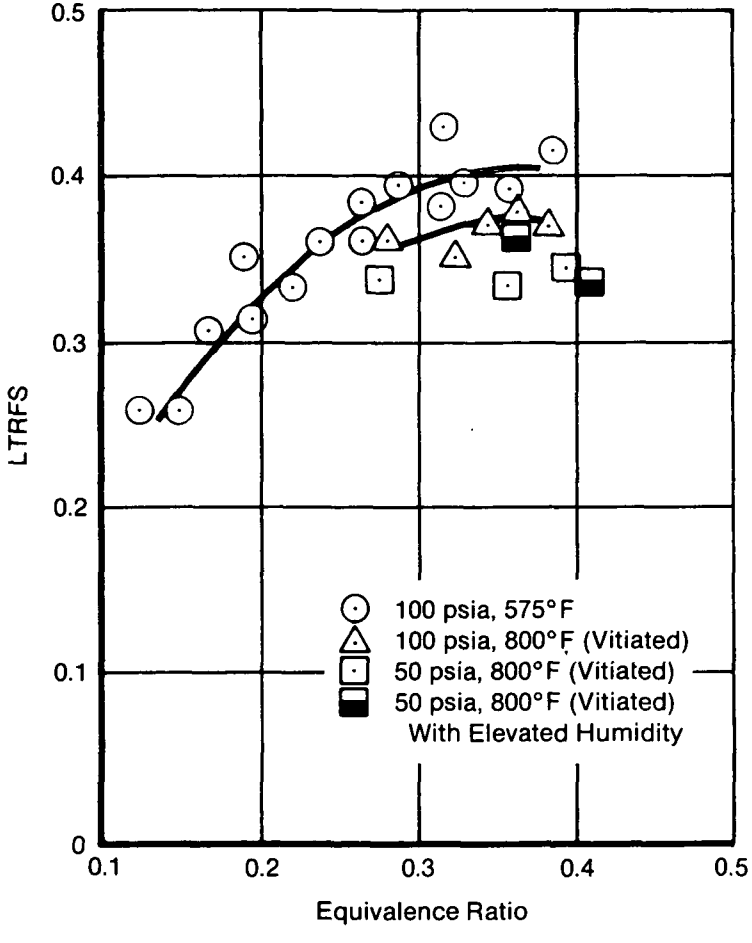

Figure 58. Effects of Equivalence Ratio, Pressure, Temperature and Humidity on Secondary Zone Liner Temperature Rise Factor Firing No. 2 Fuel in Scheme FS-08A

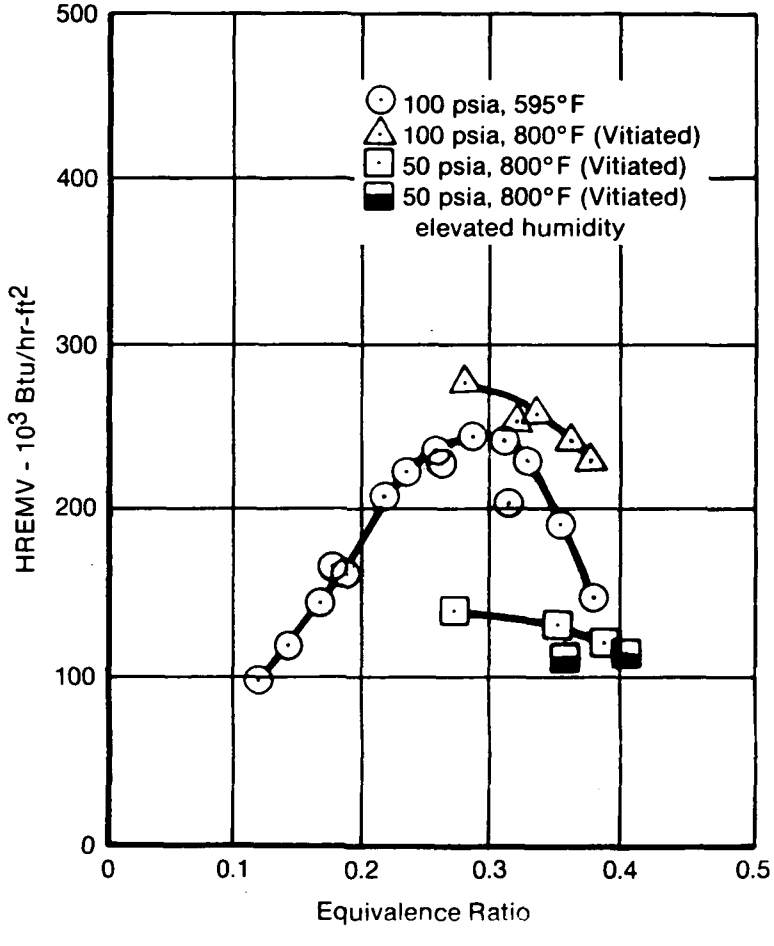

Figure 59. Variation in Heat Removed from the Primary Zone Liner by the Convective Cooling Airflow With Equivalence Ratio for Scheme FS-08A Firing No. 2 Fuel at Various Rig Inlet Conditions

At the conclusion of the test program, the primary liner shroud was removed in order to examine the thermal paint. Figure 60 is a photograph of the primary zone liner showing the pattern of colors in the thermal paint. It may be noted that the combustor liner temperature was relatively uniform with the upstream one-quarter of the finned surface being the coolest. Temperatures of 2000°F and above were seen by the downstream three-quarters of the primary liner at one time or another during the course of the test program.

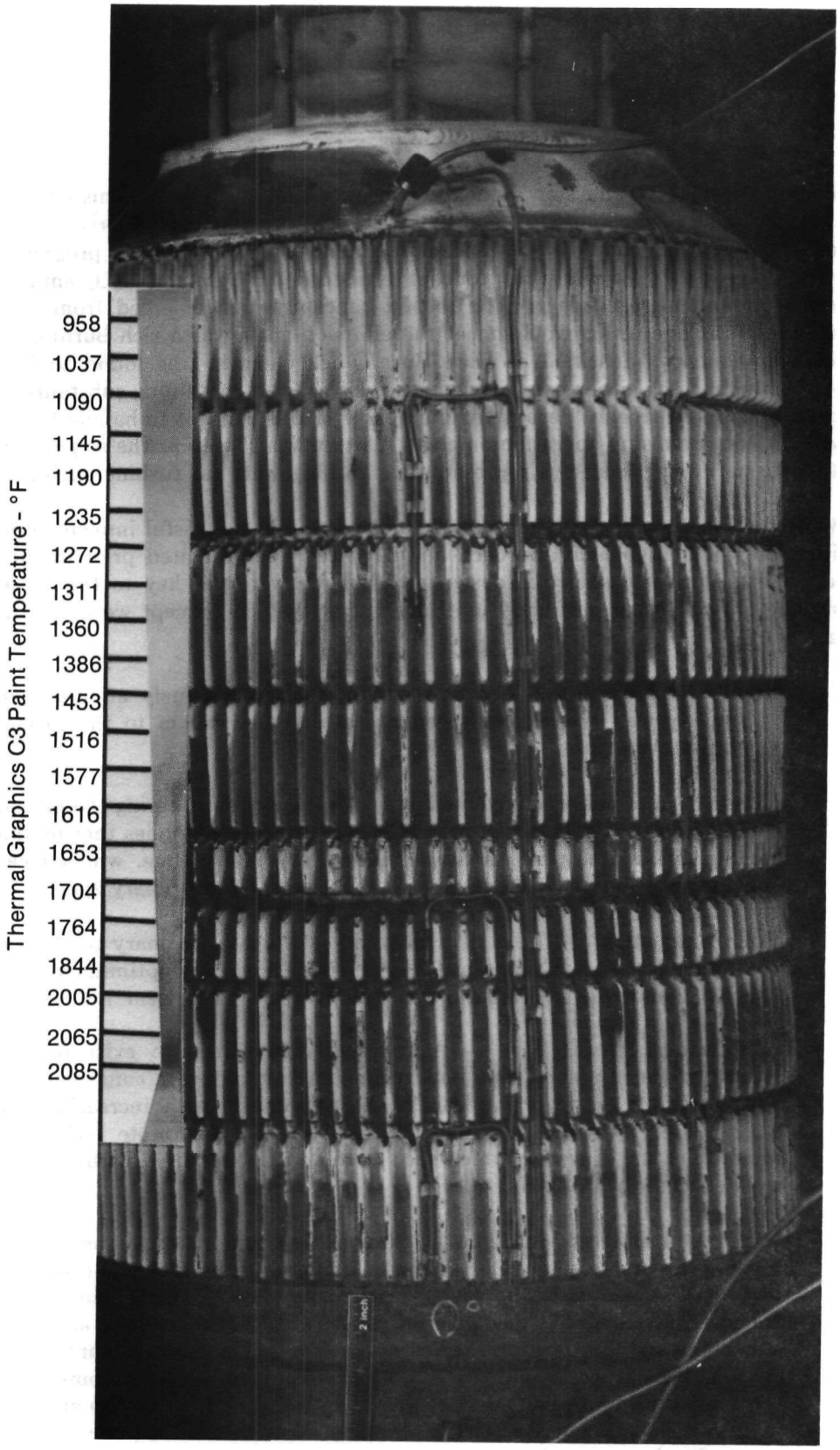

Figure 60. Primary Zone Liner Postrun Thermal Paint Analysis

SECTION 3

PROGRAM CONCLUSIONS

Many potential NO_x emission reduction concepts were evaluated in this program through subscale experimental screening; two concepts were identified as particularly successful. First, a premixed, fuel-lean combustion concept was shown to meet the program goals for non-nitrogenous fuels; however, this concept produced unacceptable NO_x emmisions when operated on bound nitrogen fuels. The second concept which emerged from the screening experimentation as one which would meet the emission goals was a rich burning combustion concept. This concept, identified as Rich Burn/Quick Quench, was found to be extremely successful while burning either non-nitrogenous fuels or fuels containing substantial quantities of chemically bound nitrogen. Because of the ability of this concept to handle bound nitrogen fuels without compromising operation on clean fuels, it was chosen as the single concept to be committed to hardware sized to a representative 25 megawatt gas turbine engine.

While fuel-rich combustion concepts are not new, fully successful implementation of the basic Rich Burn/Quick Quench approach had not been demonstrated prior to this program. Methods of executing the principal design requirments were the key to the success of this concept. The critical features of the Rich Burn/Quick Quench concept were identified as the following:

1. Good fuel preparation — The need for fuel to be finely atomized and reasonably well distributed throught the inlet airstream to the primary combustion volume.

2. Elimination of nonpremixed airflow — All the airflow entering the primary combustion volume must be premixed with fuel. This implies that no liner cooling airflow may be discharged into the primary zone, which means conventional louvered liners may not be used for the primary zone.

3. Rich combustion — The equivalence ratio within the primary combustion volume must be maintained at fuel-rich conditions. The optimum value of primary zone equivalence ratio was demonstrated to be near 1.3.

4. Sufficient residence time — A trade-off was shown to exist between primary zone residence time and attainable NO_x emission concentrations. This trade-off, however, appears to be asymptotic with increasing residence time. It is thought that the level of the asymptote (NO_x) is a function of the degree to which each of the critical features of the concept were executed.

5. Rapid and effective dilution — Composition and mixture temperature must approximate a step change in the transition from fuel-rich conditions in the primary zone to fuel-lean conditions in the secondary zone. As this transition is allowed to deviate from a near step, residence time at or near stoichiometric combustion begins to create much larger quantities of thermal NO_x. It was found that the most effective means of accomplishing the rapid dilution (quick quench) was by introducing the dilution air into a high velocity stream of the rich products. This method was found to be most effective when the mainstream velocity was great enough to incur a substantial momentum pressure loss due to mass addition. Because other methods not having this pressure loss were tried with lesser degrees of

success, it is hypothesized that this additional pressure loss is transferred into more rapid mixing. The means employed in this program to achieve the high velocity mainstream flow was to form a constriction in the burner cross sectional area into which the dilution flow was injected. The reduced cross section also acts as a region of separation between the zones of rich and lean combustion. It is also thought that since the reduced area causes the mainstream flow of rich products to accelerate to high velocity, the possibility of dilution flow recirculating upstream, forming pockets of stoichiometric combustion (resulting in high NO_x production), is lessened.

6. CO consumption — Because large quantities of carbon monoxide are present in the effluent gases of the primary and quench zones, residence time and sufficient temperature are necessary in the secondary (lean) zone. Temperatures in the range of 2100°F to 2800°F are generally considered adequate for CO oxidation in the residence times typically found in gas turbine combustors. Outside this range on the low side leaves the potential for higher CO, while on the high side, the production of thermal NO_x becomes significant. It should be noted that as combustion pressure is increased, CO concentrations decline. Implicit in the secondary zone temperature requirement is the need to inject final dilution air later in the secondary zone to lower the temperature of the gases to that required for admission to the turbine.

The requirement of maintaining a primary zone equivalence ratio near 1.3 implies that a means of varying the airflow admitted into the rich region must be provided to stage the primary zone airflow in proportion to the fuel flow. It is possible to operate the combustor on non-nitrogenous fuels over a limited range of conditions without varying the primary airflow since the characteristic NO_x curve for these fuels remains essentially constant beyond a primary zone equivalence ratio of 1.3. This non-nitrogenous fuel operating range without variable geometry is bounded by the smoke formation threshold. Variable geometry is required for proper operation with nitrogen bearing fuels.

The Rich Burn/Quick Quench combustor concept was successfully transferred from subscale to a size representative of a typical 25 megawatt gas turbine combustor. Success was evidenced by the emission trends and levels achieved. While scaling criteria dictate that there can be no exact and complete correspondence between a prototype combustor and its subscale model (with regard to physical dimensions, operating conditions, and combustion performance), computer modeling and subscale parametric data were successfully used to execute the separate full-scale design.

NO_x emission levels obtained with the Rich Burn/Quick Quench concept were demonstrated to be extremely low, and were better than the emission goals specified for the program by a wide margin. While No. 2 distillate fuel oil (unadulterated and with 0.5% nitrogen) and a shale derived diesel fuel marine were the principal test fuels used during the Phase II bench-scale screening experiments, these as well as a middle distillate solvent refined coal, SRC II (0.95% N); a residual shale oil (0.46% N); and an Indonesian/Malaysian petroleum residual (0.24% N) were tested during Phases IV and VI in the full-scale conbustors. A low Btu gas was also tested during the bench-scale program, again with excellent results. A wide range of operating conditions was spanned during the test program, and variable geometry was successfully employed to provide low emissions at all operating points. It was also shown in this program that the Rich Burn/Quick Quench concept essentially eliminates the adverse effect that increased pressure can have on NO_x formation (this effect is very evident in lean combustion and is ordinarily found to be proportional to the square root of the pressure ratio).

A high exit temperature (1600°F design point) version of the full-scale Rich Burn/Quick Quench combustor was also successfully tested on No. 2 distillate fuel oil. NO_x emission results were found to be essentially identical to the results of the normal temperature rise version. This result implies that the concept is directly applicable to advanced technology turbine engines having a high turbine inlet temperature requirement.

In summary, the Rich Burn/Quick Quench combustor concept was demonstrated to yield excellent emission results on all fuels tested, nitrogen laiden as well as non-nitrogenous. This concept is the only technique known at this time, wet (addition of water or steam to the combustion process) or dry (no water), which has demonstrated the ability to burn nitrogenous fuels containing up to 1% N while maintaining low NO_x emission levels (less than 100 ppmv at 15% O_2).

SECTION 4

RECOMMENDATIONS

Several areas remain where further study and testing may be conducted to improve and refine the Rich Burn/Quick Quench combustion concept and adapt it for application in specific industrial gas turbine engines.

1. Testing of the prototype combustor should be conducted at full pressure, full temperature conditions representative of an industrial gas turbine engine.

2. Further primary zone liner thermo/mechanical analysis should be undertaken. Studies of candidate liner materials (including nonmetallic alternatives) and coatings should be made. Heat transfer analyses of cooling schemes and cyclic testing at full-pressure full-temperature operating conditions are also indicated.

3. Improvements in temperature pattern factor should be undertaken for in-line combustor applications. Alternate methods of the final dilution air injection, perhaps including a mainstream swirl technique or a second quick quench zone, should be considered. It is also possible that the quick quench zone shape can be optimized (possibly rectangular or semi-annular) to facilitate easier pattern factor tailoring.

4. Methods of optimizing fuel preparation techniques and devices should be addressed. Fuel atomization and mixing techniques may properly be tailored for the specific fuels burned.

5. Variable geometry techniques for scheduling the airflow admitted into the various combustion zones should be proposed and evaluated. Improvements in the methods of staging and control are needed.

6. Studies of the basic processes of the Rich Burn/Quick Quench concept in areas such as the kinetic processes of rich combustion and the optimization of quenching effectiveness should be undertaken.

REFERENCES

1. Pierce, R. M., Smith, C. E., and Hinton, B. S., "Advanced Combustion Systems for Stationary Gas Turbine Engines: Volume III. Combustor Verification Testing," EPA-600/7-80-017c.

2. "Design and Performance Analysis of Gas Turbine Combustion Chamber Vol. I Theory and Practice of Design," Northern Research and Engineering Corp., 1964, NREC 1082-1.

3. Pierce, R. M., Smith, C. E., and Hinton, B. S., "Low NO_x Combustor Development for Stationary Gas Turbine Engines," EPA-600/7-79/050C.

4. Lorenzetto, G. E., and Lefebrve, A. H., "Measurements of Drop Size on a Plain-Jet Airblast Atomizer," AIAA 1976.

5. Barnett, M. C. and Hibbard, R. R., "Properties of Aircraft Fuels," NACA TN 3276, August 1956.

LIST OF SYMBOLS

The following symbols are used in the test data summaries contained in Table I through Table VII of Appendix A.

Symbol	*Definition*	*Units*
EQR	Combustor overall fuel-air equivalence ratio determined from metered fuel and air flowrates (dry)	—
PTIN	Combustor inlet total pressure	psia
TTIN	Combustor inlet total temperature	°F
WA	Total combustor airflow rate (wet)	pps
LPL	Combustor total pressure loss	%
HUM	Inlet air specific humidity	lb H_2O/lb air
FUEL	Fuel type '2' designates No. 2 fuel oil. 'SRC II' designates middle distillate solvent refined coal	—
PHIP	Primary zone equivalence ratio (dry)	—
NOX15	NO_x concentration corrected to 15% O_2 (dry)	ppmv
NO15	NO concentration corrected to 15% O_2 (dry)	ppmv
CO15	CO concentration corrected to 15% O_2 (dry)	ppmv
UHC15	Unburned hydrocarbon concentration corrected to 15% O_2 (dry)	ppmv
CO_2	CO_2 concentration, uncorrected, as measure (dry)	pctv
O_2	O_2 concentration, uncorrected, as measured (dry)	pctv
CFRAC	Carbon balance parameter; total carbon out divided by total carbon in	—
EFFGA	Combustion efficiency from gas analysis measurements	%
EQRSAM	Combustor overall fuel-air equivalence ratio determined by gas analysis measurements	—
BST1 through BST20	Combustor liner temperatures, measured at locations defined in Figure 3	°F

LIST OF SYMBOLS (Continued)

Symbol	*Definition*	*Units*
BSTD1 through BSTD4	Combustor liner dome temperatures, measured at locations defined in Figure 3	°F
WAPRI	Primary zone airflow rate (wet)	pps
WASEC	Secondary zone (quick-quench) airflow rate (wet)	pps
TPF	Temperature pattern factor	—
VREF	Primary zone reference velocity (cold)	ft/sec
EFFMB	Combustion efficiency from average of exit thermocouple data	%
T_{t41} through T_{T48}	Combustor exit total temperatures, measured at 8 locations on the exit plane traverse probe	°F
HRRV	Combustor volumetric heat release rate	10^6 Btu/ hr-ft^3-atm
HREMV	Heat transferred from primary liner to quench air, determined from quench air temperature rise	10^3 Btu/ hr-ft^2
TTQQ	Quick quench air total temperature, measured as quench air enters dilution ports (after liner cooling)	°F
LTRFP	Liner temperature rise factor of primary liner	—
LTRFS	Liner temperature rise factor of secondary liner	—
$LTRF_{avg}$	Liner temperature rise factor of combined primary and secondary liners	—
LB	Burner length	in.
AREF	Reference area	sq. in.
L/D	Length to diameter ratio	
VOLREF	Reference volume	in^3
ACDSUM	Total effective flow area	
AX	Axial location	inches
ACD	Effective flow area	
WACUM	Cumulative airflow	%
PHI	Local equivalence ratio	

APPENDIX A

TABLE I. COMBUSTOR OPERATING PARAMETER DATA

Test No.	*EQR (dry)*	P_{TIN}	T_{TIN}	*Wa (wet)*	*LPL*[1]	*Fuel*	*Hum*
FS-05A-1	0.0916	50.4	436	9.313	4.29	2	0.0180
FS-05A-2	0.1337	52.2	442	9.150	4.33	2	0.0183
FS-05A-3	0.1439	50.0	449	10.067	5.40	2	0.0182
FS-05A-4	0.1788	51.0	453	9.829	5.30	2	0.0183
FS-05B-1	0.1604	50.1	410	9.912	6.01	2	0.0155
FS-05B-2	0.1911	50.3	428	10.011	6.14	2	0.0164
FS-05B-3	0.2377	50.1	427	9.839	5.91	2	0.0164
FS-05B-4	0.2676	50.6	430	9.856	5.63	2	0.0164
FS-05B-5	0.2143	50.4	433	9.834	5.87	2	0.0164
FS-05B-6	0.2405	50.5	433	9.723	5.43	2	0.0164
FS-05B-7	0.2641	50.3	435	9.915	5.68	2	0.0164
FS-05B-8	0.1912	50.3	432	9.936	5.84	2	0.0164
FS-05B-9	0.1564	50.2	431	10.048	5.76	2	0.0164
FS-05B-10	0.1659	101.0	610	17.070	4.31	2	0.0159
FS-05B-11	0.2021	99.8	604	16.388	3.79	2	0.0159
FS-05B-12	0.2116	99.6	608	17.827	5.35	2	0.0159
FS-05B-13	0.2359	99.8	613	17.699	5.01	2	0.0159
FS-05B-14	0.2724	101.3	614	17.397	4.62	2	0.0159
FS-05B-15	0.2858	99.0	616	17.961	5.15	2	0.0159
FS-05B-16	0.1368	99.8	616	16.784	4.37	SRC II	0.0159
FS-05B-17	0.1816	101.3	617	17.848	5.09	SRC II	0.0159
FS-05B-18	0.2157	100.1	620	17.269	4.84	SRC II	0.0159
FS-05B-19	0.2389	101.8	607	17.695	4.88	2	0.0179
FS-05B-20	0.1620	100.2	606	17.428	4.82	SRC II	0.0179
FS-05B-21	0.1954	101.5	615	17.342	4.89	SRC II	0.0179
FS-05B-22	0.2134	101.3	614	16.975	4.71	SRC II	0.0179
FS-05B-23	0.2590	100.2	598	17.507	4.62	SRC II	0.0179
FS-05B-24	0.1269	101.1	606	17.559	4.59	SRC II	0.0179

TABLE I. COMBUSTOR OPERATING PARAMETER DATA (Continued)

Test No.	*EQR*	P_{TIN}	T_{TIN}	*Wa (wet)*	*LPL*	*Fuel*	*Hum*	*BAPR*
FS-05B-25	0.1421	99.66	574	16.952	4.60	SRES	0.0200	
FS-05B-26	0.1616	100.29	607	17.513	4.86	SRES	0.0200	
FS-05B-27	0.1839	100.51	612	17.586	5.16	SRES	0.0200	
FS-05B-28	0.2067	99.86	614	17.799	5.38	SRES	0.0200	
FS-05B-29	0.2366	99.66	616	17.447	5.26	SRES	0.0200	
FS-05B-30	0.2195	100.03	617	17.701	5.27	SRES	0.0200	
FS-05B-31	0.2104	100.80	584	17.721	4.32	SRES	0.0200	
FS-05B-32	0.1818	99.74	593	17.995	5.18	SRES	0.0189	
FS-05B-33	0.2490	101.12	615	17.152	4.53	SRES	0.0189	
FS-05B-34	0.2397	99.40	585	17.489	—	2	0.0186	
FS-05B-35	0.2230	100.28	607	17.748	4.84	2	0.0186	
FS-05B-36	0.1265	100.58	610	17.331	4.40	2	0.0186	
FS-05B-37	0.1357	101.12	610	17.361	4.29	2	0.0186	
FS-05B-38	0.1343	100.47	608	17.170	4.31	RESD	0.0186	
FS-05B-39	0.1670	100.86	612	17.763	4.83	RESD	0.0186	
FS-05B-40	0.2127	100.37	608	17.322	4.61	RESD	0.0186	
FS-05B-41	0.2495	100.47	612	17.396	4.67	RESD	0.0186	
FS-05B-42	0.2370	99.13	612	17.305	4.94	RESD	0.0186	
FS-05B-43	0.2047	100.44	614	17.201	4.53	RESD	0.0186	
FS-07A-1	0.1354	99.36	565	17.816	5.09	2	0.0188	2.211
FS-07A-2	0.1639	100.50	609	17.393	5.17	2	0.0188	2.216
FS-07A-3	0.1883	99.92	612	17.466	5.23	2	0.0188	2.199
FS-07A-4	0.2073	99.67	616	17.725	5.99	2	0.0188	2.204
FS-07A-5	0.2368	100.31	618	17.534	5.43	2	0.0188	2.240
FS-07A-6	0.2629	98.82	618	17.619	5.36	2	0.0188	2.274
FS-07A-7	0.1977	99.63	619	17.740	5.41	2	0.0188	2.255
FS-07A-8	0.1985	99.93	619	17.662	5.49	2	0.0188	1.648
FS-07A-9	0.1973	99.99	619	17.774	5.32	2	0.0188	1.397
FS-07A-10	0.2007	99.84	619	17.468	5.59	2	0.0188	4.154
FS-07A-11	0.1988	100.14	620	17.642	5.48	2	0.0188	2.194
FS-07A-12	0.2192	99.38	618	17.670	5.55	RESD	0.0188	2.211
FS-07A-13	0.2457	99.80	621	17.655	5.46	RESD	0.0188	2.201
FS-07A-14	0.1949	99.72	620	17.623	5.51	RESD	0.0188	2.203
FS-07A-15	0.1926	99.24	619	17.706	5.45	SRC II	0.0188	2.214
FS-07A-16	0.2190	100.22	620	17.426	5.53	SRC II	0.0188	2.192
FS-07A-17	0.2421	99.55	621	17.615	5.87	SRC II	0.0188	2.207
FS-08A-1	0.1218	99.81	540	12.519	5.38	2	0.0149	2.081
FS-08A-2	0.1440	100.45	554	12.231	5.34	2	0.0149	2.068
FS-08A-3	0.1665	101.14	558	12.028	5.49	2	0.0149	2.054
FS-08A-4	0.1887	100.73	558	11.669	5.56	2	0.0149	2.032
FS-08A-5	0.1914	99.74	562	12.579	6.53	2	0.0149	2.052
FS-08A-6	0.2145	100.33	564	12.324	6.52	2	0.0149	2.040
FS-08A-7	0.2354	100.61	566	12.195	6.31	2	0.0149	2.034
FS-08A-8	0.2612	100.74	567	11.872	6.55	2	0.0149	2.032
FS-08A-9	0.2613	100.55	571	12.387	7.08	2	0.0149	2.036
FS-08A-10	0.2875	101.51	572	12.280	6.74	2	0.0149	2.016
FS-08A-11	0.3150	101.46	574	11.808	6.63	2	0.0149	2.037
FS-08A-12	0.3100	101.02	572	12.708	7.63	2	0.0166	1.957
FS-08A-13	0.3263	102.51	576	12.744	7.63	2	0.0166	2.075
FS-08A-14	0.3532	101.32	574	12.389	7.17	2	0.0166	2.119
FS-08A-15	0.3837	101.68	576	12.022	7.09	2	0.0166	2.112
FS-08A-16	0.2792	98.19	814	12.530	9.18	2	0.0217	2.156
FS-08A-17	0.3198	99.01	806	12.335	8.56	2	0.0212	2.108
FS-08A-18	0.3399	99.41	808	12.198	8.35	2	0.0209	2.120
FS-08A-19	0.3573	100.32	806	12.235	8.23	2	0.0208	2.100
FS-08A-20	0.3802	100.85	806	12.078	7.86	2	0.0209	2.089
FS-08A-21	0.2764	49.42	799	6.488	9.57	2	0.0239	2.483
FS-08A-22	0.3525	49.94	808	6.231	9.00	2	0.0245	2.397
FS-08A-23	0.3914	50.03	800	6.128	8.63	2	0.0246	2.452
FS-08A-24	0.4022	50.38	795	6.170	8.48	2	0.0454	2.376
FS-08A-25	0.3579	50.02	800	6.261	8.91	2	0.0455	2.393

APPENDIX A (Continued)

TABLE II. EMISSION CONCENTRATION DATA

Test No.	*EQR*	*PHIP*	*NO_x15*	*CO15*	*UHC15*
FS-05A-1	0.0916	—	27.3	14.4	—
FS-05A-2	0.1337	—	123.3	76.8	—
FS-05A-3	0.1439	—	103.5	144.6	—
FS-05A-4	0.1788	—	31.7	243.9	—
FS-05B-1	0.1604	0.8589	53.9	269.3	—
FS-05B-2	0.1911	1.0229	37.3	242.7	—
FS-05B-3	0.2377	1.2861	27.3	169.2	—
FS-05B-4	0.2676	1.4443	20.6	115.0	—
FS-05B-5	0.2143	1.1477	20.3	155.6	—
FS-05B-6	0.2405	1.2981	19.6	112.2	—
FS-05B-7	0.2641	1.4418	19.6	86.1	—
FS-05B-8	0.1912	1.0368	41.7	240.6	—
FS-05B-9	0.1564	0.8554	82.1	203.4	—
FS-05B-10	0.1659	0.9061	155.2	78.9	—
FS-05B-11	0.2021	1.1139	65.0	64.8	24.2*
FS-05B-12	0.2116	1.1404	53.0	68.0	18.3*
FS-05B-13	0.2359	1.2863	43.7	46.5	15.7*
FS-05B-14	0.2724	1.4307	48.5	23.6	6.8
FS-05B-15	0.2858	1.5356	48.0	19.0	5.5
FS-05B-16	0.1368	0.8553	394.9	103.4	16.6*
FS-05B-17	0.1816	1.1305	105.1	101.9	10.6*
FS-05B-18	0.2157	1.3190	100.9	66.2	7.3
FS-05B-19	0.2389	1.3454	43.7	50.7	—
FS-05B-20	0.1620	1.9520	223.8	116.0	—
FS-05B-21	0.1954	1.1510	97.8	91.2	—
FS-05B-22	0.2134	1.2791	93.3	75.9	15.6*
FS-05B-23	0.2590	1.5208	143.8	52.7	—
FS-05B-24	0.1269	0.8384	361.4	129.1	—

*Sample lines saturated with fuel

APPENDIX A (Continued)

TABLE II. EMISSION CONCENTRATION DATA (Continued)

Test No.	*EQR*	*PHIP*	*NOX15*	*CO15*	*UHC15*
FS-05B-25	0.1421	0.8011	245.7	88.1	—
FS-05B-26	0.1616	0.9236	136.3	110.5	—
FS-05B-27	0.1839	1.0527	81.3	94.2	—
FS-05B-28	0.2067	1.1877	65.1	80.8	11.7
FS-05B-29	0.2366	1.3508	94.5	53.2	5.0
FS-05B-30	0.2195	1.2605	75.8	—	0.2
FS-05B-31	0.2104	1.1808	73.5	76.1	0.0
FS-05B-32	0.1818	1.0448	99.2	97.4	—
FS-05B-33	0.2490	1.4035	121.2	49.2	8.0
FS-05B-34	0.2397	—	46.2	50.8	5.4
FS-05B-35	0.2230	1.2093	47.5	63.3	4.7
FS-05B-36	0.1265	0.6967	372.2	67.1	4.0
FS-05B-37	0.1357	0.7509	365.3	71.5	0.5
FS-05B-38	0.1343	0.7310	253.6	80.2	0.0
FS-05B-39	0.1670	0.9052	122.4	91.6	2.9
FS-05B-40	0.2127	1.1495	67.3	74.4	1.8
FS-05B-41	0.2495	1.3475	87.5	59.7	2.4
FS-05B-42	0.2370	1.3190	75.6	64.3	1.2
FS-05B-43	0.2047	1.0980	71.2	94.1	1.5
FS-07A-1	0.1354	0.7375*	120.0	68.6	12.6
FS-07A-2	0.1639	0.8928*	108.0	94.7	6.6
FS-07A-3	0.1883	1.0258*	65.4	100.8	4.8
FS-07A-4	0.2073	1.1297*	48.7	96.2	3.4
FS-07A-5	0.2368	1.2903*	42.9	67.8	1.8
FS-07A-6	0.2629	1.4322*	43.8	54.2	1.4
FS-07A-7	0.1977	1.0770*	54.2	93.3	2.2
FS-07A-8	0.1985	1.0816*	62.8	83.7	2.5
FS-07A-9	0.1973	1.0750*	73.6	78.9	2.8
FS-07A-10	0.2007	1.0934*	43.6	111.3	2.6
FS-07A-11	0.1988	1.0804*	54.2	91.1	2.6
FS-07A-12	0.2192	1.1943*	57.7	92.6	2.1
FS-07A-13	0.2457	1.3389*	65.5	77.7	1.6
FS-07A-14	0.1949	1.0618*	82.4	102.5	2.2
FS-07A-15	0.1926	1.0492*	134.4	106.8	2.9
FS-07A-16	0.2190	1.1932*	80.3	92.7	1.8
FS-07A-17	0.2421	1.3193*	91.7	76.8	1.7
FS-08A-1	0.1218	0.4192*	24.7	29.1	—
FS-08A-2	0.1440	0.4956*	55.4	25.7	—
FS-08A-3	0.1665	0.5728*	72.9	25.6	—
FS-08A-4	0.1887	0.6494*	113.0	31.6	—
FS-08A-5	0.1914	0.6587*	123.7	32.8	—
FS-08A-6	0.2145	0.7381*	134.0	40.7	—
FS-08A-7	0.2354	0.8098*	115.4	43.1	—
FS-08A-8	0.2612	0.8987*	82.2	35.7	—
FS-08A-9	0.2613	0.8989*	85.8	36.8	—
FS-08A-10	0.2875	0.9893*	59.4	22.2	—
FS-08A-11	0.3150	1.0838*	45.7	12.6	—
FS-08A-12	0.3100	1.0668*	50.2	13.9	—
FS-08A-13	0.3263	1.1229*	45.2	10.3	—
FS-08A-14	0.3532	1.2154*	45.0	8.1	—
FS-08A-15	0.3837	1.3202*	47.1	7.6	—
FS-08A-16	0.2792	0.9617*	88.5	10.6	13.4
FS-08A-17	0.3198	1.1013*	53.2	7.9	9.9
FS-08A-18	0.3399	1.1704*	43.1	7.4	7.8
FS-08A-19	0.3573	1.2306*	39.4	7.1	7.4
FS-08A-20	0.3802	1.3093*	38.4	7.1	6.6
FS-08A-21	0.2764	0.9524*	50.4	20.0	7.0
FS-08A-22	0.3525	1.2148*	31.2	8.0	5.1
FS-08A-23	0.3914	1.3487*	30.9	7.3	4.6
FS-08A-24	0.4022	1.3865*	26.9	7.4	6.0
FS-08A-25	0.3579	1.2335*	26.5	8.3	6.7

*Approximate value, based on primary airflow estimate

APPENDIX A (Continued)

TABLE III. GAS ANALYSIS PARAMETER DATA

Test No.	*EQR*	*CO2*	*O2*	*CFRAC*	*EFFGA*	*EQRSAM*
FS-05A-1	0.0916	1.31	19.32	—	99.98	0.0916
FS-05A-2	0.1337	1.89	18.43	—	99.91	0.1337
FS-05A-3	0.1439	2.06	18.05	—	99.82	0.1439
FS-05A-4	0.1788	2.56	17.46	—	99.70	0.1788
FS-05B-1	0.1604	2.19	17.41	0.9706	99.68	0.1526
FS-05B-2	0.1911	2.76	16.58	1.0275	99.71	0.1919
FS-05B-3	0.2377	3.41	15.79	1.0202	99.80	0.2355
FS-05B-4	0.2676	3.81	15.33	1.0145	99.86	0.2616
FS-05B-5	0.2143	2.98	17.75	0.9846	99.82	0.2049
FS-05B-6	0.2405	3.37	17.15	0.9946	99.87	0.2311
FS-05B-7	0.2641	3.70	16.65	0.9947	99.90	0.2544
FS-05B-8	0.1912	2.72	17.37	1.0093	99.72	0.1875
FS-05B-9	0.1564	2.29	18.05	1.0321	99.76	0.1584
FS-05B-10	0.1659	2.49	18.08	1.0581	99.91	0.1715
FS-05B-11	0.2021	2.94	17.51	1.0278	99.92	0.2020
FS-05B-12	0.2116	3.09	17.45	1.0314	99.92	0.2122
FS-05B-13	0.2359	3.49	16.95	1.0448	99.94	0.2384
FS-05B-14	0.2724	4.05	15.82	1.0526	99.97	0.2762
FS-05B-15	0.2858	4.25	15.52	1.0542	99.98	0.2907
FS-05B-16	0.1368	2.40	18.30	1.1055	99.88	0.1416
FS-05B-17	0.1816	3.07	17.51	1.0689	99.89	0.1802
FS-05B-18	0.2157	3.62	16.87	1.0628	99.93	0.2123
FS-05B-19	0.2389	3.49	16.62	1.0323	99.94	0.2413
FS-05B-20	0.1620	2.72	18.00	1.0599	99.87	0.1596
FS-05B-21	0.1954	3.21	17.44	1.0391	99.90	0.1879
FS-05B-22	0.2134	3.48	17.23	1.0333	99.92	0.2033
FS-05B-23	0.2590	4.24	15.99	1.0416	99.94	0.2471
FS-05B-24	0.1269	2.11	17.86	1.0469	99.86	0.1235

TABLE III. GAS ANALYSIS PARAMETER DATA (Continued)

Test No.	*EQR*	*CO_2*	*O_2*	*CFRAC*	*EFFGA*	*EQRSAM*
FS-05B-25	0.1421	2.14	17.79	1.0369	99.679	0.1450
FS-05B-26	0.1616	2.36	17.43	1.0191	99.745	0.1608
FS-05B-27	0.1839	2.65	16.98	1.0034	99.851	0.1795
FS-05B-28	0.2067	2.94	16.53	0.9934	99.865	0.1982
FS-05B-29	0.2366	3.34	15.94	0.9857	99.920	0.2254
FS-05B-30	0.2195	3.08	16.17	0.9793	99.993	0.2082
FS-05B-31	0.2104	3.02	16.24	1.0033	99.911	0.2039
FS-05B-32	0.1818	2.74	16.82	1.0228	99.830	0.1824
FS-05B-33	0.2490	3.56	15.66	1.0011	99.915	0.2398
FS-05B-34	0.2397	3.46	15.92	1.0016	99.923	0.2369
FS-05B-35	0.2230	3.18	16.34	0.9976	99.910	0.2195
FS-05B-36	0.1265	1.86	18.25	1.0203	99.908	0.1279
FS-05B-37	0.1357	2.04	18.08	1.0436	99.915	0.1410
FS-05B-38	0.1343	2.16	17.94	1.0835	99.908	0.1416
FS-05B-39	0.1670	2.64	17.51	1.0628	99.885	0.1725
FS-05B-40	0.2127	3.31	16.55	1.0482	99.908	0.2173
FS-05B-41	0.2495	3.87	15.75	1.0446	99.923	0.2524
FS-05B-42	0.2370	3.68	15.95	1.0438	99.922	0.2398
FS-05B-43	0.2047	3.17	16.69	1.0422	99.887	0.2075
FS-07A-1	0.1354	1.98	18.21	1.0168	99.876	0.1352
FS-07A-2	0.1639	2.28	17.70	0.9806	99.866	0.1570
FS-07A-3	0.1883	2.58	17.34	0.9658	99.864	0.1773
FS-07A-4	0.2073	2.84	17.06	0.9689	99.874	0.1962
FS-07A-5	0.2368	3.21	16.98	0.9598	99.913	0.2209
FS-07A-6	0.2629	3.88	15.98	1.0471	99.930	0.2660
FS-07A-7	0.1977	2.81	—	1.0018	99.882	0.1933
FS-07A-8	0.1985	2.85	16.82	1.0117	99.892	0.1962
FS-07A-9	0.1973	2.88	17.30	1.0291	99.8969	0.1977
FS-07A-10	0.2007	2.91	17.09	1.0230	99.859	0.2006
FS-07A-11	0.1988	2.85	17.32	1.0132	99.882	0.1962
FS-07A-12	0.2192	3.37	16.66	1.0341	99.886	0.2201
FS-07A-13	0.2457	3.69	16.72	1.0110	99.905	0.2412
FS-07A-14	0.1949	2.88	17.92	0.9946	99.875	0.1886
FS-07A-15	0.1926	2.93	18.42	0.9525	99.873	0.1724
FS-07A-16	0.2190	3.39	18.02	0.9808	99.890	0.1982
FS-07A-17	0.2421	3.80	16.82	0.9978	99.908	0.2226
FS-08A-1	0.1218	1.85	18.10	1.0536	99.966	0.1279
FS-08A-2	0.1440	2.15	17.67	1.0342	99.970	0.1482
FS-08A-3	0.1665	2.37	17.45	0.9894	99.970	0.1628
FS-08A-4	0.1887	2.72	17.06	0.9988	99.963	0.1860
FS-08A-5	0.1914	2.73	16.84	0.9880	99.962	0.1875
FS-08A-6	0.2145	3.04	16.49	0.9828	99.952	0.2078
FS-08A-7	0.2354	3.35	16.03	0.9885	99.950	0.2296
FS-08A-8	0.2612	3.78	15.67	1.0044	99.958	0.2587
FS-08A-9	0.2613	3.80	15.47	1.0101	99.957	0.2601
FS-08A-10	0.2875	4.21	14.86	1.0145	99.974	0.2863
FS-08A-11	0.3150	4.56	14.30	1.0046	99.985	0.3103
FS-08A-12	0.3100	4.55	14.33	1.0177	99.984	0.3096
FS-08A-13	0.3263	4.86	14.03	1.0331	99.988	0.3314
FS-08A-14	0.3532	5.25	13.42	1.0302	99.990	0.3561
FS-08A-15	0.3837	5.76	12.95	1.0394	99.991	0.3895
FS-08A-16	0.2792	5.20*	13.70*	1.0388	99.990	0.2706
FS-08A-17	0.3198	5.65*	13.08*	1.0316	99.992	0.3032
FS-08A-18	0.3399	6.01*	12.76*	1.0446	99.970	0.3261
FS-08A-19	0.3573	6.21*	12.34*	1.0367	99.972	0.3392
FS-08A-20	0.3802	6.60*	11.92*	1.0423	99.974	0.3634
FS-08A-21	0.2764	5.52*	13.59*	1.0092	99.966	0.2639
FS-08A-22	0.3525	6.82*	12.20*	1.0209	99.980	0.3410
FS-08A-23	0.3914	7.50*	11.26*	1.0399	99.981	0.3853
FS-08A-24	0.4022	7.86*	11.39*	1.0312	99.978	0.3900
FS-08A-25	0.3579	7.22*	12.78*	1.0407	99.976	0.3514

*Includes effect of vitiation of airflow by preheater.

APPENDIX A (Continued)

TABLE IV. COMBUSTOR LINER TEMPERATURE DATA

Test No.	*EQR*	*BSTD1*	*BSTD2*	*BSTD3*	*BSTD4*	*BST1*	*BST2*
FS-05A-1	0.0916	—	954	941	992	1092	1076
FS-05A-2	0.1337	—	1089	1140	1150	1315	1303
FS-05A-3	0.1439	—	1117	1163	1196	1329	1339
FS-05A-4	0.1788	—	1170	1217	1260	1442	1455
FS-05B-1	0.1604	—	1133	1157	1179	1386	1380
FS-05B-2	0.1911	—	1209	1240	1289	1460	1457
FS-05B-3	0.2377	—	1203	1198	1240	1475	1437
FS-05B-4	0.2676	—	1164	1155	1227	1214	1490
FS-05B-5	0.2143	—	1106	1164	1199	1507	1483
FS-05B-6	0.2405	—	1184	1173	1218	1458	1405
FS-05B-7	0.2641	—	1116	1163	1177	1173	1431
FS-05B-8	0.1912	—	1268	1330	1218	1450	1433
FS-05B-9	0.1564	—	1167	1226	1161	1367	1350
FS-05B-10	0.1659	—	1317	1359	1478	1572	1718
FS-05B-11	0.2021	—	1392	1420	1543	1640	1802
FS-05B-12	0.2116	—	1373	1419	1542	1630	1777
FS-05B-13	0.2359	–	1440	1467	1555	1658	1830
FS-05B-14	0.2724	—	1480	1428	1470	1614	1814
FS-05B-15	0.2858	—	1491	1446	1450	1570	1833
FS-05B-16	0.1368	—	1360	1450	1598	1620	1790
FS-05B-17	0.1816	—	1470	1550	1576	1731	1950
FS-05B-18	0.2157	—	1558	1600	1701	1760	1890
FS-05B-19	0.2389	—	1461	1479	1605	1839	—
FS-05B-20	0.1620	—	1405	1411	1590	1730	—
FS-05B-21	0.1954	—	1528	1512	1687	1894	—
FS-05B-22	0.2134	—	1580	1574	1744	1960	—
FS-05B-23	0.2590	—	1595	1575	1670	—	—
FS-05B-24	0.1269	—	1340	1420	1594	—	—

TABLE IV. COMBUSTOR LINER TEMPERATURE DATA (Continued)

Test No.	*EQR*	*BST3*	*BST4*	*BST5*	*BST6*	*BST7*	*BST8*
FS-05A-1	0.0916	—	1048	983	1005	939	1017
FS-05A-2	0.1337	—	1258	1550	1272	1310	1295
FS-05A-3	0.1439	—	1287	—	1265	1328	1333
FS-05A-4	0.1788	—	1355	—	1345	1387	1380
FS-05B-1	0.1604	—	1289	—	1302	1343	1419
FS-05B-2	0.1911	—	1381	—	1331	1467	1478
FS-05B-3	0.2377	—	1338	—	1361	1160	1210
FS-05B-4	0.2676	—	1049	—	1213	894	768
FS-05B-5	0.2143	—	1190	—	1339	931	803
FS-05B-6	0.2405	—	1252	—	1448	995	989
FS-05B-7	0.2641	—	1124	—	1255	835	887
FS-05B-8	0.1912	—	1319	—	1351	1011	981
FS-05B-9	0.1564	—	1382	—	1267	1503	1504
FS-05B-10	0.1659	—	1534	—	1635	1711	1735
FS-05B-11	0.2021	—	1548	—	1686	1702	1708
FS-05B-12	0.2116	—	1499	—	1659	1635	1651
FS-05B-13	0.2359	—	1504	—	1708	1594	1602
FS-05B-14	0.2724	—	1514	—	1788	1598	1504
FS-05B-15	0.2858	—	1513	—	1656	1191	1118
FS-05B-16	0.1368	—	1572	—	1660	1719	1754
FS-05B-17	0.1816	—	1574	—	1814	1741	1744
FS-05B-18	0.2157	—	1392	—	1895	1660	1694
FS-05B-19	0.2389	—	1478	—	—	1535	—
FS-05B-20	0.1620	—	1793	—	—	1700	—
FS-05B-21	0.1954	—	1882	—	—	1793	—
FS-05B-22	0.2134	—	1693	—	—	1790	—
FS-05B-23	0.2590	—	—	—	—	—	—
FS-05B-24	0.1269	—	—	—	—	—	—

APPENDIX A (Continued)

TABLE IV. COMBUSTOR LINER TEMPERATURE DATA (Continued)

Test No.	*EQR*	*BST9*	*BST10*	*BST11*	*BST12*	*BST13*	*BST14*
FS-05A-1	0.0916	—	998	986	1004	512	468
FS-05A-2	0.1337	—	1260	1267	1299	555	530
FS-05A-3	0.1439	—	1249	1284	1333	560	537
FS-05A-4	0.1788	—	1322	1358	1384	590	561
FS-05B-1	0.1604	—	1296	1321	1332	551	543
FS-05B-2	0.1911	—	1298	1447	1442	574	565
FS-05B-3	0.2377	—	1298	1259	1137	623	602
FS-05B-4	0.2676	—	972	928	752	690	660
FS-05B-5	0.2143	—	1190	988	921	600	594
FS-05B-6	0.2405	—	1327	1161	1034	638	625
FS-05B-7	0.2641	—	1024	922	791	682	652
FS-05B-8	0.1912	—	1292	1053	1086	578	569
FS-05B-9	0.1564	—	1293	1357	1424	553	548
FS-05B-10	0.1659	—	1474	1652	1591	751	731
FS-05B-11	0.2021	—	1505	1638	1600	772	751
FS-05B-12	0.2116	—	1471	1558	1535	775	756
FS-05B-13	0.2359	—	1503	1564	1531	808	784
FS-05B-14	0.2724	—	1570	1595	1510	860	822
FS-05B-15	0.2858	—	1140	1133	1185	877	834
FS-05B-16	0.1368	—	1427	1653	1546	737	708
FS-05B-17	0.1816	—	1503	1690	1580	785	743
FS-05B-18	0.2157	—	1622	1701	1629	847	787
FS-05B-19	0.2389	—	1730	1546	1469	826	780
FS-05B-20	0.1620	—	1573	1650	1618	743	728
FS-05B-21	0.1954	—	1764	1771	1752	803	772
FS-05B-22	0.2134	—	1868	1798	1750	851	810
FS-05B-23	0.2590	—	1773	—	—	930	884
FS-05B-24	0.1269	—	1482	—	—	722	707

TABLE IV. COMBUSTOR LINER TEMPERATURE DATA (Continued)

Test No.	*EQR*	*BST15*	*BST16*	*BST17*	*BST18*	*BST19*	*BST20*
FS-05A-1	0.0916	456	477	499	467	452	469
FS-05A-2	0.1337	504	526	537	529	494	514
FS-05A-3	0.1439	507	527	548	538	500	520
FS-05A-4	0.1788	524	546	573	560	514	538
FS-05B-1	0.1604	486	517	537	555	480	509
FS-05B-2	0.1911	516	549	557	577	505	536
FS-05B-3	0.2377	537	578	604	615	526	567
FS-05B-4	0.2676	583	634	676	684	569	619
FS-05B-5	0.2143	532	569	584	608	522	556
FS-05B-6	0.2405	556	601	622	640	545	589
FS-05B-7	0.2641	575	629	665	674	562	613
FS-05B-8	0.1912	526	557	561	582	517	543
FS-05B-9	0.1564	511	538	539	560	504	526
FS-05B-10	0.1659	684	714	733	752	680	705
FS-05B-11	0.2021	695	724	749	776	686	712
FS-05B-12	0.2116	696	725	755	779	686	712
FS-05B-13	0.2359	716	747	784	807	705	732
FS-05B-14	0.2724	753	784	826	843	741	769
FS-05B-15	0.2858	769	791	837	846	756	772
FS-05B-16	0.1368	677	706	723	730	672	698
FS-05B-17	0.1816	701	737	765	761	694	724
FS-05B-18	0.2157	738	779	814	800	729	757
FS-05B-19	0.2389	730	770	812	803	715	754
FS-05B-20	0.1620	684	715	726	741	677	707
FS-05B-21	0.1954	724	764	785	787	717	757
FS-05B-22	0.2134	761	807	830	823	755	798
FS-05B-23	0.2590	807	896	890	922	784	869
FS-05B-24	0.1269	674	728	709	722	671	724

TABLE IV. COMBUSTOR LINER TEMPERATURE DATA (Continued)

Test No.	*EQR*	*BSTD2*	*BSTD3*	*BSTD4*	*BST13*	*BST14*	*BST15*
FS-05B-25	0.1421	1323	1374	1501	708	696	656
FS-05B-26	0.1616	1410	1442	1567	749	738	695
FS-05B-27	0.1839	1470	1473	1645	783	773	718
FS-05B-28	0.2067	1447	1521	1702	829	809	743
FS-05B-29	0.2366	1627	1402	1478	880	860	775
FS-05B-30	0.2195	1582	1453	1647	851	831	759
FS-05B-31	0.2104	1483	1566	1699	815	777	737
FS-05B-32	0.1818	1436	1525	—	762	746	693
FS-05B-33	0.2490	1570	1604	—	891	862	800
FS-05B-34	0.2397	—	1530	—	828	779	732
FS-05B-35	0.2230	—	1519	—	800	760	717
FS-05B-36	0.1265	—	1385	—	718	697	669
FS-05B-37	0.1357	—	1408	—	726	701	673
FS-05B-38	0.1343	—	1403	—	730	705	672
FS-05B-39	0.1670	—	1462	—	767	745	704
FS-05B-40	0.2127	—	1556	—	860	823	765
FS-05B-41	0.2495	—	1480	—	927	885	818
FS-05B-42	0.2370	—	1451	—	904	864	801
FS-05B-43	0.2047	—	1606	—	859	817	769
FS-07A-1	0.1354	—	1369	—	696	675	653
FS-07A-2	0.1639	—	1325	—	755	727	704
FS-07A-3	0.1883	—	1634	—	797	755	731
FS-07A-4	0.2073	—	1694	—	833	780	756
FS-07A-5	0.2368	—	1682	—	870	815	784
FS-07A-6	0.2629	—	1320	—	896	841	808
FS-07A-7	0.1977	—	1660	—	819	771	743
FS-07A-8	0.1985	—	—	—	804	—	—
FS-07A-9	0.1973	—	—	—	783	—	—
FS-07A-10	0.2007	—	—	—	803	—	—
FS-07A-11	0.1988	—	1682	—	825	770	745
FS-07A-12	0.2192	—	1760	—	877	820	786
FS-07A-13	0.2457	—	1737	—	916	852	815
FS-07A-14	0.1949	—	1790	—	828	782	750
FS-07A-15	0.1926	—	1681	—	822	783	748
FS-07A-16	0.2190	—	1947	—	900	849	803
FS-07A-17	0.2421	—	1761	—	927	870	835
FS-08A-1	0.1218	—	—	—	733	690	657
FS-08A-2	0.1440	—	—	—	781	726	689
FS-08A-3	0.1665	—	—	—	844	783	751
FS-08A-4	0.1887	—	—	—	911	852	807
FS-08A-5	0.1914	—	—	—	896	824	785
FS-08A-6	0.2145	—	—	—	950	879	832
FS-08A-7	0.2354	—	—	—	1010	948	884
FS-08A-8	0.2612	—	—	—	1080	1020	936
FS-08A-9	0.2613	—	—	—	1065	996	924
FS-08A-10	0.2875	—	—	—	1150	1084	991
FS-08A-11	0.3150	—	—	—	1263	1191	1057
FS-08A-12	0.3100	—	—	—	1148	1101	1003
FS-08A-13	0.3263	—	—	—	1203	1169	1042
FS-08A-14	0.3532	—	—	—	1235	1216	1078
FS-08A-15	0.3837	—	—	—	1312	1292	1145
FS-08A-16	0.2792	—	—	—	1215	1242	1198
FS-08A-17	0.3198	—	—	—	1253	1300	1244
FS-08A-18	0.3399	—	—	—	1298	1368	1295
FS-08A-19	0.3573	—	—	—	1327	1406	1322
FS-08A-20	0.3802	—	—	—	1364	1442	1350
FS-08A-21	0.2764	—	—	—	1181	1195	1197
FS-08A-22	0.3525	—	—	—	1252	1288	1258
FS-08A-23	0.3914	—	—	—	1310	1364	1315
FS-08A-24	0.4022	—	—	—	1318	1460	1365
FS-08A-25	0.3579	—	—	—	1267	1426	1320

TABLE IV. COMBUSTOR LINER TEMPERATURE DATA (Continued)

Test No.	*EQR*	*BST16*	*BST17*	*BST18*	*BST19*	*BST20*
FS-05B-25	0.1421	714	690	707	650	705
FS-05B-26	0.1616	754	728	750	688	745
FS-05B-27	0.1839	778	758	792	710	767
FS-05B-28	0.2067	812	793	830	739	797
FS-05B-29	0.2366	848	842	881	765	827
FS-05B-30	0.2195	834	819	853	749	816
FS-05B-31	0.2104	796	781	791	724	784
FS-05B-32	0.1818	739	736	752	684	735
FS-05B-33	0.2490	855	847	879	781	841
FS-05B-34	0.2397	770	793	785	720	764
FS-05B-35	0.2230	755	771	768	707	747
FS-05B-36	0.1265	698	703	701	664	696
FS-05B-37	0.1357	704	708	706	668	701
FS-05B-38	0.1343	701	713	707	669	708
FS-05B-39	0.1670	751	742	745	699	744
FS-05B-40	0.2127	825	822	824	762	813
FS-05B-41	0.2495	880	876	887	804	854
FS-05B-42	0.2370	867	863	867	792	844
FS-05B-43	0.2047	831	822	816	766	820
FS-07A-1	0.1354	708	667	669	642	688
FS-07A-2	0.1639	759	711	717	687	734
FS-07A-3	0.1883	785	739	742	709	756
FS-07A-4	0.2073	815	768	767	734	783
FS-07A-5	0.2368	849	798	802	756	810
FS-07A-6	0.2629	872	819	821	772	830
FS-07A-7	0.1977	818	760	756	725	784
FS-07A-8	0.1985	—	758	—	—	—
FS-07A-9	0.1973	—	748	—	—	—
FS-07A-10	0.2007	—	757	—	—	—
FS-07A-11	0.1988	812	768	757	728	779
FS-07A-12	0.2192	852	814	806	764	814
FS-07A-13	0.2457	888	846	837	789	844
FS-07A-14	0.1949	813	782	776	737	783
FS-07A-15	0.1926	806	771	771	732	773
FS-07A-16	0.2190	874	836	832	787	834
FS-07A-17	0.2421	901	855	853	806	852
FS-08A-1	0.1218	748	709	633	648	666
FS-08A-2	0.1440	799	757	659	680	705
FS-08A-3	0.1665	869	815	718	737	765
FS-08A-4	0.1887	951	874	782	790	829
FS-08A-5	0.1914	929	859	745	769	815
FS-08A-6	0.2145	986	912	792	811	860
FS-08A-7	0.2354	1056	967	845	857	911
FS-08A-8	0.2612	1138	1032	904	915	972
FS-08A-9	0.2613	1115	1020	872	894	955
FS-08A-10	0.2875	1206	1100	950	966	1020
FS-08A-11	0.3150	1289	1181	1034	1045	1104
FS-08A-12	0.3100	1223	1094	961	980	1056
FS-08A-13	0.3263	1260	1141	1018	1026	1074
FS-08A-14	0.3532	1287	1170	1077	1066	1093
FS-08A-15	0.3837	1368	1237	1158	1154	1160
FS-08A-16	0.2792	1357	1169	1155	1242	1264
FS-08A-17	0.3198	1311	1199	1205	1291	1300
FS-08A-18	0.3399	1443	1243	1269	1347	1317
FS-08A-19	0.3573	1455	1270	1296	1377	1320
FS-08A-20	0.3802	1449	1305	1323	1403	1312
FS-08A-21	0.2764	1176	1291	1127	1099	1185
FS-08A-22	0.3525	1397	1191	1166	1260	1270
FS-08A-23	0.3914	1464	1246	1239	1318	1329
FS-08A-24	0.4022	1381	1257	1380	1381	1114
FS-08A-25	0.3579	1321	1212	1344	1335	1092

APPENDIX A (Continued)

TABLE V. PERFORMANCE PARAMETER DATA

Test No.	*EQR*	*WAPRI*	*WASEC*	*VREF*	*EFFMB*	*TPF*
FS-05A-1	0.0916	—	3.472		137.3	0.502
FS-05A-2	0.1337	—	3.506		121.9	0.371
FS-05A-3	0.1439	—	3.812		126.8	0.437
FS-05A-4	0.1788	—	3.680		129.3	0.471
FS-05B-1	0.1604	1.851	3.590		134.3	0.370
FS-05B-2	0.1911	1.871	3.485		131.4	0.298
FS-05B-3	0.2377	1.818	3.405		134.8	0.416
FS-05B-4	0.2676	1.826	3.522		124.3	0.491
FS-05B-5	0.2143	1.836	3.492		112.2	0.381
FS-05B-6	0.2405	1.801	3.399		120.2	0.589
FS-05B-7	0.2641	1.816	3.532		118.5	0.619
FS-05B-8	0.1912	1.832	3.496		108.5	0.551
FS-05B-9	0.1564	1.838	3.498		111.3	0.572
FS-05B-10	0.1659	3.125	5.789		105.6	0.481
FS-05B-11	0.2021	2.973	5.484		106.7	0.477
FS-05B-12	0.2116	3.307	6.226		105.2	0.457
FS-05B-13	0.2359	3.247	6.155		106.6	0.464
FS-05B-14	0.2724	3.312	5.958		104.2	0.323
FS-05B-15	0.2858	3.343	6.200		105.9	0.289
FS-05B-16	0.1368	2.642	5.879		111.0	0.387
FS-05B-17	0.1816	2.823	6.415		106.5	0.467
FS-05B-18	0.2157	2.825	6.215		112.8	0.396
FS-05B-19	0.2389	3.144	6.076		—	—
FS-05B-20	0.1620	2.966	5.864		—	—
FS-05B-21	0.1954	2.944	5.802		—	—
FS-05B-22	0.2134	2.832	5.960		—	—
FS-05B-23	0.2590	2.981	6.128		—	—
FS-05B-24	0.1269	2.659	6.037		—	—

TABLE V. PERFORMANCE PARAMETER DATA (Continued)

Test No.	*EQR*	*WAPRI*	*WASEC*	*VREF*	*EFFMB*	*TPF*
FS-05B-25	0.1421	3.007	5.964	22.1	—	—
FS-05B-26	0.1616	3.065	5.996	23.1	—	—
FS-05B-27	0.1839	3.072	6.034	23.2	—	—
FS-05B-28	0.2067	3.097	5.983	23.6	—	—
FS-05B-29	0.2366	3.055	6.005	23.3	—	—
FS-05B-30	0.2195	3.034	6.198	23.1	—	—
FS-05B-31	0.2104	3.158	6.004	23.1	—	—
FS-05B-32	0.1818	3.131	6.160	23.4	73.4	0.389
FS-05B-33	0.2490	3.043	5.943	22.9	—	—
FS-05B-34	0.2397	—	5.891	—	—	—
FS-05B-35	0.2230	3.273	5.936	24.6	—	—
FS-05B-36	0.1265	3.148	5.965	23.7	—	—
FS-05B-37	0.1357	3.137	5.740	23.5	—	—
FS-05B-38	0.1343	3.154	5.565	23.7	—	—
FS-05B-39	0.1670	3.276	5.773	24.6	—	—
FS-05B-40	0.2127	3.205	5.657	24.1	—	—
FS-05B-41	0.2495	3.220	5.746	24.3	—	—
FS-05B-42	0.2370	3.109	5.538	23.8	—	—
FS-05B-43	0.2047	3.206	5.495	24.2	—	—
FS-07A-1	0.1354	3.270*	6.034	23.9	—	—
FS-07A-2	0.1639	3.192*	5.892	24.0	—	—
FS-07A-3	0.1883	3.206*	5.979	24.3	—	—
FS-07A-4	0.2073	3.253*	6.082	24.8	—	—
FS-07A-5	0.2368	3.218*	6.098	24.5	—	—
FS-07A-6	0.2629	3.234*	6.139	25.0	—	—
FS-07A-7	0.1977	3.256*	6.048	24.9	—	—
FS-07A-8	0.1985	3.242*	6.035	24.8	—	—
FS-07A-9	0.1973	3.262*	5.893	24.9	—	—
FS-07A-10	0.2007	3.206*	5.843	24.5	—	—
FS-07A-11	0.1988	3.245*	6.063	24.8	—	—
FS-07A-12	0.2192	3.243*	6.090	24.9	—	—
FS-07A-13	0.2457	3.240*	6.151	24.8	—	—
FS-07A-14	0.1949	3.234*	5.947	24.8	—	—
FS-07A-15	0.1926	3.250*	6.055	25.0	—	—
FS-07A-16	0.2190	3.198*	6.064	24.4	—	—
FS-07A-17	0.2421	3.233*	6.204	24.8	—	—
FS-08A-1	0.1218	3.638*	6.013	25.8	—	—
FS-08A-2	0.1440	3.555*	5.942	25.4	—	—
FS-08A-3	0.1665	3.496*	6.077	24.9	—	—
FS-08A-4	0.1887	3.391*	6.044	24.2	—	—
FS-08A-5	0.1914	3.656*	6.346	26.5	—	—
FS-08A-6	0.2145	3.582*	6.328	25.9	—	—
FS-08A-7	0.2354	3.544*	6.322	25.6	—	—
FS-08A-8	0.2612	3.450*	6.188	24.9	—	—
FS-08A-9	0.2613	3.600*	6.381	26.1	—	—
FS-08A-10	0.2875	3.569*	6.332	25.7	—	—
FS-08A-11	0.3150	3.432*	6.159	24.7	—	—
FS-08A-12	0.3100	3.693*	6.828	26.7	—	—
FS-08A-13	0.3263	3.704*	6.862	26.5	—	—
FS-08A-14	0.3532	3.600*	6.498	26.0	—	—
FS-08A-15	0.3837	3.494*	6.238	25.2	—	—
FS-08A-16	0.2792	3.641*	6.923	33.4	—	—
FS-08A-17	0.3198	3.585*	6.734	32.4	—	—
FS-08A-18	0.3399	3.545*	6.768	32.0	—	—
FS-08A-19	0.3573	3.556*	6.593	31.7	—	—
FS-08A-20	0.3802	3.510*	6.477	31.2	—	—
FS-08A-21	0.2764	1.886*	3.457	34.0	—	—
FS-08A-22	0.3525	1.811*	3.367	32.5	—	—
FS-08A-23	0.3914	1.781*	3.297	31.7	—	—
FS-08A-24	0.4022	1.793*	3.225	31.6	—	—
FS-08A-25	0.3579	1.820*	3.270	32.4	—	—

*Estimate, value based on constant fraction of total airflow.

TABLE VI. COMBUSTOR LINER HEAT TRANSFER DATA

Test No.	*EQR*	*HRRV* $*10^6$	*HREMV* $*10^3$	*TTQQ*	*LTRFP*	*LTRFS*	*LTRF avg*	*Note*
FS-05A-1	0.0916	1.0884	54.7	515	0.9342	0.0641	0.5862	1
FS-05A-2	0.1337	1.1397	92.6	574	1.2045	0.1222	0.7717	1
FS-05A-3	0.1439	1.2672	100.0	580	1.2670	0.1246	0.8100	1
FS-05A-4	0.1788	1.3351	108.5	600	1.2521	0.1381	0.8064	1
FS-05B-1	0.1604	1.3921	117.6	574	1.2157	0.1542	0.7912	1
FS-05B-2	0.1911	1.6672	125.0	607	1.1090	0.1398	0.7214	1
FS-05B-3	0.2377	2.0454	91.8	562	0.8117	0.1477	0.5461	1
FS-05B-4	0.2676	2.2847	64.6	522	0.5478	0.1796	0.4004	1
FS-05B-5	0.2143	1.8327	89.3	561	0.7566	0.1448	0.5119	1
FS-05B-6	0.2405	2.0289	83.5	556	0.7450	0.1599	0.5110	1
FS-05B-7	0.2641	2.2812	57.7	517	0.5557	0.1707	0.4017	1
FS-05B-8	0.1912	1.6547	102.8	579	0.9380	0.1430	0.6200	1
FS-05B-9	0.1564	1.3725	119.8	602	1.2771	0.1470	0.8251	1
FS-05B-10	0.1659	1.2294	194.2	774	1.2500	0.1493	0.7320	2
FS-05B-11	0.2021	1.4548	194.0	777	1.0760	0.1462	0.6384	2
FS-05B-12	0.2116	1.6603	203.6	768	0.9890	0.1386	0.5888	2
FS-05B-13	0.2359	1.8347	136.8	722	0.9092	0.1453	0.5497	2
FS-05B-14	0.2724	2.0509	185.2	766	0.7917	0.1604	0.4946	2
FS-05B-15	0.2858	2.2737	144.2	730	0.6037	0.1605	0.3951	2
FS-05B-16	0.1368	1.0702	194.9	778	1.4667	0.1420	0.8433	2
FS-05B-17	0.1816	1.4890	239.2	799	1.1759	0.1454	0.6909	2
FS-05B-18	0.2157	1.7145	234.4	804	1.0251	0.1647	0.6202	2
FS-05B-19	0.2389	1.8186	196.2	765	0.9386	0.1624	0.5733	2
FS-05B-20	0.1620	1.3085	222.0	791	1.3256	0.1444	0.7697	2
FS-05B-21	0.1954	1.5501	256.1	830	1.2518	0.1666	0.7412	2
FS-05B-22	0.2134	1.6604	269.2	834	1.1733	0.1965	0.7136	2
FS-05B-23	0.2590	2.1011	156.1	723	0.9111	0.2373	0.4619	3
FS-05B-24	0.1269	1.0238	219.9	784	1.4231	0.1687	0.5869	3

Number of T/C's used in LTRF calculations

Note	*Primary*	*Secondary*	*Total*
1	12	8	20
2	9	8	17
3	4	8	12

TABLE VI. COMBUSTOR LINER HEAT TRANSFER DATA (Continued)

Test No.	*EQR*	*HRRV*	*HREMV*	*TTQQ*	*LTRFP*	*LTRFS*	*LTRF*	*Note*
		$*10^6$	$*10^3$					
FS-05B-25	0.1421	1.0594	222	757	1.2195	0.1784	—	
FS-05B-26	0.1616	1.2371	242	804	1.1728	0.1742	—	
FS-05B-27	0.1839	1.4104	263	824	1.0709	0.1841	—	
FS-05B-28	0.2067	1.6147	263	828	1.0134	0.2011	—	
FS-05B-29	0.2366	1.8152	222	796	0.7759	0.2162	—	
FS-05B-30	0.2195	1.7026	248	812	0.8828	0.2080	—	
FS-05B-31	0.2104	1.6213	289	819	1.0536	0.2060	—	
FS-05B-32	0.1818	1.4392	275	811	1.1578	0.1714	—	
FS-05B-33	0.2490	1.8533	236	809	0.9304	0.2154	—	
FS-05B-34	0.2397	1.8441	220	768	0.9060	0.1783	—	
FS-05B-35	0.2230	1.7261	210	780	0.9510	0.1522	—	
FS-05B-36	0.1265	0.9535	192	767	1.3864	0.1485	—	
FS-05B-37	0.1357	1.0188	193	774	1.3344	0.1472	—	
FS-05B-38	0.1343	1.0197	212	794	1.3228	0.1564	—	
FS-05B-39	0.1670	1.3064	263	834	1.1502	0.1691	—	
FS-05B-40	0.2127	1.6311	286	854	1.0216	0.2198	—	
FS-05B-41	0.2495	1.9190	226	804	0.8082	0.2365	—	
FS-05B-42	0.2370	1.8380	242	825	0.8177	0.2320	—	
FS-05B-43	0.2047	1.5572	284	865	1.1084	0.2212	—	
FS-07A-1	0.1354	1.0612	211	737	1.2622	0.1727	—	
FS-07A-2	0.1639	1.2398	223	794	0.9986	0.1604	—	
FS-07A-3	0.1883	1.4389	253	818	1.2524	0.1716	—	
FS-07A-4	0.2073	1.6121	264	827	1.2072	0.1836	—	
FS-07A-5	0.2368	1.8099	240	810	1.0524	0.1899	—	
FS-07A-6	0.2629	2.0491	167	751	0.6307	0.1923	—	
FS-07A-7	0.1977	1.5388	257	826	1.2190	0.1792	—	
FS-07A-8	0.1985	1.5341	265	833	—	0.1727	—	1
FS-07A-9	0.1973	1.5334	257	831	—	0.1596	—	1
FS-07A-10	0.2007	1.5350	233	813	—	0.1699	—	1
FS-07A-11	0.1988	1.5310	264	832	1.2392	0.1785	—	
FS-07A-12	0.2192	1.7313	296	854	1.1971	0.2086	—	
FS-07A-13	0.2457	1.9311	231	804	1.0538	0.2143	—	
FS-07A-14	0.1949	1.5298	296	862	1.3716	0.1887	—	
FS-07A-15	0.1926	1.5939	307	865	1.2109	0.1790	—	
FS-07A-16	0.2190	1.7666	317	874	1.3445	0.2219	—	
FS-07A-17	0.2421	1.9879	281	841	1.0526	0.2225	—	
FS-08A-1	0.1218	0.6707	98	621	—	0.2616	—	
FS-08A-2	0.1440	0.7696	115	650	—	0.2632	—	
FS-08A-3	0.1665	0.8688	148	678	—	0.3068	—	
FS-08A-4	0.1887	0.9596	182	706	—	0.3505	—	
FS-08A-5	0.1914	1.0596	179	701	—	0.3155	—	
FS-08A-6	0.2145	1.1564	205	723	—	0.3344	—	
FS-08A-7	0.2354	1.2520	225	741	—	0.3607	—	
FS-08A-8	0.2612	1.3508	236	754	—	0.3849	—	
FS-08A-9	0.2613	1.4126	231	749	—	0.3629	—	
FS-08A-10	0.2875	1.5266	245	762	—	0.3951	—	
FS-08A-11	0.3150	1.6088	203	736	—	0.4294	—	
FS-08A-12	0.3100	1.7089	242	746	—	0.3806	—	
FS-08A-13	0.3263	1.7776	226	758	—	0.3949	—	
FS-08A-14	0.3532	1.8925	193	720	—	0.3933	—	
FS-08A-15	0.3837	1.9877	147	692	—	0.4114	—	
FS-08A-16	0.2792	1.5613	279	1006	—	0.3614	—	
FS-08A-17	0.3198	1.7457	254	986	—	0.3540	—	
FS-08A-18	0.3399	1.8272	260	991	—	0.3763	—	
FS-08A-19	0.3573	1.9096	243	982	—	0.3794	—	
FS-08A-20	0.3802	1.9950	234	978	—	0.3727	—	
FS-08A-21	0.2764	1.5898	138	990	—	0.3405	—	
FS-08A-22	0.3525	1.9273	134	998	—	0.3233	—	
FS-08A-23	0.3914	2.1006	118	971	—	0.3403	—	
FS-08A-24	0.4022	2.1169	116	967	—	0.3575	—	
FS-08A-25	0.3579	1.9252	113	965	—	0.3635	—	

Note:
1 — LTRFS based on estimate of average liner temperature projected from 2 thermocouples
— HREMV based on estimate of average TTQQ projected from 1 thermocouple

TABLE VII. COMBUSTOR EXIT TEMPERATURE DATA

Test No.	*EQR*	T_{T41}	T_{T42}	T_{T43}	T_{T44}	T_{T45}	T_{T46}	T_{T47}	T_{T48}
FS-05A-1	0.0916	574	705	828	955	1083	1160	1118	918
FS-05A-2	0.1337	741	932	1120	1258	1379	1443	1385	1116
FS-05A-3	0.1439	720	948	1194	1379	1541	1619	1515	1184
FS-05A-4	0.1788	804	1082	1382	1631	1872	1952	1764	1292
FS-05B-1	0.1604	—	993	1248	1475	1689	1750	1490	1073
FS-05B-2	0.1911	—	1141	1480	1709	1830	1884	1621	1184
FS-05B-3	0.2377	—	1277	1664	1963	2223	2424	1981	1327
FS-05B-4	0.2676	—	1342	1758	2047	2591	—	2107	1429
FS-05B-5	0.2143	—	1171	1547	1905	—	1638	—	1233
FS-05B-6	0.2405	845	1275	1693	2064	2451	2029	1932	1336
FS-05B-7	0.2641	846	1262	1672	2050	2643	2345	2127	1445
FS-05B-8	0.1912	745	1068	1395	1655	1870	—	1599	1183
FS-05B-9	0.1564	696	970	1239	1460	1668	—	1416	1076
FS-05B-10	0.1659	862	1142	1378	1570	1750	—	1647	1309
FS-05B-11	0.2021	939	1263	1555	1775	1995	—	1856	1442
FS-05B-12	0.2116	945	1278	1582	1807	2018	—	1930	1473
FS-05B-13	0.2359	1009	1381	1725	1955	2196	—	2038	1557
FS-05B-14	0.2724	1134	1586	1934	2057	2211	—	2200	1623
FS-05B-15	0.2858	1147	1797	2022	2164	2267	—	2217	1667
FS-05B-16	0.1368	822	—	1257	1432	1595	—	1555	1271
FS-05B-17	0.1816	916	1186	1496	1720	1924	—	1853	1462
FS-05B-18	0.2157	971		1676	1944	2163	—	2035	1561
FS-05B-19	0.2389	—	—	—	1992	2359	—	2161	1696
FS-05B-20	0.1620	—	—	—	—	1885	—	2011	1581
FS-05B-21	0.1954	—	—	—	—	—	—	—	—
FS-05B-22	0.2134	—	—	—	—	—	—	—	—
FS-05B-23	0.2590	—	—	—	—	—	—	—	—
FS-05B-24	0.1269	—	—	—	—	—	—	—	—

TABLE VII. COMBUSTOR EXIT TEMPERATURE DATA (Continued)

Test No.	*EQR*	T_{T41}	T_{T42}	T_{T43}	T_{T44}	T_{T45}	T_{T46}	T_{T47}	T_{T48}
FS-05B-25	0.1421	—	—	—	—	—	—	—	—
FS-05B-26	0.1616	—	—	—	—	—	—	—	—
FS-05B-27	0.1839	—	—	—	—	—	—	—	—
FS-05B-28	0.2067	—	—	—	—	—	—	—	—
FS-05B-29	0.2366	—	—	—	—	—	—	—	—
FS-05B-30	0.2195	—	—	—	—	—	—	—	—
FS-05B-31	0.2104	—	—	—	—	—	—	—	—
FS-05B-32	0.1818	818	939	1129	1299	1378	1413	1357	1135
FS-05B-33	0.2490	937	—	1352	1586	1689	—	1582	1331
FS-05B-34	0.2397	—	—	1799	2231	—	—	2314	1835
FS-05B-35	0.2230	—	—	—	2089	—	—	2222	1748
FS-05B-36	0.1265	—	—	—	1430	—	2002	1572	1333
FS-05B-37	0.1357	—	—	—	1494	—	2143	1638	1371
FS-05B-38	0.1345	—	—	—	1530	—	2365	1664	1377
FS-05B-39	0.1670	—	—	—	1714	—	2798	1862	1508
FS-05B-40	0.2127	—	—	—	—	—	—	2134	1716
FS-05B-41	0.2495	—	—	—	—	—	—	2420	1845
FS-05B-42	0.2370	—	—	—	2230	—	—	2382	1824
FS-05B-43	0.2047	—	—	1789	1938	—	2437	2098	1634
FS-07A-1	0.1354	—	—	—	1407	—	—	1434	1273
FS-07A-2	0.1639	—	—	—	1519	—	—	1610	1434
FS-07A-3	0.1883	—	—	—	1767	—	—	1748	1542
FS-07A-4	0.2073	—	—	—	1823	—	—	1837	1659
FS-07A-5	0.2368	—	—	—	1971	—	—	2067	1860
FS-07A-6	0.2629	—	—	—	—	—	—	—	—
FS-07A-7	0.1977	—	—	—	—	—	—	1809	1688
FS-07A-8	0.1985	—	—	—	—	—	—	1861	1621
FS-07A-9	0.1973	—	—	—	—	—	—	1860	1592
FS-07A-10	0.2007	—	—	—	—	—	—	1830	1595
FS-07A-11	0.1988	—	—	—	—	—	—	1831	1648
FS-07A-12	0.2192	—	—	—	—	—	—	1872	1752
FS-07A-13	0.2457	—	—	—	—	—	—	2144	1915
FS-07A-14	0.1949	—	—	—	—	—	—	1803	1611
FS-07A-15	0.1926	—	—	—	—	—	—	1753	1530
FS-07A-16	0.2190	—	—	—	—	—	—	1952	1733
FS-07A-17	0.2421	—	—	—	—	—	—	2107	1860
FS-08A-1	0.1218	—	—	—	—	—	—	1290	1218
FS-08A-2	0.1440	—	—	—	—	—	—	1455	1363
FS-08A-3	0.1665	—	—	—	—	—	—	1502	1435
FS-08A-4	0.1887	—	—	—	—	—	—	1606	1536
FS-08A-5	0.1914	—	—	—	—	—	—	1663	1578
FS-08A-6	0.2145	—	—	—	—	—	—	1750	1660
FS-08A-7	0.2354	—	—	—	—	—	—	—	—
FS-08A-8	0.2612	—	—	—	—	—	—	—	—
FS-08A-9	0.2613	—	—	—	—	—	—	—	—
FS-08A-10	0.2875	—	—	—	—	—	—	—	—
FS-08A-11	0.3150	—	—	—	—	—	—	—	—
FS-08A-12	0.3100	—	—	—	—	—	—	—	—
FS-08A-13	0.3263	—	—	—	—	—	—	—	—
FS-08A-14	0.3532	—	—	—	—	—	—	—	—
FS-08A-15	0.3837	—	—	—	—	—	—	—	—
FS-08A-16	0.2792	—	—	—	—	—	—	—	—
FS-08A-17	0.3198	—	—	—	—	—	—	—	—
FS-08A-18	0.3399	—	—	—	—	—	—	—	—
FS-08A-19	0.3573	—	—	—	—	—	—	—	—
FS-08A-20	0.3802	—	—	—	—	—	—	—	—
FS-08A-21	0.2764	—	—	—	—	—	—	—	—
FS-08A-22	0.3525	—	—	—	—	—	—	—	—
FS-08A-23	0.3914	—	—	—	—	—	—	—	—
FS-08A-24	0.4022	—	—	—	—	—	—	—	—
FS-08A-25	0.3579	—	—	—	—	—	—	—	—

APPENDIX B

SI UNIT CONVERSION TABLE

English	*SI*	*Multiply by*
°F	°C	°C = (5/9)(°F−32)
in.	cm	2.54
$in.^2$	cm^2	0.1550
$in.^3$	liters	0.0164
ft	m	0.3048
ft^2	m^2	0.0929
ft^3	m^3	0.0283
ft/sec	m/sec	0.3048
in. Hg	N/m^2	3.3863
lb_m/sec	kg/sec	0.4535
lb_m/hr	kg/hr	0.4535
gal	m^3	0.003785
Btu/ft^2 hr	w/m^2	315.24808
psi	N/m^2	6894.7572

TECHNICAL REPORT DATA
(Please read Instructions on the reverse before completing)

1. REPORT NO.	2.	3. RECIPIENT'S ACCESSION NO.
EPA-600/7-80-017d		

4. TITLE AND SUBTITLE	5. REPORT DATE
Advanced Combustion Systems for Stationary Gas Turbine Engines: Volume 4. Combustor Verification Testing (Addendum)	January 1980
	6. PERFORMING ORGANIZATION CODE
7. AUTHOR(S)	8. PERFORMING ORGANIZATION REPORT NO.
R.M. Pierce, C.E. Smith, and B.S. Hinton	FR-11405
9. PERFORMING ORGANIZATION NAME AND ADDRESS	10. PROGRAM ELEMENT NO.
Pratt and Whitney Aircraft Group United Technologies Corporation P.O. Box 2691 West Palm Beach, Florida 33402	INE829
	11. CONTRACT/GRANT NO.
	68-02-2136
12. SPONSORING AGENCY NAME AND ADDRESS	13. TYPE OF REPORT AND PERIOD COVERED
EPA, Office of Research and Development Industrial Environmental Research Laboratory Research Triangle Park, NC 27711	Final; 7/79 - 10/79
	14. SPONSORING AGENCY CODE
	EPA/600/13

15. SUPPLEMENTARY NOTES IERL-RTP project officer is W.S. Lanier, Mail Drop 65, 919/541-2432.

16. ABSTRACT The reports describe an exploratory development program to identify, evaluate, and demonstrate dry techniques for significantly reducing NOx from stationary gas turbine engines. (Volume 1 describes Phase I research activities to compile a series of combustor design concepts which could potentially meet the program's low emission goals. Volume 2 covers the Phase II bench-scale testing program which experimentally singled out the rich-burn/quick-quench (RB/QQ) combustor concept as being capable of low NOx and CO operation on both clean fuels and fuels containing significant amounts of bound nitrogen. Volume 3 covers the Phase III and IV scaleup and full-scale testing of the RB/QQ concept, documenting the fact that all emission goals could be met with the RB/QQ combustor.) Volume 4 describes an additional series of tests to evaluate the performance of the combustor on heavy fuels such as petroleum or shale residual oil and solvent refined coal (SRC). Results from the tests show that all exhaust emission goals were met while burning three test fuels: a middle-cut distillate SRC, a residual shale oil, and an Indonesian/Malaysian residual oil. It was also demonstrated that the exhaust emission goals were met when operating a RB/QQ combustor at a high turbine inlet temperature (1426 C design) firing No. 2 fuel oil.

17. KEY WORDS AND DOCUMENT ANALYSIS

a. DESCRIPTORS		b. IDENTIFIERS/OPEN ENDED TERMS	c. COSATI Field/Group	
Pollution	Residual Oils	Pollution Control	13B	21D
Gas Turbine Engines	Shale Oil	Stationary Sources	21E	
Stationary Engines	Coal	Combustor Design	21K	
Nitrogen Oxides	Liquefaction	Staged Combustion	07B	07D
Combustion		Dry Controls	21B	
Combustion Chambers		Fuel-bound Nitrogen		

18. DISTRIBUTION STATEMENT	19. SECURITY CLASS *(This Report)*	21. NO. OF PAGES
Release to Public	Unclassified	116
	20. SECURITY CLASS *(This page)*	22. PRICE
	Unclassified	

EPA Form 2220-1 (9-73)